MASTER THESIS

Alternative ways to set the blue water footprint cap at sub-catchment level: a case study for the Yellow River basin in China

Luc T. Albers

S1497804

University of Twente

Faculty of Engineering Technology (ET)

Water Engineering and Management

EXAMINATION COMMITTEE

Dr. Ir. M. J. Booij (University of Twente, Enschede, the Netherlands)

Dr. Ir. J.F. Schyns (University of Twente, Enschede, the Netherlands)

Dr. L. Zhuo (Northwest A&F University, Yangling, China)

28/5/2020

Preface

This thesis is part of my graduation for the Master study 'Civil Engineering and Management' with the specialization 'Integrated Water Management'. This finished thesis marks the end of my period at the University of Twente.

The research preceding the thesis was carried out at the University of Twente. However, I had the privilege to visit the Northwest A&F University in Yangling China, where I gathered the data required for my research. I would like to thank La Zhuo, who helped me with setting up the research, addressed my questions regarding the methods and data, and arranged everything for me to assure a pleasant stay in China. Furthermore, I would like to thank my fellow students for helping me during my stay in Yangling, especially Pengxuan Xie who translated daily life for me and assisted me with data simulation, both the setup of the model and data preparation.

From the University of Twente, I would like to thank Martijn Booij and Joep Schyns. They both helped me with structuring and writing my thesis by providing me with useful and necessary feedback, thereby improving the quality of my thesis. Besides, they were available to help me with adjusting and improving the methods required for my research.

In addition, I am grateful that despite the difficult situation due to the outbreak of the COVID-19 virus, I could continue my research and finish my thesis.

Finally, I would like to pay my respects to all friends and family of Arjen Hoekstra, the former supervisor of my thesis. He sadly passed away last November and has been very important in the field of the blue water footprint research.

Kind regards,

Luc Albers
May 2020, Enschede

Summary

The growing water demand of the world's population burden the renewable freshwater or blue water resources globally. The supply of blue water reduces locally and becomes more erratic due to climate change. This combination threatens and has already affected ecosystems in river basins that depend on blue water resources. The consumption of blue water resources is referred to as the blue water footprint (BWF). The ecosystems can be protected by setting an upper limit of blue water consumption which ensures the sustainability of the BWF. The upper limit of sustainable consumption is defined as the natural runoff minus a certain amount of blue water that is reserved for the environment defined as the environmental flow requirements (EFR). The upper limit of blue water consumption can be implemented in a river basin as a policy tool in the form of a BWF cap.

Until recently BWF caps were calculated monthly at river basin level. However, this spatial resolution does not capture the spatial variability of consumption or generation of blue water. For the practical implication that captures this variability, the BWF cap needs to be defined at a smaller spatial scale. How to spatially define the BWF cap remains a point of interest. The objective of this study is to examine the effect on the blue water scarcity of defining alternative monthly BWF caps at sub-catchment level. Four alternative allocation principles using two EFR methods for BWF cap setting at sub-catchment level were investigated. The effect of the allocation principles and EFR methods were evaluated by computing monthly blue water scarcity at sub-catchment level in a case study for the Yellow River basin (YRB) from 2010 to 2014.

The natural runoff is simulated using the Soil and Water Assessment Tool (SWAT). The SWAT model used physical characteristics and meteorological data of the basin to determine the natural runoff. The blue water availability (BWA) for consumption is calculated for every sub-catchment by subtracting EFRs from the natural runoff. The BWA was allocated over the sub-catchments according to four scenarios for the calculation of the BWF caps: 1) natural conditions and *not accounting* for other sub-catchments (default scenario), 2) presence of reservoirs and *not accounting* for other sub-catchments (reservoir scenario), 3) presence of reservoirs and *accounting* for other sub-catchments based on relative population (population-based scenario) and 4) presence of reservoirs and *accounting* for other sub-catchments based on relative past demand of blue water in the form of BWF (demand-based scenario). All these four scenarios have been assessed for two different methods to compute EFR: the presumptive standard approach (PRE) and the variable monthly flow method (VMF).

Blue water scarcity was most prominently present during spring and summer for every scenario and more so for PRE than VMF. The default scenario showed the largest number of sub-catchments with water scarcity in the highest category due to mismatch in timing between BWA and BWF. The reservoir scenario decreased this number by changing the timing of BWA and its spatial distribution over sub-catchments. The population-based scenario decreased the water scarcity and it was more equally distributed over the sub-catchments. Finally, the demand-based scenario decreased water scarcity to the lowest level over the sub-catchments with smaller regional differences between sub-catchments.

The timing of BWA is influenced by its natural temporal and spatial variability, and the operation of reservoirs. An allocation based on the use-what-is-there principle leads to large regional differences in BWF caps and water scarcity, increasing from upstream to downstream. An allocation principle that considers other sub-catchments mitigates regional differences between upstream and downstream BWF caps, and water scarcity. The allocation considering other sub-catchments and based on past demand shows the most equal distribution of water scarcity if the pattern of past demand and actual demand correspond.

List of symbols

$BWA_{x,t}$	Blue water availability. Sustainable available blue water in sub-catchment x at time t.
$BWA_{down,x,t}$	BWA that is available downstream of sub-catchment x at time t. This is calculated as a future value for the demand-based scenario.
$BWA_{local,x,t}$	Locally generated BWA in sub-catchment x at time t.
$BWA_{up,x,t}$	BWA entering a sub-catchment x at time t from an upstream sub-catchment. This can be a mainstream sub-catchment or a tributary sub-catchment.
$BWF_{x,t}$	Blue water footprint in sub-catchment x at time t.
$BWF_{cap,x,t}$	Blue water footprint cap in sub-catchment x at time t.
EFR	Environmental flow requirements. The amount of natural runoff that is reserved for the environment to sustain it.
$EFR_{frac,x,t}$	Fraction of natural runoff to determine the environmental flow requirements in sub-catchment x at time t.
PRE	Presumptive standard approach. A method to estimate the environmental flow requirements.
$Q_{nat,x,t}$	Natural streamflow. The amount of water flowing through the river channel in sub-catchment x at time t without human influence.
$RO_{nat,x,t}$	Natural runoff. The amount of generated blue water in sub-catchment x that adds to the streamflow at time t without human influence.
$\Delta S_{x,t}$	Adjusted storage change of a reservoir located in sub-catchment x at time t.
T_x	Travel time through the river channel in sub-catchment x.
$T_{i,x}$	Travel time through the river channel from sub-catchment x to i.
VMF	Variable monthly flow method. A method to estimate the environmental flow requirements.

Table of contents

1. Introduction

1.1. Problem analysis

The growing water demand of the increasing world population and its increasing consumption levels burden the renewable freshwater resources around the world more and more (Postel, 2000). The United Nations (2017) project that the world population will continue to increase towards 2030, 2050, and 2100. This increases the freshwater consumption globally. In addition, the predicted economic growth and increased GDP lead to a more water-intensive freshwater consumption pattern (Liu & Savenije, 2008; United Nations, 2019). The projected population and economic growth increase the pressure on the world's limited freshwater resources. It is not merely the demand side that affects the pressure on global freshwater resources. It is also a matter of freshwater supply. The freshwater supply locally reduces and becomes more erratic due to climate change (Hoekstra, 2013).

The amount of freshwater consumed from ground and surface water bodies in a river basin is referred to as the blue water footprint (BWF) of the basin. Consumption here relates to loss of water, i.e. the amount of water that is not returned to the system and should not be confused with water withdrawal (Hoekstra, 2013; Hoekstra et al., 2011). This study focusses on the pressure of human consumption on blue water resources in riverine systems. This pressure has resulted in four billion people, two-thirds of the world's population, facing severe water scarcity for at least one month per year (Mekonnen & Hoekstra, 2016). Human blue water consumption causes major rivers, or parts of it, around the world to run dry completely or are reduced to a mere trickle for a number of days each year, e.g. Colorado River in the United States, Yellow River in China, Indus River in Pakistan and the Ganges River in India (Postel, 1999; Brown, 2006).

This overutilization of blue water resources from rivers affects the ecosystem in and around it (Richter et al., 2006). The principle of environmental flow requirements (EFR) was introduced as a theoretical measure for the adverse effects of unsustainable blue water consumption on ecosystems. The EFR indicates what part of the natural flow should be reserved for maintaining the river's ecosystem (Richter et al., 2006). The natural flow or natural runoff (RO_{nat}) is the amount of water that would have become streamflow if human activities would not have altered it (Roos, 1991; Karimi et al., 2012). The EFR indirectly indicates what part of the natural runoff is sustainably available for consumption or the blue water availability (BWA).

The BWA is defined as the natural runoff minus the EFR (Hoekstra, 2014). The extent of sustainable consumption can be evaluated by computing the water scarcity. The water scarcity is calculated by dividing the actual BWF by the BWA (Mekonnen & Hoekstra, 2016). The environment can be actively protected by setting an upper limit of blue water consumption in a river basin to assure sustainable consumption. This upper limit of sustainable consumption is the blue water footprint cap (BWF cap). There is still discussion on setting the BWF cap. The discussion considers the temporal and spatial variability of BWA and the actual BWF within a basin. For example, annual water scarcity studies hide the intra-annual difference and cause an underestimation of water scarcity. In addition, water scarcity is often calculated at river basin level and thereby not accounting for the spatial variation of BWA and BWF (Hoekstra et al., 2012).

Mekonnen & Hoekstra (2016) calculated the global monthly water scarcity at grid level to deal with the temporal and spatial variability of BWA. Furthermore, Veldkamp et al. (2017) showed that human interventions like reservoir construction and land-use change over the past decades, reduce water scarcity in upstream parts of river basins and aggravate it downstream. Zhuo et al. (2019) studied the influence of the presence of reservoirs on the water scarcity between different sections of the Yellow River basin in China. In the studies by Mekonnen & Hoekstra (2016) and Zhuo et al. (2019), the BWF cap was determined

by considering the dependency of the different grid cells or areas of a basin. The dependency was expressed as water flowing through the flow paths of grid cells or areas. In combination with actual BWF, the amount of water present was used as the BWF cap. However, the BWF cap can be spatially defined differently than based on the total BWA present in a certain grid cell or area. BWA in an upstream part of a basin does not necessarily have to be consumed in that specific part but could also be consumed somewhere downstream instead. Blue water can be reserved in an upstream part of the basin for consumption downstream, thereby changing the BWF cap in both locations. It is thus possible to transfer a part of the theoretical BWF cap from an upstream area to a downstream area. How to spatially allocate water over different areas of a basin using this possible transfer has not been studied yet.

The objective of this study is to examine the effect on the blue water scarcity of defining alternative monthly BWF caps at sub-catchment level. The BWF caps are based on four alternative allocation principles and two EFR methods. Paragraph 1.2. shows the research questions that are used to fulfil the objective. The Yellow River basin (YRB) from 2010 – 2014 is taken as a case study. The period from 2010 to 2014 is chosen as a case study for the YRB, because of the detailed level of available BWF and the years cover a variety of hydrological years, i.e. dry, wet, and average. Information about the YRB is given in paragraph 1.3. Paragraph 1.4. shows the outline of the report.

1.2. Research questions

The research objective consists of formulating alternative BWF caps and evaluating them by calculating the blue water scarcity. The former is the result of the research question one to three, and the latter is the result of research question four. As stated in paragraph 1.1., the BWF cap setting starts with determining the natural runoff. Leading to the first sub-question:

1. *What is the monthly natural runoff of per sub-catchment in the YRB from 2010 to 2014?*

Now with the local natural runoff determined, the BWA for each sub-catchment can be estimated to determine the BWF caps. In this research, the BWA is determined using two different EFR methods to gain an insight into the effect on water scarcity of applying different EFR methods for setting BWF caps. The second sub-question is formulated as follows:

2. *What is the monthly BWA per sub-catchment using two alternative EFR methods from 2010 to 2014?*

The allocation of BWA over the sub-catchments lead to the BWF cap for each sub-catchment. The way of allocating the resources affects the BWF caps. In this study, four alternative allocation principles are proposed. Therefore, the third sub-question:

3. *What is the monthly BWF cap per sub-catchment for four alternative allocation principles from 2010 to 2014?*

The final step in achieving the objective of this study is to evaluate the formulated BWF caps using BWF data of each sub-catchment and identifying the level of water scarcity, resulting in the fourth and final sub-question.

4. *What is the water scarcity of each sub-catchment per month of the defined BWF caps using BWF data for the period 2010 – 2014?*

1.3. Background information

The YRB is the second largest river basin in China with a drainage area of 7.53 x 10^5 km^2. The main river channel's length is around 5464 km (Wu et al., 2018). The basin is located in the northern area of China, and its elevation ranges from 1 to 6199 m, decreasing from west to east (Jiang et al, 2016). The YRB's location within China and its elevation are displayed in Figure 1.

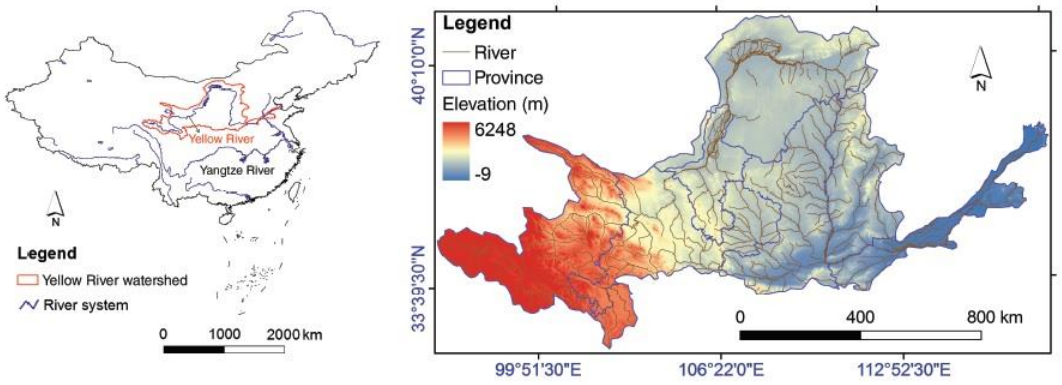

FIGURE 1: LOCATION OF YRB IN CHINA (LEFT) AND LONGITUDE AND LATITUDE COORDINATES, AND ELEVATION OF THE YRB (RIGHT) (WU ET AL., 2018).

In literature the basin is other divided into three reaches. The division of the three reaches is displayed in Figure 2 (Zhuo et al., 2019). The Yellow River originates on the eastern Tibetan Plateau; this part of the river is called the Upper Reach of the river basin. The Middle Reach of the river flows across the Loess Plateau, and the Lower Reach flows across a fluvial plain before discharging into the Bohai Sea. In addition, the river flows through arid, semi-arid, and semi-humid areas. The temporal and spatial distribution of the precipitation are heterogeneous. Most precipitation occurs in the period between June and September and increases from northwest to southeast (Tang et al., 2008a). The average annual natural runoff of the Yellow River is 58 x 10^9 m^3/year or 77 mm/year, accounting for 2.1% of the total of China's seven largest rivers. The freshwater resources of the YRB are important for nature and are the lifeblood of at least nine important wetlands (Hua & Cui, 2018).

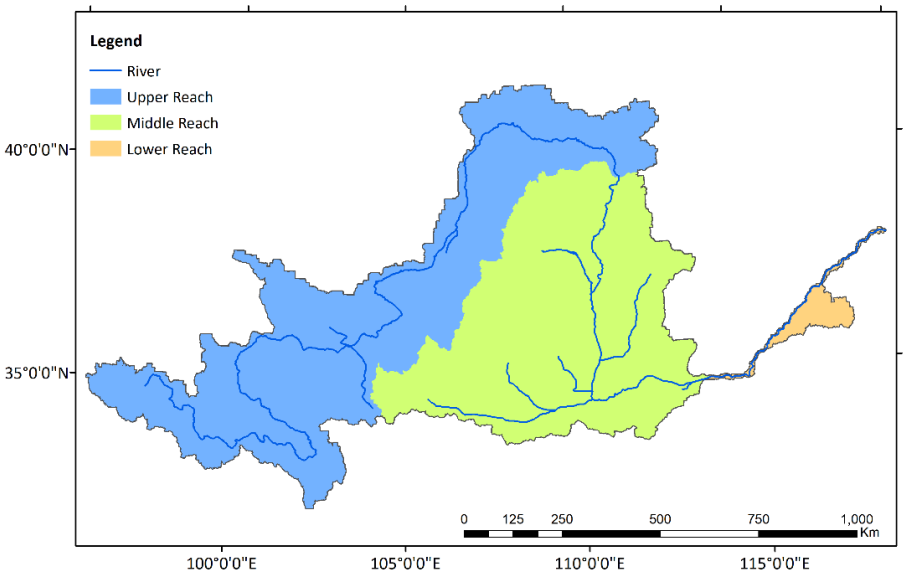

FIGURE 2: THE YELLOW RIVER'S UPPER, MIDDLE AND LOWER REACH.

The importance of the YRB can be illustrated by the 107 million people that are directly supported by it (Liu et al., 2008). The YRB plays a vital role in China's agricultural production. The total cultivated area in the basin is 129.000 km^2, 13% of China's total, but it holds only 2% of the country's freshwater resources. The irrigated area increased with 650% from 1950 to 2000. Irrigation, together with the rapid growth of industrial and municipal water uses, has resulted in dramatic water withdrawals and consumption over the entire basin (Zhu et al., 2004). After the completion of the irrigation projects and the increase of industrial and municipal consumption, the Lower Reach of the Yellow River has suffered from extreme low flow conditions. Eventually leading to the zero-flow phenomenon to occur in the Lower Reach of the basin (Tang et al., 2008b). The phenomenon started to occur in 1972 (Yang, et al., 2004). A total of 21 events of drying up in the lower reach have been recorded between 1972 and 1999 (Hua & Cui, 2018). The frequency and length of the zero-flow phenomenon rapidly increased in the 1990s (Yang, et al., 2009a). The phenomenon seemed to have disappeared in the 2000s. The strengthening of administrative and water rights management, employing economic measures to promote water conservation, for example to stimulate the improvement of agricultural water efficiency, and the development of new water projects to regulate the streamflow have led to this disappearance (Changming & Shifeng, 2002; Wang et al., 2019b). Nevertheless, the overconsumption of freshwater resources is still an issue that threatens the YRB and should be considered (Zhuo et al., 2016; Zhuo et al., 2019).

Additionally, future predictions of climate change and blue water consumption pose an increasing threat for the YRB. Yin et al. (2017) studied the future blue water scarcity using the 8.5 RCP climate scenario and ten global gridded hydrological models. They showed that the freshwater resources are expected to decrease slightly from 1995 to 2035 and increase from 2036 to 2084. The general trend is a slight decrease. However, they show that blue water consumption is expected to pose a larger threat to blue water scarcity than climate change. The main reason for this larger threat, is the increase in irrigation and industrial water consumption. The current blue water scarcity make the YRB a suitable case study for assessing the effect of alternative allocation principles for BWF cap setting on blue water scarcity.

1.4. Outline report

This report is structured as follows. In chapter 2 the methods and data employed for the simulation and calculations of the results are described. In chapter 3 the results are presented and briefly reviewed. chapter 2 and 3 follow the order of the research question, i.e. both chapters consist of four sections corresponding with the research questions. In chapter 4 the study's methods and its results are discussed. Finally, in chapter 5 the conclusion and recommendations are presented.

2. Methods and data

This chapter elaborates on the methods and data used to achieve the objective and answer the research questions. Firstly, the method for natural runoff simulation is discussed in 2.1. Second, the method to obtain the BWA according to two EFR methods in 2.2. Third, the methods for calculation of the four BWF cap scenarios in 2.3. And fourth, the method for water scarcity calculation in 2.4. Figure 3 shows a summary of what is explained in each paragraph and how the different paragraphs are related.

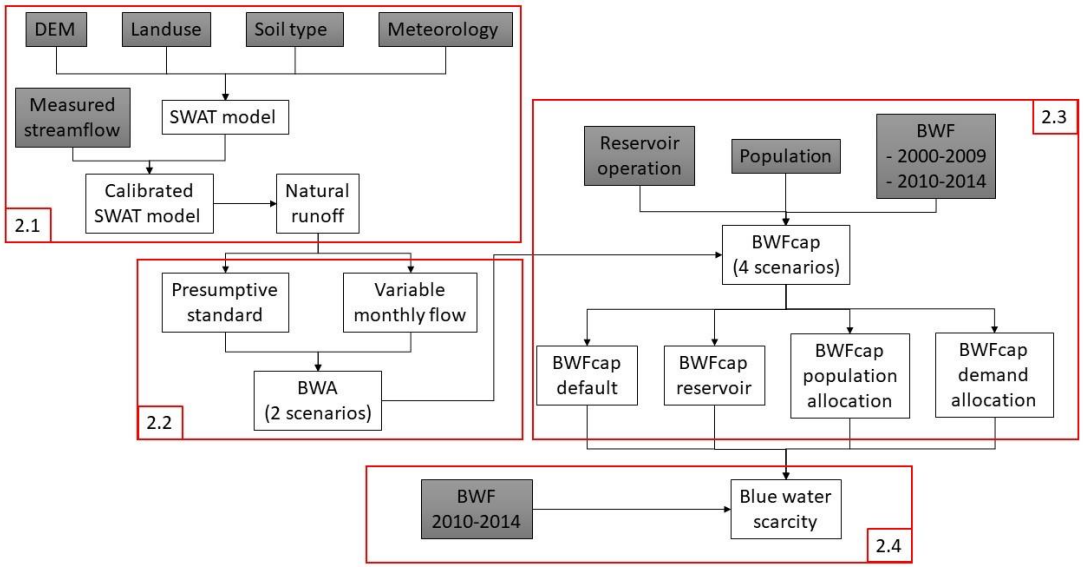

FIGURE 3: SUMMARY OF METHODS. GREY BOXES REPRESENT EXTERNAL DATA SOURCES, WHITE BOXES REPRESENT RESULTS/INPUT FROM/FOR OTHER STEPS, AND THE ARROWS INDICATE THE DEPENDENCIES BETWEEN THE DIFFERENT COMPONENTS. DEM: DIGITAL ELEVATION MODEL, EFR: ENVIRONMENTAL FLOW REQUIREMENT, BWF: BLUE WATER FOOTPRINT, BWFCAP: BLUE WATER FOOTPRINT CAP.

The natural runoff results are input for the calculation of BWA that is determined according to two EFR methods. The BWA is used to determine the BWF cap according to four scenarios. Finally, the BWF caps are evaluated by calculating the blue water scarcity.

2.1. Natural runoff

Studies on water scarcity report two options to determine the natural runoff. Hoekstra et al. (2012) and Mekonnen & Hoekstra (2016) used the actual, measured streamflow and BWF data to reconstruct the natural runoff. The other option often applied is using hydrological models to simulate the natural runoff on a global or local scale (Zang et al., 2012; Zhuo et al., 2016; Zhuo et al., 2019). The natural runoff for this study is determined using a hydrological model called the Soil and Water Assessment Tool, hereafter SWAT (Arnold et al., 1998).

SWAT is used for the simulation of natural runoff in the YRB, because it has already proven to yield satisfactory results in a wide variety of locations around the world both for quantity and quality (Gassman et al., 2007; Faramarzi et al., 2009; Zang et al., 2012). Secondly, it has been applied successfully for the YRB or parts of it (Hao et al., 2004; Zhang et al., 2008; Wang et al., 2019c).

2.1.1. SWAT model

SWAT is a conceptual, semi-distributed and computationally efficient hydrological model (Neitsch et al., 2011). SWAT is a model that divides an entire basin into sub-catchments. Each sub-catchment possesses a

geographic position in the basin, and the sub-catchments are spatially related to each other, i.e. outflow of one sub-catchment is the inflow for another sub-catchment. The delineation of the entire basin is based on a digital elevation model (DEM) and a stream network. The delineation of the sub-catchments is based on the principle that the entire surface area of a sub-catchment drains to the outlet of the specific sub-catchment (Neitsch et al., 2004). Outlets are added, and sub-catchments are formed where tributaries enter the mainstream and at manually assigned locations. Each sub-catchment is further divided into hydrological response units (HRUs). An HRU is used as the minimum hydrological simulation unit to simulate the various parts of the water cycle and thereby to optimize the computational efficiency (Wang et al., 2019c). The HRUs represent a percentage of the sub-catchments area, possessing unique land use, soil, and slope class attributes. Not all combinations are considered, only the HRUs that exceed a certain percentage per characteristic. To assure the entire sub-catchment is part of an HRU, the HRUs are scaled based on their relative size in the sub-catchment. An HRU is not spatially defined in the sub-catchment, i.e. while the individual areas with a specific combination of attributes may be scattered throughout the sub-catchment, the areas are lumped together to form one specific HRU. The natural runoff is simulated separately for these HRUs and then summed together to obtain the total natural runoff for the sub-catchment (Arnold, et al., 2012).

The first step in the operation of the land phase of the hydrological cycle is to determine what part of the precipitation becomes surface runoff, and what part infiltrates into the soil. Once the water enters the soil, it either evaporates through soil or plant transpiration, enters a shallow aquifer or enters the streamflow as lateral flow. Water entering the shallow aquifer can percolate further to a deep aquifer, where it is considered a loss from the system, or it can enter the streamflow as groundwater flow. The surface runoff enters surface water bodies, e.g. river channel or lakes. There are three options for what happens with water in the surface water bodies. The water can enter the shallow aquifer through seepage, evaporate, or in case it is not in a river channel it can become streamflow in a river channel. A flowchart of the hydrological operation is given in Appendix A. A more detailed description of all hydrological processes can be found in Neitsch et al. (2011). The climatic variables required by SWAT to simulate this hydrologic cycle are daily precipitation, maximum and minimum air temperature, solar radiation, wind speed and relative humidity.

In this study, the YRB is divided into multiple sub-catchments, and the BWF caps are monthly calculated. To match the actual timing of BWA at a certain location, the travel time through the different parts of the river channel are considered. The travel time (T_x) through the river channel within sub-catchment x is defined as the time it takes water to travel from the inlet to the outlet of sub-catchment x. The travel time is calculated in hours for every time step of the simulation (Neitsch et al., 2011). The travel time is converted to days for the implementation in this study. Therefore, natural runoff is simulated on a daily scale. The average travel time over all days of the study period, 2010 – 2014 is taken as the travel time for further calculations.

2.1.2. Model setup

In this section, the model setup for the YRB and required data are described. The first step is to delineate the sub-catchments of the YRB. Figure 4 displays the DEM and stream network used for the delineation of sub-catchments. The DEM is available from the National Elevation Dataset by the United States Geological Survey (USGS) at 15-sec grid level. Likewise, the USGS provided the data on the predefined stream network (USGS, 2019).

Additional outlets are required for calibration, validation and including reservoirs in this study. The additional outlets are added manually at the location of hydrological stations used for calibration and validation, and at the location of the reservoirs considered in this study. More detailed descriptions are given in sections 2.1.3. and 2.3.2., respectively.

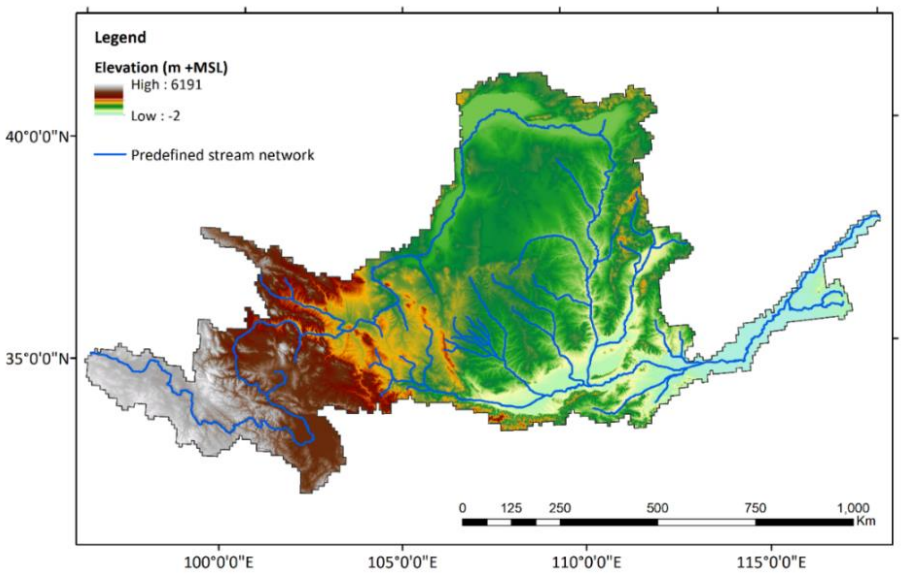

FIGURE 4: DIGITAL ELEVATION MODEL AND THE PREDEFINED STREAM NETWORK OF THE YELLOW RIVER BASIN (USGS, 2019).

The land use data required for HRU formation is provided by the Resource and Environment Data Cloud Platform from 2015 at 1x1 km scale (REDCP, 2015). A map of the land use in the YRB is given in Figure 5. The soil data required is provided by the Harmonized World Soil Database at a scale of 1:1,000,000 (HWSD, 2009). For a map of soil classes in the YRB, see Appendix B.

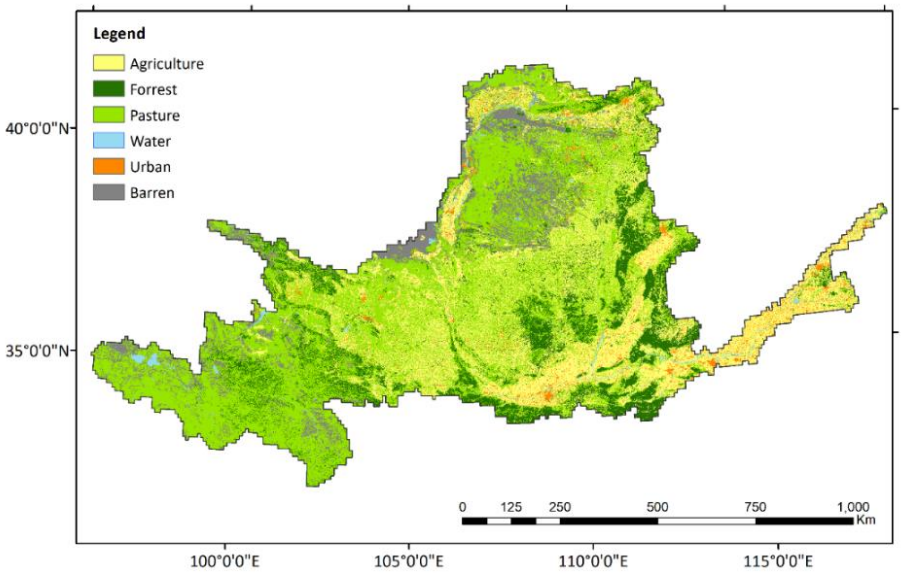

FIGURE 5: LAND USE MAP YELLOW RIVER BASIN 1X1 KM^2 (REDCP, 2015).

These inputs lead to the delineated SWAT model in Figure 6, and the HRUs in Appendix C. The basin is divided into 31 sub-catchments. The mainstream includes 19 sub-catchments and consists of sub-catchment 31 to 18. The remaining 12 sub-catchments are tributary sub-catchments. See Figure 7 for this distribution and for the division of sub-catchments over the three reaches. This schematization is used to

route the available blue water through the sub-catchments using the travel time for the calculation of the BWF caps.

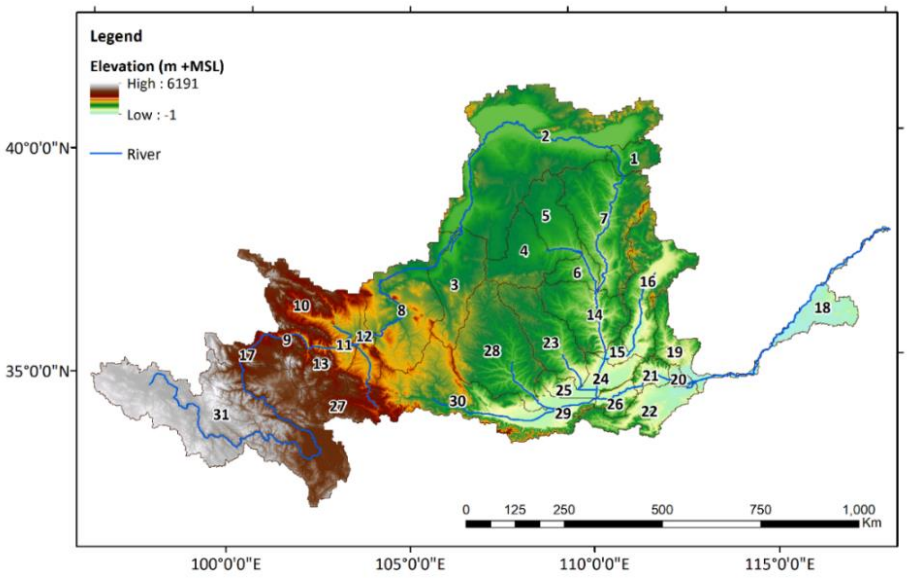

FIGURE 6: THE DELINEATED SUB-CATCHMENTS ACCORDING TO SWAT FOR THE YRB.

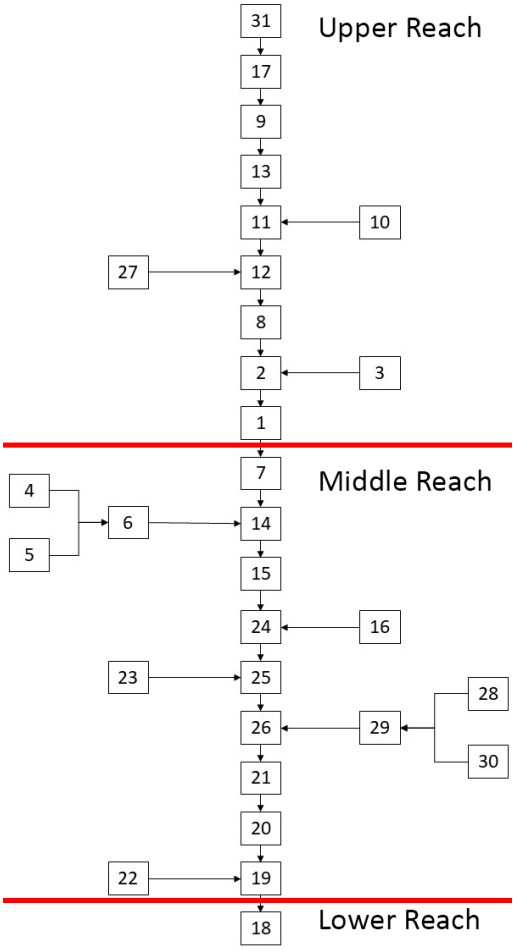

FIGURE 7: SCHEMATIZATION OF SUB-CATCHMENTS.

TABLE 1: TRAVEL TIME SUB-CATCHMENTS.

Mainstream sub-catchment nr	Travel time from previous sub-catchment (day)	Travel time from sub-catchment 31 (day)
31	-	-
17	5	5
9	4	9
13	6	15
11	0	15
12	4	19
8	7	26
2	12	34
1	2	36
7	6	42
14	5	47
15	0	47
24	1	48
25	0	48
26	2	50
21	2	52
20	1	53
19	1	54
18	9	63

The travel time through the river channel in a sub-catchments and the time it takes water to flow through the entire mainstream river channel are given in Table 1. Blue water coming from a tributary sub-catchment enters a certain mainstream sub-catchment. From there on, it follows the travel time corresponding to the mainstream sub-catchment it entered.

The daily meteorological data for climatic variables required to simulate the hydrological cycle are provided by the Chinese National Meteorological Information Center. The data are available for 840 meteorological stations throughout China (CNMIC, 2019). For this study 112 meteorological stations were considered for the YRB. The spatial distribution of these meteorological stations is displayed in Figure 8.

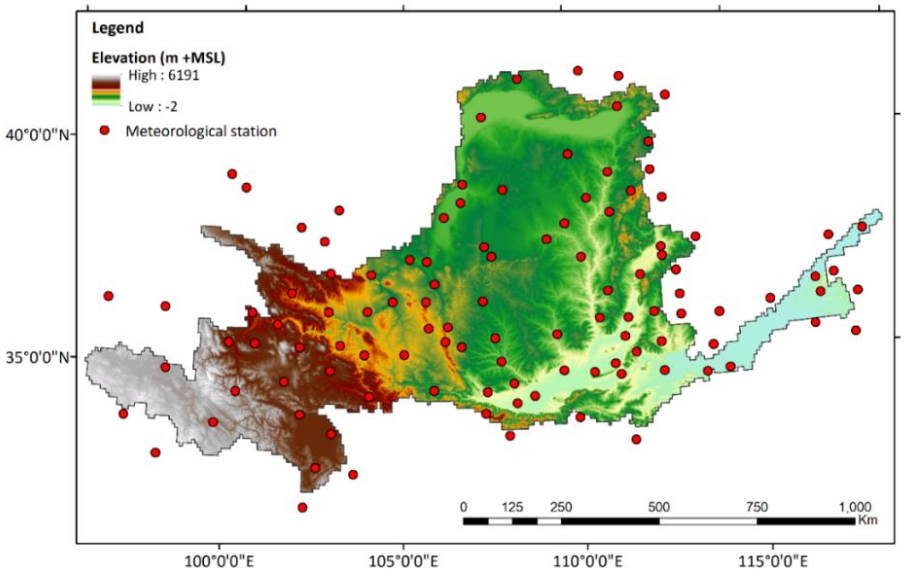

FIGURE 8: SPATIAL DISTRIBUTION OF METEOROLOGICAL STATIONS (CNMIC, 2019).

This study considers the period from 2010 to 2014. However, a warm-up period is included in the simulation of natural runoff to provide realistic initial conditions for the simulation of natural runoff from 2010 to 2014. A period of two years prior to the actual study period is used as suggested by Zang et al. (2012) and Parikh & Parekh (2019). The model is simulated from 2008 to 2014 to include the warm-up period. Accordingly, meteorological data from 2008 to 2014 is used for the simulation of the natural runoff.

2.1.3. Model calibration and validation

The SWAT model needs to be calibrated and validated to obtain reliable results (Gassman et al., 2007). The model used for the simulation of natural runoff has been previously calibrated and validated outside this study using monthly streamflow data (Xie, et al., 2020). Daily natural runoff data are required for this study. Therefore, the model is additionally validated using daily streamflow data to assure the reliability of natural runoff. The model should be validated using observed natural streamflow to assess the daily model performance for natural conditions. However, observed natural streamflow (Q_{nat}) is somewhat problematic to obtain for the YRB. The early presence of human interventions and their influence on streamflow cause a lack of observed natural streamflow data (Gao et al., 2011). A solution to this issue is presented by Zang et al. (2012). In their study of the Heihe River basin in Northwest China they encountered a similar obstacle. To circumvent the issue, they selected upstream hydrological stations where human influence on streamflow was minimal. In addition, the selected upstream area was responsible for a large part of the generated annual natural runoff, thereby a large part of the natural runoff could be calibrated and validated for natural conditions.

This is applicable for the YRB as well. The area upstream of the Tangnaihai or Source Region has experienced minimal human influence, see Figure 9. This area in combination with the area between Tangnaihai and Lanzhou is on average accountable for two-thirds of the total annual generated natural runoff in the YRB (Li et al., 2008; Gu et al., 2019; Zhuo et al., 2019). However, the area between Tangnaihai and Lanzhou has experienced more human influence on the streamflow than upstream of Tangnaihai. This should be kept in mind. The two hydrological stations at Tangnaihai and Lanzhou were used for the initial calibration and validation using monthly observed streamflow by Xie et al. (2020). The additional daily validation is performed using these two hydrological stations as well.

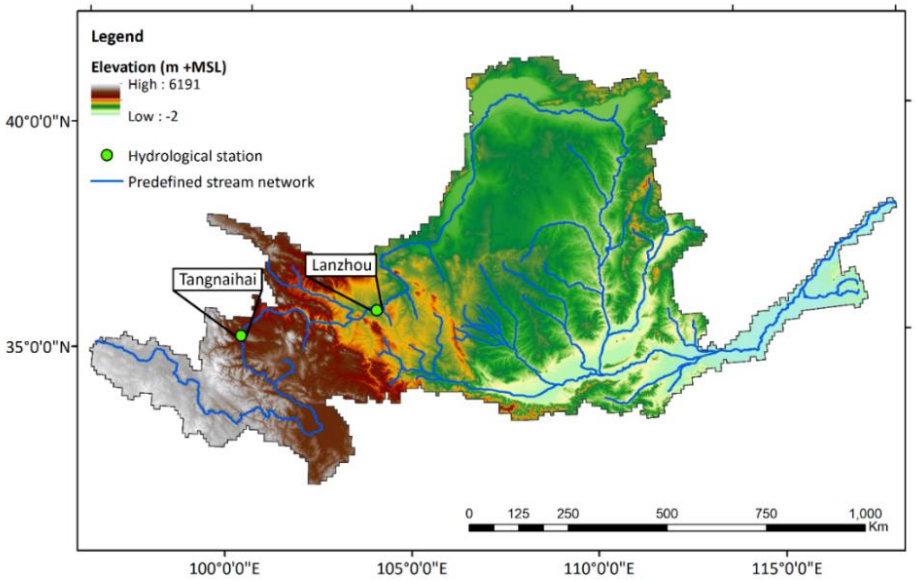

FIGURE 9: HYDROLOGICAL STATIONS FOR MODEL CALIBRATION AND VALIDATION.

As mentioned in section 2.1.2., these two hydrological stations were considered in the setup of the SWAT model by adding the locations as outlets. The locations were added to obtain streamflow data from SWAT at those locations required for the comparison of simulated and observed streamflow data.

The model calibration was performed using SWAT-CUP, a computer program that links different calibration methods to SWAT. More specifically, SUFI-2 was used for the calibration. SUFI-2 is a semi-automated, stochastic, inverse modelling procedure for a combined calibration and uncertainty analysis (Abbaspour, 2015). The manual input for the calibration is the parameter ranges. SUFI-2 uses the ranges to find a value that gives the best calibration results. The parameter ranges are defined by the user and are restricted by the physical limits of the parameter or the user's wishes. For a detailed description of SWAT-CUP and SUFI-2 consult Abbaspour (2015).

Xie et al. (2020) used the Nash-Sutcliffe, E_{ns}, and the coefficient of determination, R^2, for the monthly calibration and validation. Gassman et al. (2007) reviewed over 250 studies reporting on calibration and validation of streamflow and surface runoff simulated by SWAT using these similar evaluation criteria. Therefore, these two evaluation criteria are applied in this study. The Nash-Sutcliffe evaluation criterion is widely used and a reliable criterion for the goodness of fit of the entire hydrograph. E_{ns} quantifies the squared error between observed and simulated streamflow and scales this by the variability around the mean of the observed variability (McCuen et al., 2006). It ranges from $-\infty$ to 1, where 1 represent a perfect fit and 0 or smaller than 0 implies that the mean of the observed data is a better prediction (Gassman et al., 2007). R^2 measures how well the simulated versus the observed regression line approaches an ideal match. It ranges from 0 to 1, where 0 indicates no correlation and a value of 1 represent that the predicted dispersion equals the measured dispersion (Krause et al., 2005).

The acceptable values of E_{ns} and R^2 are based on site-specific in literature reported values. Zhang et al. (2008) in their study of the source region of the YRB report very good monthly results for E_{ns} and R^2 for values above 0.80. Liu et al. (2011) studied the SWAT results in the Upper and the Middle reaches of the Yellow River and reported monthly values of 0.5 for R^2 as satisfactory and >0.70 as good results, similarly for E_{ns}. Xu et al. 2011 used a SWAT model in their study for the YRB and reported acceptable results for calibration and validation with values of 0.64 and 0.66 for E_{ns} and of 0.61 and 0.66 for R^2. However, no daily results are reported for a SWAT model of the YRB. Moriasi et al. (2007) state that there should be a relaxing of acceptable evaluation criterion values from monthly to daily results. That includes the priorly found values for the YRB. Based on the previous, the daily validation of the SWAT model is considered sufficient for E_{ns} > 0.6 and R^2 > 0.6. The calibration and validation in the previous study were performed monthly for the period 2010 – 2014 and 2015 – 2018, respectively and proved to be good and very good for Tangnaihai, and good and sufficient compared to the previously mentioned values for E_{ns} and R^2, see Table 2.

TABLE 2: MONTHLY EVALUATION CRITERIA RESULTS FOR CALIBRATION (2010-2014) AND VALIDATION (2015 – 2018) (XIE, ET AL., 2020).

	E_{ns}	R^2
Calibration		
Tangnaihai	0.81	0.82
Lanzhou	0.69	0.74
Validation		
Tangnaihai	0.71	0.72
Lanzhou	0.66	0.78

The additional daily validation in this study is performed manually for the period 2010 to 2014. The daily streamflow data at Tangnaihai and Lanzhou hydrological station were provided by the Chinese Ministry of Resources (MWR, 2019).

2.2. Blue water availability

The BWA is calculated as the natural runoff minus the EFR (Mekonnen & Hoekstra, 2016). The presumptive standard approach (PRE) and the variable monthly flow method (VMF) are both used as EFR methods to determine the BWA in this study. The presumptive standard approach is applied in many studies to estimate EFRs (Hoekstra et al., 2012; Hoekstra, 2014; Mekonnen & Hoekstra, 2016; Zhuo et al., 2016; Zhuo et al., 2019). However, the presumptive standard approach could be considered precautious because there are other methods available that reserve a smaller percentage of the natural runoff for the environment. Examples are Pastor et al. (2014), Yang et al. (2009b), and Smakhtin et al. (2004). All set the EFR at a lower percentage of natural runoff (Zhuo et al., 2016). For the purpose of comparison, the less precautious variable monthly flow method is included. The methods to determine the EFRs for the calculation of BWA are discussed in this paragraph.

2.2.1. Presumptive standard approach

The presumptive standard approach is presented by Richter et al. (2012) to protect the planet's rivers from exploitation without limits. They describe that the approach aims at maintaining a certain percentage-based range around natural or historic flow variability of the river system. The approach states that for moderate ecological protection, 80% of natural runoff should be reserved for the environment. It then becomes obvious that a maximum of 20% of natural runoff can sustainably be consumed.

2.2.2. Variable monthly flow

The VMF method presented by Pastor et al. (2014) reserves a certain percentage of the natural runoff for the environment. The VMF method follows the natural variability of river streamflow in defining EFRs by distinguishing flow seasons: low, medium, and high. Every month is categorized into one of these flow seasons. The method was developed to protect ecosystems by reserving 60% of the natural runoff during the low flow season, 45% during medium flow season, and 30% during the high flow. The remaining blue water is available for consumption. The reason for the difference in percentages between flow seasons is that the environment is prone to damage and needs additional protection in those months (Pastor et al., 2014). The flow seasons are determined based on mean annual flow (MAF) and mean monthly flow (MMF).

For this method, each month is classified in one of the three flow seasons and EFR of the specific month can be calculated accordingly. The classification of flow seasons and corresponding EFR percentages are displayed in Table 3.

TABLE 3: EFR FRACTION ACCORDING TO VMF.

Flow season	Definition	EFR
Low	MMF $\leq$ 0.4 MAF	0.6 MMF
Medium	0.4 MAF $<$ MMF $\leq$ 0.8 MAF	0.45 MMF
High	MMF $>$ 0.8 MAF	0.3 MMF

The EFRs are estimated daily for the BWA calculations. In contrast to the presumptive standard approach, estimating daily EFR values is less straightforward for the VMF method due to the distinction of flow seasons. The flow seasons for each sub-catchment are determined for every month. The percentage of

natural runoff that is reserved for the environment is calculated for each month by taking the monthly sum of daily natural runoff. The monthly value is compared with the annual, monthly mean according to Table 3. The calculated percentage is assigned to all days of the specific month to obtain daily EFR estimations.

2.3. Blue water footprint caps

In this paragraph, the BWF caps are determined according to four different scenarios as a function of the previously calculated BWA. Each scenario based on an allocation principle. First, the BWF cap is calculated for the sub-catchments under natural circumstances for the YRB, the default BWF cap scenario. The default scenario is included to compare the influence on BWF caps and water scarcity of the other three allocation principles. Second, the BWF cap per sub-catchment is calculated with five major reservoirs present in the mainstream. Third, the BWF cap per sub-catchment is determined based on the relative population size of a sub-catchment. Finally, the BWF cap per sub-catchment is calculated based on the relative demand of a sub-catchment. An overview of the different BWF cap scenarios and the data necessary for each BWF cap calculation is displayed in Table 4. The BWF data from 2010 – 2014 is used in the BWF cap calculations for all scenarios. These BWF data are included in the BWF cap calculations to determine what part of the blue water flow to the next sub-catchment after blue water consumption. The BWF data from 2000 to 2009 are required to determine the past demand of a certain sub-catchment. This past demand is required for computing an allocation factor for each sub-catchment in the demand-based scenario. More on this allocation factor can be found in section 2.3.4.

All BWF caps are calculated daily at the outlet of a sub-catchment. To obtain monthly BWF caps, the daily data are summed for each month after the BWF cap calculations for each scenario is concluded. In addition, each BWF cap calculation scenario is performed twice, once for each EFR methods.

TABLE 4: BWF CAP SCENARIOS (ROWS) AND THE REQUIRED DATA (COLUMNS).

	Natural runoff and EFR	BWF data 2010 – 2014	Reservoir operation	BWF data 2000 – 2009	Population data 2010
Default BWF cap	**x**	**x**			
Reservoir BWF cap	**x**	**x**	**x**		
Population based BWF cap	**x**	**x**	**x**		**x**
Demand-based BWF cap	**x**	**x**	**x**	**x**	

The BWF data on agriculture were taken from Wang et al. (2019a) and is monthly available at a grid level of 5 x 5 arcmin. All grid cells within a sub-catchment are assigned to the sub-catchment. The sum of these grid cells is the sub-catchment's total monthly agricultural BWF. The BWF of households and industry are annually available for an area between two hydrological stations and is provided by the Yellow River Conservancy Commission (YRCC) (YRCC, 2015). The total annual BWF in such an area is divided equally over the 12 months, because there is no clear indication for an alternative distribution. In addition, the total monthly values were divided proportionally to the relative surface area of a sub-catchment with respect to the total surface area. The division of the BWF for household and industry with respect to the hydrological stations is based on the areas draining to the part of the mainstream between two hydrological stations. This leads to the division of the YRB displayed in Figure 10. The total BWF per sub-catchment can now be computed by adding the agricultural BWF and the BWF of household and industry. The BWF data on agriculture, households and industry are provided from 2000 to 2014 to include the BWF in BWF cap setting and past demand for the allocation factor. The monthly BWF from 2010 to 2014 is divided equally over the

days of the month for the daily BWF cap calculations. The population data are provided by the Data Center for Resources and Environmental Sciences, Chinese Academy of Sciences (REDCP) as population/km^2 (REDCP, 2010).

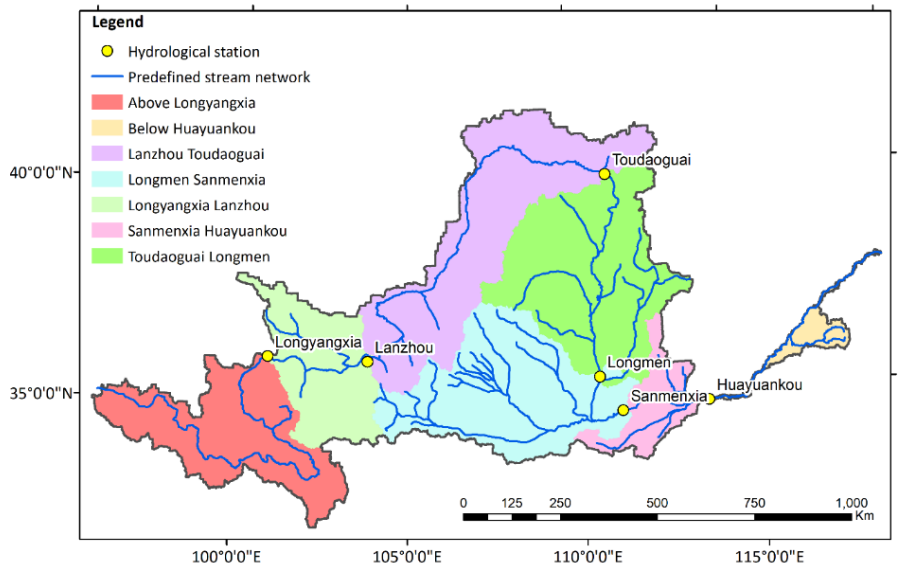

FIGURE 10: BWF HOUSEHOLD AND INDUSTRY DIVISION.

2.3.1. BWF cap default

The default scenario BWF cap is calculated under natural circumstances. Other sub-catchments are not taken into account in BWF cap calculations. This means the allowed blue water consumption in a sub-catchment is equal to the BWA at that moment. Hereafter this is referred to as the use-what-is-there principle. The natural runoff for a time step in the SWAT simulation is the amount of water that enters the river channel during that time step (Arnold, et al., 2011). This means the natural runoff enters the river everywhere along the river channel. Therefore, the travel time of the generated natural runoff in a sub-catchment to its outlet is not equal to the travel time of the entire river channel in a sub-catchment. This is illustrated in Figure 11. The travel time of natural runoff generated closer to the outlet of the sub-catchment is shorter than for natural runoff generated further upstream in the sub-catchment. The average travel time through the river channel in the sub-catchment to its outlet, is used to account for the spatial component of the generated natural runoff. The average travel time for the generated natural runoff is equal to half the travel time for the river channel in the sub-catchment. Hereafter, this is referred to as the internal travel time of a sub-catchment. The travel time from the inlet to the outlet of a sub-catchment is used for external water sources and is referred to as the external travel time.

The BWF cap per sub-catchment depends on the local BWA (BWA_{local}). The local BWA of a sub-catchment is calculated by reserving a part of the natural runoff as EFR (Hoekstra et al., 2011; Hoekstra et al., 2012). The BWA of sub-catchment x at time t is determined using Equation 1. It includes the previously mentioned internal travel time for the generated natural runoff in sub-catchment x ($\frac{1}{2}T_x$). EFR is expressed as a fraction of the natural runoff for sub-catchment x at time t and has a value between 0 and 1.

$$BWA_{local,x,t} = RO_{nat,x,t-\frac{1}{2}T_x} * (1 - EFR_{frac,x,t}) \quad (1)$$

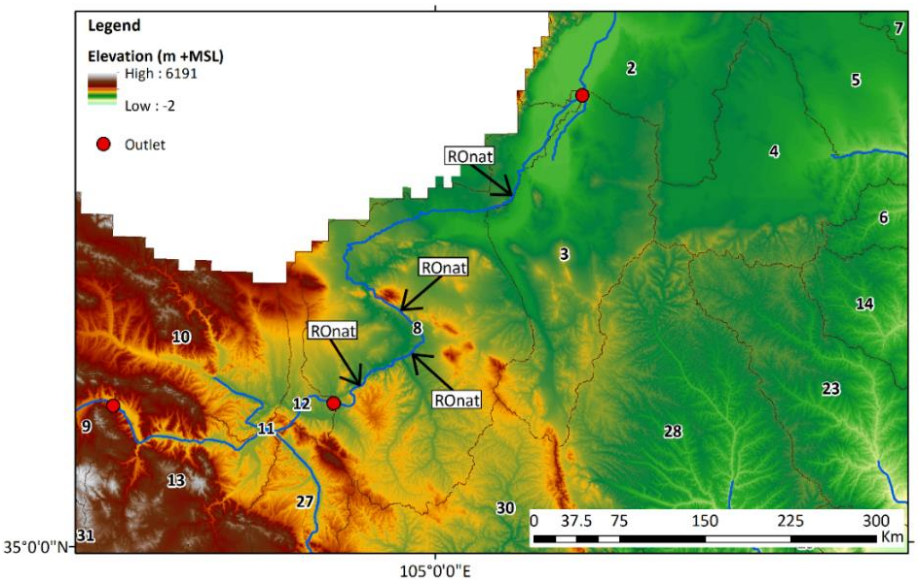

FIGURE 11: LOCAL NATURAL RUNOFF AND INTERNAL TRAVEL TIME. THE GREY LINES REPRESENT SUB-CATCHMENT BOUNDARIES AND THE NUMBERS THE SUB-CATCHMENT'S NUMBER.

Since the basin is divided into multiple sub-catchments, the BWF cap of a sub-catchment is influenced by blue water from other sub-catchments. The blue water that is consumed in an upstream sub-catchment is unavailable for downstream sub-catchments. However, if the local BWA is not completely consumed, the leftover BWA flows to the next sub-catchment. Therefore, the BWF cap of a sub-catchment has two components, the local available blue water and blue water coming from upstream sub-catchments if any is present (Mekonnen & Hoekstra, 2016). The local BWA and the BWA from an upstream sub-catchment (BWA_{up}) determine the BWF cap of sub-catchment x at time t, see Equation 2.

$$BWF_{cap,x,t} = BWA_{local,x,t} + BWA_{up,x,t} \quad (2)$$

$BWA_{up,x,t}$ consists of the upstream sub-catchment's BWF cap, $x-1$, at time t minus the travel time through the river channel in sub-catchment x, $BWF_{cap,x-1,t-T_x}$, and the corresponding actual BWF, $BWF_{x-1,t-T_x}$. These components lead to Equation 3 and determine if any blue water is left after consumption in the upstream sub-catchment. This component cannot be smaller than zero, or else it would imply that downstream blue water compensates for upstream blue water shortage. Sub-catchment x can have multiple BWA_{up} components in case blue water enters the sub-catchment from a mainstream and tributary sub-catchment(s).

$$BWA_{up,x,t} = \max\left(BWF_{cap,x-1,t-T_x} - BWF_{x-1,t-T_x}, 0\right) \quad (3)$$

2.3.2. BWF cap with reservoirs

The BWF cap in this section is calculated with five of the seven largest reservoirs present in the mainstream of the Yellow River. Near the end of 2014, there were 29 large and 174 medium-size reservoirs present in the YRB (YRCC, 2015). The total storage capacity of all reservoirs was around 1.2 times the annual natural runoff, $\pm 72 * 10^9$ m^3 (Ran & Lu, 2011). The reservoirs are included in the study because they have been proven to influence the BWF caps (Zhuo et al., 2019) and to show what the effect is of the alternative allocation principles on water scarcity under realistic conditions. The reservoirs considered are the same reservoirs Zhuo et al. (2019) used in their study to estimate the effect of these reservoirs on the BWF cap for the three reaches of the Yellow River. The reservoirs considered are Longyangxia, Liujiaxia, Wanjiazhai,

Sanmenxia, and Xiaolangdi. The total sum of their storage capacity accounts for 78% of the basin's total reservoir storage capacity (Zhuo et al., 2019). See Table 5 for the characteristics of the considered reservoirs and Figure 12 for their locations.

TABLE 5: THE FIVE MAJOR RESERVOIRS IN THE MAINSTREAM (ZHUO ET AL., 2019).

Reservoir	Longitude	Latitude	Storage capacity (10^9 m^3)	Area (10^6 m^2)	Year of completion
Longyangxia	100°54'57"	36°7'15"	27.6	353	1989
Liujiaxia	111°48'26"	36°7'3"	5.7	113	1974
Wanjiazhai	111°25'42"	39°34'45"	0.9	20	2000
Sanmenxia	111°20'41"	34°49'47"	9.6	120	1961
Xiaolangdi	112°21'37"	34°55'26"	12.7	263	2001

End of month storage data of the reservoirs are provided by the YRCC. The end of month storage changes are used to define whether the reservoir retains or releases water. Daily data are required for the BWF cap calculations. Therefore, the monthly values are converted to daily values. There is no indicator to determine the daily distribution of the amount being retained or released. Therefore, the monthly storage change is divided equally over the days of the specific month. In addition, retention and release are not the sole causes of the change in reservoir storage. The evaporation from and precipitation on the reservoir's surface area are included to estimate the actual reservoir storage change due to retention or release. Evaporation has a negative effect on the storage, whereas the precipitation affects the storage positively. The adjusted storage change is obtained by considering the original storage change and adding evaporation and subtracting precipitation according to Equation 4.

$$\Delta S = \Delta S_{org} + \Delta S_{evap} - \Delta S_{pre} \quad (4)$$

ΔS is the adjusted storage change, ΔS_{org} the original storage change, ΔS_{evap} the storage change as a result of evaporation, and ΔS_{pre} the storage change due to precipitation. The daily values for evaporation and precipitation from and on the surface area of the reservoir, are obtained from the meteorological stations closest to the reservoirs. The location of these meteorological stations is displayed in Figure 12. The evaporation and precipitation volumes are calculated by multiplying the daily data with the surface area of the reservoir. The surface area of a reservoir is a variable component and depends on the stored volume in the reservoir. The surface area of the reservoir is simplified for the purpose of implication in the calculations. The surface area is set at the principal spillway surface area. This is the surface area when the stored volume is equal to the regular volume required for water supply, power generation, and possibly recreation (Neitsch et al., 2011).

The adjusted storage change is implemented in the daily BWF cap calculations using the use-what-is-there-principle. The locations of reservoirs were manually added to the SWAT model as outlets, i.e. reservoirs at the end of the sub-catchments. This characterization of the reservoirs in the model causes two solutions to occur depending on retention or release. Retention is a positive storage change and affects the BWF cap of the sub-catchment itself because a part of BWA is reserved for retention. It indirectly affects the BWF cap downstream of the reservoir by reducing the available water flowing downstream. The release is a negative storage change and affects the BWF cap in the sub-catchment directly downstream of the reservoir due to release of additional available blue water. The sub-catchments further downstream might indirectly benefit from the additional released water.

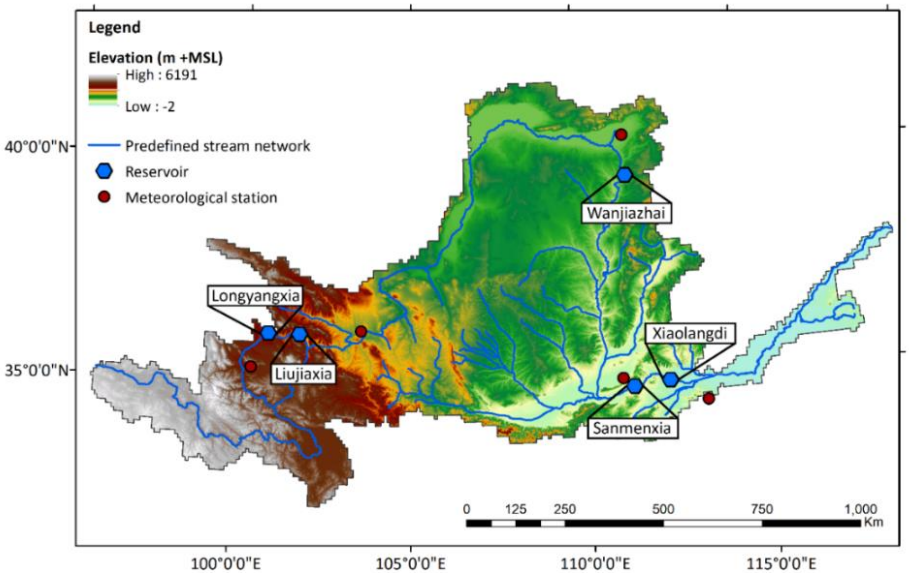

FIGURE 12: LOCATIONS OF RESERVOIRS AND METEOROLOGICAL STATIONS FOR PRECIPITATION AND EVAPORATION.

Two equations are used for the BWF cap calculation for the sub-catchment containing the reservoir, $BWF_{cap,x}$, and two for the sub-catchment downstream of the reservoir, $BWF_{cap.x+1}$. Equation 5 and 6 are used in case of water retention in the reservoir, whereas Equation 7 and 8 are used in case of water release from the reservoir.

$If\ \Delta S_{x,t} \geq 0$

$$BWF_{cap,x,t} = \max\left(BWA_{local,x,t} + BWA_{up,x,t} - \Delta S_{x,t}, 0\right) \quad (5)$$

$$BWF_{cap,x+1,t} = BWA_{local,x+1,t} + BWA_{up,x,t} \quad (6)$$

$If\ \Delta S_{x,t} < 0$

$$BWF_{cap,x,t} = BWA_{local,x,t} + BWA_{up,x,t} \quad (7)$$

$$BWF_{cap,x+1,t} = BWA_{local,x+1,t} + BWA_{up,x,t} - \Delta S_{x,t-T_{x+1}} \quad (8)$$

The travel time through the river channel in the sub-catchment downstream of the reservoir is only included in Equation 8. In that situation, the sub-catchment downstream of the reservoir benefits from the additionally released blue water. This blue water travels like BWA_{up}, through the river channel in sub-catchment x before it reaches its outlet. Therefore, travel time is included. Retention of blue water does not include travel time, because it occurs at the outlet of the reservoir's sub-catchment. The BWF cap can never be smaller than zero, hence the max-function in Equation 5 to set the minimum after retention at zero.

2.3.3. BWF cap population-based

The previous BWF cap scenarios favored upstream sub-catchments by applying the use-what-is-there principle. However, as indicated by Figure 13, the population density is larger further downstream in the basin. Therefore, a population-based allocation scenario is introduced to divide the blue water resources more equally over the population. The total population per sub-catchment is determined by multiplying the average population density by the surface area of the sub-catchment.

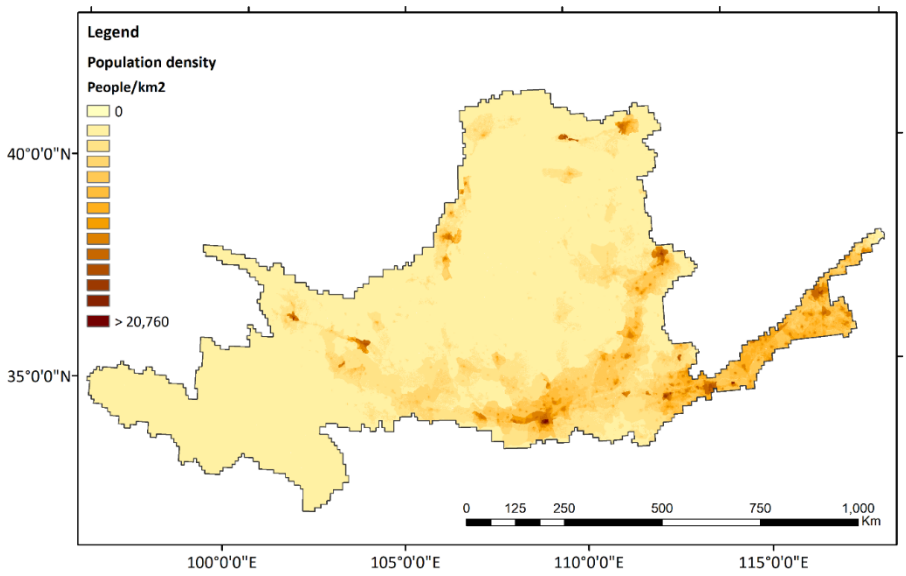

FIGURE 13: POPULATION DENSITY YRB 2010 (REDCP, 2010).

The allocation for the population-based BWF cap scenario is based on the work of Van der Zaag et al. (2002). They propose an allocation principle that aims at dividing annual blue water resources equally over the serial configurated riparian countries of the basin and their population. The interdependency between countries is expressed as the responsibility of a country to supply blue water to countries downstream. The share of blue water a country is entitled to is calculated according to Equation 9. The share is calculated by taking all blue water that is sustainably available from country x to the most downstream country n. That includes the generated blue water in that area and the blue water available from an upstream country. The right to the amount of blue water is then calculated by multiplying the available blue water in the system by the relative population of country x. The relative population is calculated by dividing the population of country x by the entire population that depends on the blue water, so the sum of the population from country x to n. This is referred to as the population allocation factor.

$$Share_x = \left(BWA_{up,x} + \sum_{x}^{n} BWA_{local,x}\right) * \frac{p_x}{\sum_{i=x}^{n} p_i} \quad (9)$$

In this study, an adjusted version of this method is applied. First, the scale of the calculation is translated to daily instead of annually. Second, reservoirs are added to the system and the equation. Third, the configuration of the sub-catchment is not merely serial, but a combination of serial and parallel. And fourth, the share a sub-catchment is entitled to is translated to a BWF cap.

The first adjustment is a transition from an annual to a daily scale. To determine the amount a sub-catchment is entitled to, the amount of water that is going to be available in the system is calculated. This means that the downstream BWA (BWA_{down}), from sub-catchment x to n, is integrated as a future value. The local BWA in a downstream sub-catchment i is calculated at the same moment the water from sub-catchment x would arrive at the outlet of sub-catchment i. This future value is determined by using the travel time through each sub-catchment between x and i. The downstream local available blue water in sub-catchment i for sub-catchment x is available at $t + T_{i,x}$, time t plus travel time from x to i.

The second adjustment is the inclusion of reservoirs. This inclusion of reservoirs has a two-sided effect on the calculation of the BWF cap. On the one hand, it influences BWA_{up} by retention or release in an

upstream reservoir. On the other hand, it influences the downstream BWA by retention or release in a downstream reservoir. The influence on BWA_{up} is straightforward, either a decrease or an increase due to retention or release. However, downstream availability is more complex. The downstream availability is not merely the sum of the local BWA of all downstream sub-catchments and storage change of the reservoirs. Local BWA cannot be considered for retention in an upstream reservoir, i.e. water only flows downstream and does not affect upstream retention. The method in this study assumes that local BWA in a sub-catchment affects the retention of the first downstream reservoir. This suggests that the downstream BWA should be determined by looking at different sections of the mainstream individually. The sections are illustrated in Figure 14.

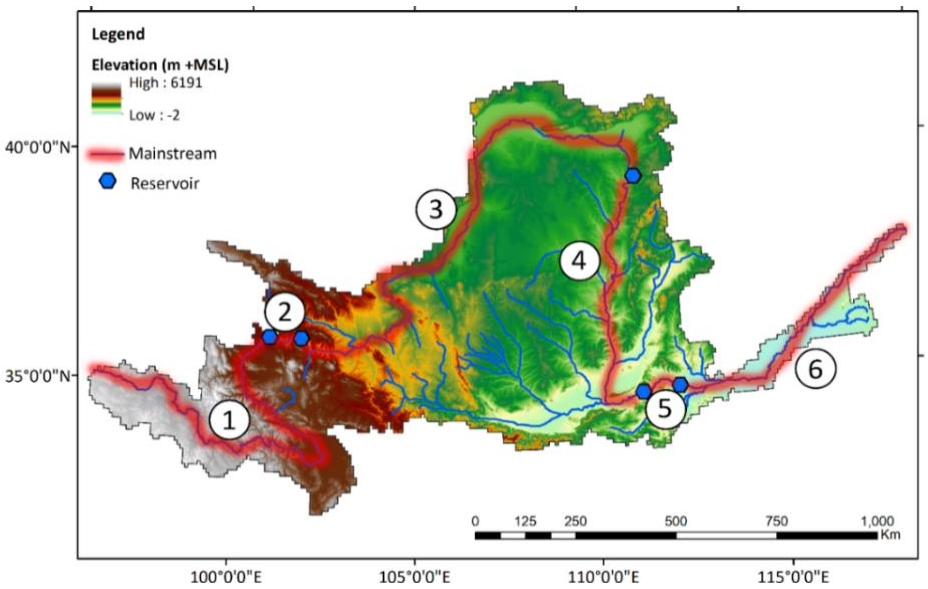

FIGURE 14: RESERVOIRS AND SIX SECTIONS FOR DOWNSTREAM BWA.

The mainstream is divided into six sections based on the locations of the five reservoirs. The BWA of every section is calculated to determine BWA_{down} of sub-catchment x. This is the sum of the BWA in all six sections. The first step in calculating the BWA of a section is to determine the location of a certain section with respect to sub-catchment x. There are three possibilities: the section is upstream of x, x is within the section is, or the section is downstream of x. These options are given in Figure 15 and denoted by 1 to 3.

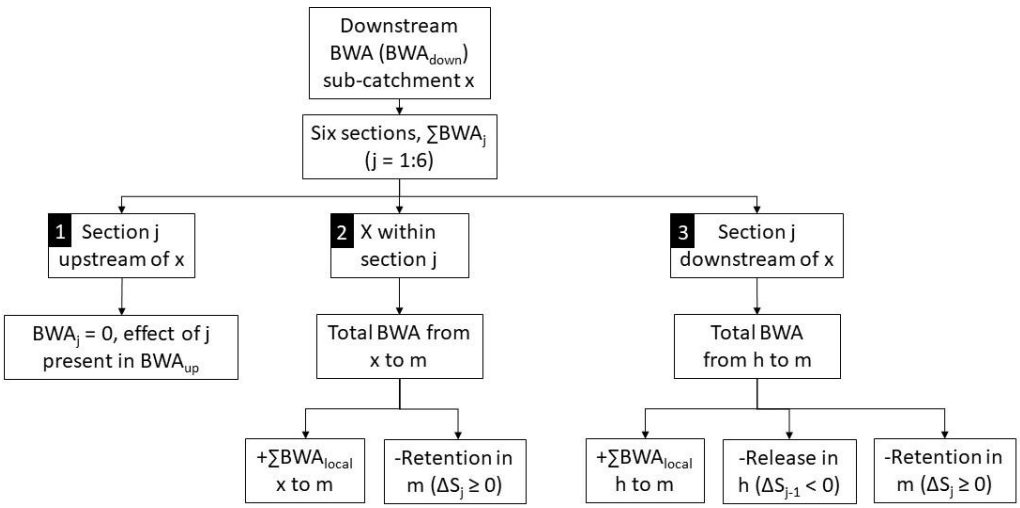

FIGURE 15: SCHEMATIZATION OF DOWNSTREAM BWA CALCULATION PER SECTION. THREE OPTIONS FOR THE BWA IN A SECTION DEPENDING ON THE LOCATION OF SUB-CATCHMENT X WITH RESPECT TO SECTION J.

A visualization of the locations of the sub-catchments indicated by the letters x, m and h in Figure 15 is given in Figure 16. The section considered for the calculation of its BWA is referred to as section j. In case the entire section is upstream of x it is not considered in BWA_{down}. The generated blue water and effect of consumption are present in the BWA_{up} component of the BWF cap calculation. The second option is that x is located within j. For BWA_{down} the local BWA from sub-catchment x to m is summed, where m is the most downstream sub-catchment of section j and contains a reservoir (ΔS_j). The most downstream section, section 6, is the exception because there is no reservoir. The amount of BWA in this section available for consumption depends on the retention of the reservoir in sub-catchment m. If this reservoir releases water instead of retaining it, it is not considered since the release affects the BWA in the next section. In case the entire section j is downstream of x the third option applies. For this option, the sum of the local BWA from the first sub-catchment of the section, h, to m is taken. The amount of water available for consumption in section j depends on the retention in reservoir at m, but is influenced by the reservoir in section $j-1$ (ΔS_{j-1}) as well. However, the reservoir in $j-1$ solely affects the BWA in j if it releases water. Retention of the reservoir influences the BWA in the section upstream of $j-1$. This is not applicable to the most downstream section, section 1, because there is no reservoir upstream of this section.

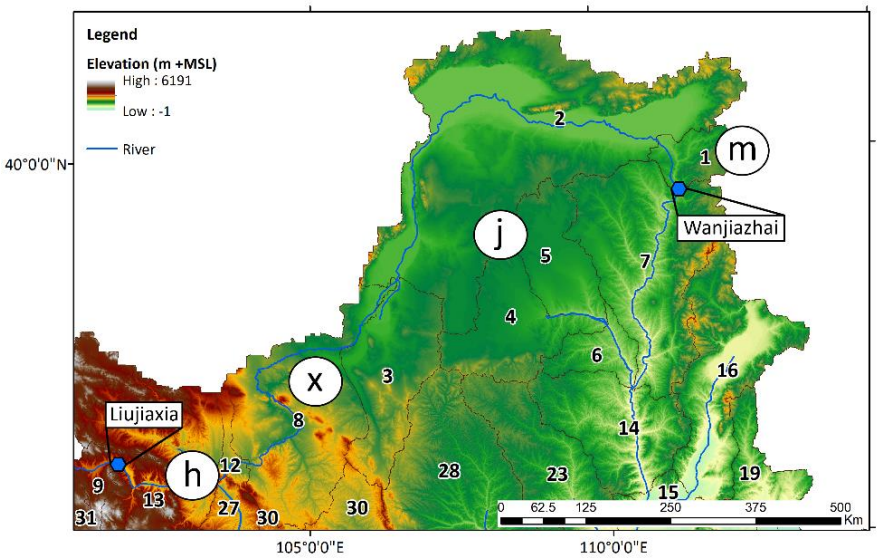

FIGURE 16: LOCATION SUB-CATCHMENTS H,X AND M FOR SECTION J BETWEEN LIUJIAXIA AND WANJIAZHAI RESERVOIRS, WHERE X IS LOCATED IN J, OPTION 2. X CAN BE DOWNSTREAM OF M OR UPSTREAM OF H FOR OPTION 1 AND 3, RESPECTIVELY.

The three options for BWA in section j are translated to equations for the implementation in the population-based BWF cap calculation. For the first option, the downstream BWA is 0 because the section is not downstream of x. The second option is translated to Equation 10.

$$BWA_{down,x,t,j} = \max\left(\sum_{i=x}^{m} BWA_{local,i,t+T_{i,x}} - max\left(\Delta S_{j,t+T_{m,x}}, 0\right), 0\right) \quad (10)$$

The summation of local BWA starts at x and ends at m. Since the downstream BWA in a sub-catchment is implemented as a future value the travel time is added to time t. $T_{i,x}$ represents the travel time from a sub-catchment downstream, i in the summation, to sub-catchment x. The second component in the equation is the retention of section j's reservoir in sub-catchment m and includes the travel time from this sub-catchment to x $T_{m,x}$. A negative storage change means a release and is excluded by the max-function. The overall max- function is added to assure a positive value for BWA. The third option is translated to Equation 11.

$$BWA_{down,x,t,j} = \max\left(\begin{matrix}\sum_{i=h}^{m} BWA_{local,i,t+T_{i,x}} - \\ max\left(\Delta S_{j,t+T_{i,x}}, 0\right) - min\left(\Delta S_{j-1,t+T_{h,x}}, 0\right), 0\end{matrix}\right) \quad (11)$$

The additional component in this equation compared to the previous, is the influence of possible release from the reservoir in section $j-1$ entering section j at sub-catchment h. This reservoir is included with a min-function to assure only negative storage change is considered. The travel time for the additional released water is implemented as the travel time from h to x.

The third adjustment is changing the configuration from serial to serial and parallel. The parallel parts of the configuration are the tributary sub-catchments. For the serial and parallel configuration see the schematization in 2.1.2. The tributary sub-catchments are considered as the most upstream sub-catchment of their river system. This river system consists of the tributary sub-catchment, the first sub-catchments in the mainstream and all mainstream sub-catchments further downstream. The tributary sub-catchments contribute to the blue water availability in the mainstream. The amount of blue water coming from a tributary sub-catchment is part of the BWA_{down} of sub-catchment x. An example is illustrated in Figure 17.

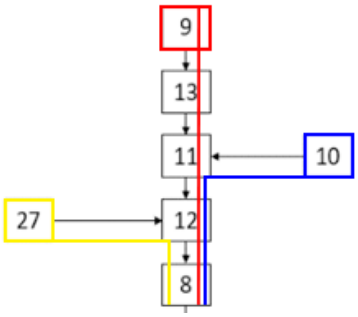

FIGURE 17: SCHEMATIZATION OF DOWNSTREAM BWA FOR MAINSTREAM AND TRIBUTARY SUB-CATCHMENTS.

The three colors indicate the sub-catchments that are included in the BWA_{down} calculations for the corresponding sub-catchment. The BWA_{down} of sub-catchment 9 depends on the blue water from sub-catchments 10 and 27 and the mainstream sub-catchments. Therefore, the BWF cap of all tributary sub-catchments is calculated firstly. The BWF cap of tributary sub-catchment 10 depends on the water entering the mainstream from sub-catchment 27. This shows that the BWF cap of sub-catchment 27 must be calculated before the BWF cap of sub-catchment 10 can be calculated. This indicates that the BWF cap for the most downstream tributary sub-catchment is calculated firstly, then the second most downstream tributary sub-catchment and so on till the most upstream one. The amount of blue water entering the mainstream from these tributary sub-catchments depends on their local BWA, calculated BWF cap and actual BWF. The BWF cap in the population-based scenario considers other sub-catchments in BWF cap setting and is not necessarily equal to the BWA. The BWA from a tributary sub-catchment that enters and adds to the BWA in sub-catchment x, is calculated by subtracting the minimum of the BWF cap and actual BWF from the BWA according to Equation 12. The BWA entering x depends on the BWA in the tributary at time $t-T_x$ and the minimum of the BWF cap and actual BWF at the corresponding moment. The min-function indicates that calculated cap is the maximum amount that is consumed in the tributary sub-catchment.

$$BWA_{tributary,x,t} = BWA_{tributary,t-T_x} - \min\left(BWF_{cap,tributary,t-T_x}, BWF_{tributary,t-T_x}\right) \quad (12)$$

After the BWF caps for tributary sub-catchments and the BWA entering the mainstream are determined, the BWF caps for the mainstream sub-catchments are from upstream to downstream.

Equation 10 and 11 are adjusted for the inclusion of tributary sub-catchments in the BWA_{down} of x for section j. BWA from tributary sub-catchments if any is present, is included as the amount entering sub-catchment i. Equation 13 shows the calculation of BWA_{down} for when x is within section j.

$$BWA_{down,x,t,j} = \max\left(\sum_{i=x}^{m}(BWA_{local,i,t+T_{i,x}} + BWA_{tributary,i,t+T_{i,x}}) - max\left(\Delta S_{j,t+T_{i,x}}, 0\right), 0\right) \quad (13)$$

Equation 14 displays the calculation of BWA_{down} for when section j is downstream of x.

$$BWA_{down,x,t,j} = \max\left(\begin{matrix}\sum_{i=h}^{m}(BWA_{local,i,t+T_{i,x}} + BWA_{tributary,i,t+T_{i,x}}) - \\ max\left(\Delta S_{j,t+T_{i,x}}, 0\right) - min\left(\Delta S_{j-1,t+T_{h,x}}, 0\right), 0\end{matrix}\right) \quad (14)$$

The total downstream available blue water is given in Equation 15. With j as the section, having a value from 1 to 6 and being one of the three options for the calculation of BWA_{down}.

$$BWA_{down,x,t} = \sum_{j=1}^{6} BWA_{down,x,t,j} \quad (15)$$

The BWF cap according to this allocation principle is not equal to the BWA in a sub-catchment, because other sub-catchments are taken into account for the BWF cap setting. Therefore, the upstream blue water entering sub-catchment x depends on the BWA and the minimum of the calculated BWF cap and actual BWF in $x-1$, see Equation 16.

$$BWA_{up,x,t} = BWA_{x-1,t-T_x} - \min\left(BWF_{cap,x-1,t-T_x}, BWF_{x-1,t-T_x}\right) \quad (16)$$

The final adjustment is converting the right a sub-catchment is entitled to, to an actual BWF cap. This adjustment is to test the rightful amount of a sub-catchment with the actual BWA in sub-catchment x at time t, $BWA_{x,t}$. This ensures that no more blue water is allocated to the BWF cap than present in the sub-catchment. Resulting in Equation 17 for the population-based BWF cap.

$$BWF_{cap,x,t} = \min\left(\left(BWA_{up,x,t} + BWA_{down,tot,x,t}\right) * \frac{p_x}{\sum_{i=x}^{n} p_i}, BWA_{x,t}\right) \quad (17)$$

The sum of the calculated BWA_{up} and BWA_{down} is multiplied with a population-based allocation factor. This factor is the same as proposed by Van der Zaag et al. (2002) in Equation 9.

2.3.4. BWF cap demand-based

The demand-based BWF cap scenario is based on a similar allocation principle as the population-based scenario. The main difference is the allocation factor applied for calculating the BWF cap. The assumption for this scenario is that the BWF is not necessarily highest for sub-catchments with the largest population. This assumption is illustrated in Figure 18 and the land use map in Figure 5. Figure 18 shows that the BWF of agriculture is in general larger than the BWF of household and industry. Blue water consumption of household and industry primarily occurs in more populated areas. Figure 5 indicates that agriculture does not always occur in more populated areas. By allocating the blue water resources over the population, a mismatch between BWF cap distribution and actual BWF might follow.

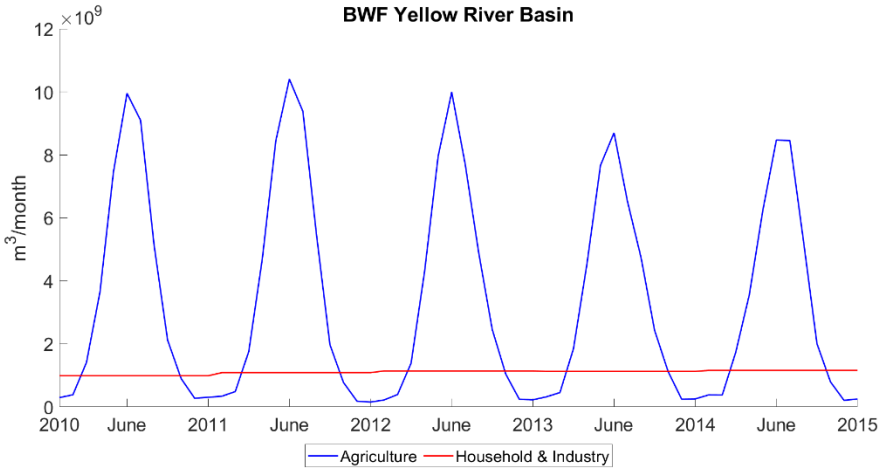

FIGURE 18: BWF DIVISION AGRICULTURE AND HOUSEHOLD & INDUSTRY YRB (WANG ET AL. 2019A; YRCC, 2015).

The demand-based allocation factor is determined using a multi-year monthly average of past BWF for each sub-catchment. The BWF data used for this monthly multi-year average is from a 10-year period from 2000 to 2009. The calculation of the monthly BWF cap is explained in 2.3. The monthly multi-year averages are used to determine a monthly demand factor per sub-catchment. Equation 18 shows the calculation of the BWF cap according to the demand-based scenario.

$$BWF_{cap,x,t} = \min\left(\left(BWA_{down,x,t} + BWA_{up,x,t}\right) * \frac{BWF_{2000-2009,x,m}}{\sum_{i=x}^{n} BWF_{2000-2009,i,m}}, BWA_{x,t}\right) \quad (18)$$

Where $BWF_{2000-2009,m}$ is the average BWF in month m over the period 2000 – 2009. This is divided by the summation of average BWF from 2000 to 2009 of all sub-catchments x is responsible for, from sub-catchment x to most downstream sub-catchment n. All other components are similar to the components in Equation 17.

2.4. Blue water scarcity

The monthly blue water scarcity is computed for four scenarios and for two EFR methods per sub-catchment to evaluate the effect of applying alternative allocation principles and EFR methods. The general calculation for blue water scarcity is given by Mekonnen & Hoekstra (2016) and is defined as the monthly BWF divided by the monthly BWA. The blue water scarcity in this study is calculated according to Equation 19, where BWA is replaced by the BWF cap. The blue water scarcity is determined from 2010 to 2014.

$$WS_{x,t} = \frac{BWF_{x,t}}{BWF_{cap,x,t}} \quad (19)$$

The blue water scarcity classification is given in Table 6. No or low water scarcity occurs if water scarcity is equal or smaller than 1, indicating blue water consumption does not exceed the BWF cap. Moderate water scarcity occurs for a value between 1 and 1.5, significant between 1.5 and 2. If the blue water consumption is equal to or larger than twice the BWF cap, severe water scarcity occurs.

TABLE 6: BLUE WATER SCARCITY CLASSIFICATION (MEKONNEN & HOEKSTRA, 2016).

WS category	WS
Low	≤ 1.0
Moderate	1.0 – 1.5
Significant	1.5 – 2.0
Severe	≥ 2.0

The effect of the BWF cap scenarios on the blue water scarcity is visualized by maps with seasonal average water scarcity per sub-catchment. The seasonal average is computed by taking the monthly average blue water scarcity for the period 2010 – 2014. These monthly values are averaged over the months of a season.

3. Results

Results are presented in sequential order similar to the research questions. Natural runoff in paragraph 3.1., BWA in 3.2, BWF caps according to the four scenarios in 3.3. and evaluation of the BWF caps in 3.4.

3.1. Natural runoff

In this paragraph, natural runoff results are displayed. Section 3.1.1. shows the results of the additional daily validation and section 3.1.2. the actual natural runoff results for the sub-catchments from 2010-2014.

3.1.1. Additional daily validation

The SWAT model proved to be calibrated and validated sufficiently. However, an additional validation is performed to check its daily accuracy. The additional validation is performed for 2010 – 2014 using daily streamflow data.

TABLE 7: ADDITIONAL DAILY STREAMFLOW VALIDATION RESULTS (2010-2014).

	E_{ns}	R^2
Tangnaihai	0.66	0.68
Lanzhou	0.24	0.46

Table 7 shows the daily validation results. See 2.1.3. for the criteria for unsatisfactory, satisfactory, and good values of E_{ns} and R^2. The results for Tangnaihai indicate satisfactory simulated daily streamflow and insufficient for Lanzhou. The reason for the unsatisfactory results at Lanzhou can be explained by the human influence of reservoirs and BWF on the observed streamflow. Appendix D shows the simulated and observed daily streamflow at Tangnaihai and Lanzhou in combination with reservoir operation and BWF. These human influences are larger at Lanzhou. Reservoir retention and BWF cause the observed streamflow to decrease, whereas reservoir release causes an increase. This leads to a situation where the observed time series do not represent the natural streamflow.

The reservoir storage change and BWF are added to the observed streamflow to circumvent the issue of human influence in the area between Tangnaihai and Lanzhou on the additional validation. These adjustments to the observed streamflow generate new adjusted observed streamflow time series. The resulting adjusted streamflow is given in Figure 19. The adjusted streamflow time series are used to validate the SWAT model a second time. Now both the observed and simulated time series present the streamflow under natural conditions since human influences are eliminated from the data.

TABLE 8: ADJUSTED DAILY STREAMFLOW VALIDATION RESULTS (2010-2014).

	E_{ns}	R^2
Tangnaihai	0.66	0.68
Lanzhou	0.60	0.66

Table 8 displays the E_{ns} and R^2 results for Tangnaihai and Lanzhou using the adjusted observed streamflow. The results indicate that the simulated daily streamflow is validated satisfactorily. The values at Tangnaihai for the adjusted daily streamflow are similar because the human influence is minimal. Lanzhou shows a clear improvement. This corresponds with the larger human influence on the daily streamflow at Lanzhou. There is more to the graphs of observation and simulation than these two evaluation criteria as both E_{ns} and R^2 have their drawbacks. E_{ns} prioritizes the model performance during peak flows and deprioritizes it during low flows. For R^2 only the dispersion is quantified for the model

performance. The two evaluation criteria are not sensitive to systematic over- or underestimation (Krause et al., 2005).

The timing of the peaks for the daily simulated streamflow correspond with the observed streamflow at Tangnaihai and Lanzhou, as shown in Figure 19. In general, the timing of the peaks in the simulated and observed streamflow agree, but the simulated peaks are smaller. This indicates that there is less water available in the wet season than in the actual situation. The streamflow values during the regression part of the hydrograph show a different pattern. This part of the simulated hydrograph has a structural delay compared to the observed hydrograph. The issue is visible at both locations, but more strongly present at Tangnaihai. This causes a structural overestimation of streamflow in the low flow season. This means that more water is available during the dry season compared to the actual situation

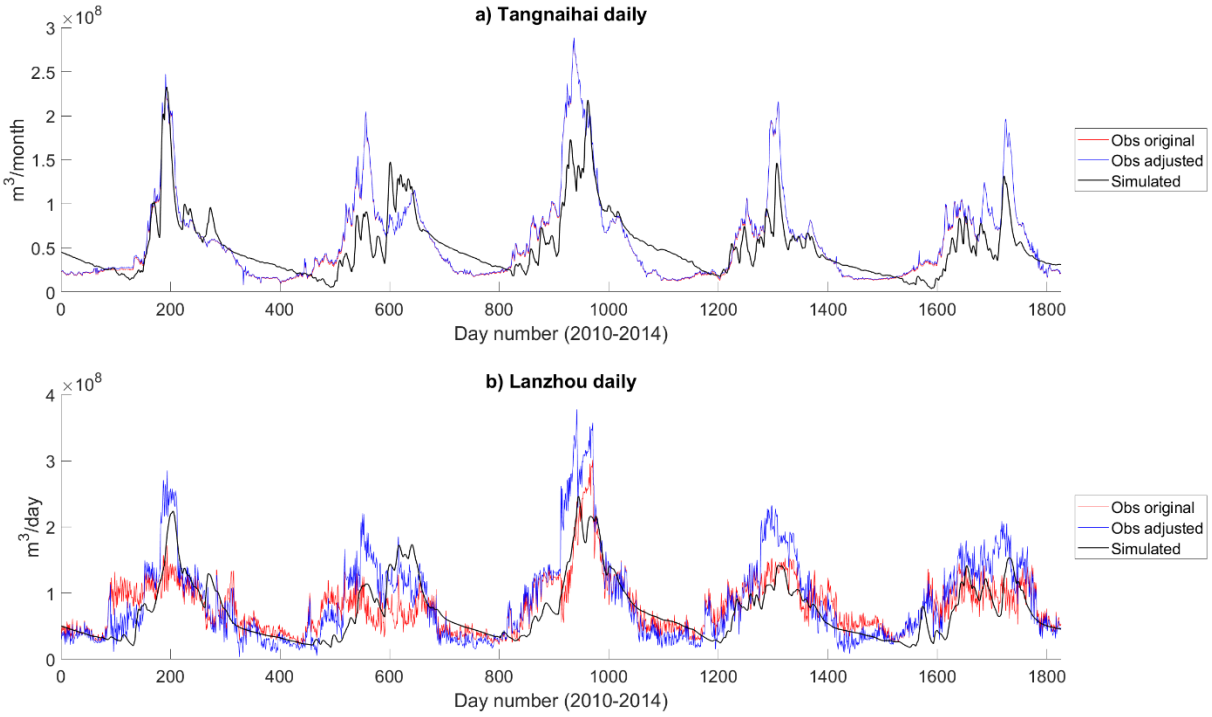

FIGURE 19: A) MONTHLY AND B) DAILY OBSERVED (OBS ORIGINAL), ADJUSTED OBSERVED (OBS ADJUSTED), AND SIMULATED STREAMFLOW AT LANZHOU.

3.1.2. Natural runoff per sub-catchment

The natural runoff for the entire basin and per reach is displayed in Figure 20. The natural runoff is displayed per reach instead of for every sub-catchment for the purpose of overview. The reaches are the same as mentioned in paragraph 1.3. The graphs indicate that the absolute natural runoff contributions are largest in the Upper and the Middle Reaches. The monthly average absolute contribution of the natural runoff and its spatial distribution over the basin are displayed in Appendix E. The results in Appendix E show that the area upstream of Lanzhou is important for the natural runoff generation in the YRB, especially the most upstream sub-catchment 31. However, this is not true for all months. From June to September, the sub-catchments in the other reaches become more important. During those months, the precipitation is largest for all reaches and natural runoff depends more on precipitation than during other months. After September, the importance of the area upstream of Lanzhou increases again. The graphs in Figure 20 confirm these findings.

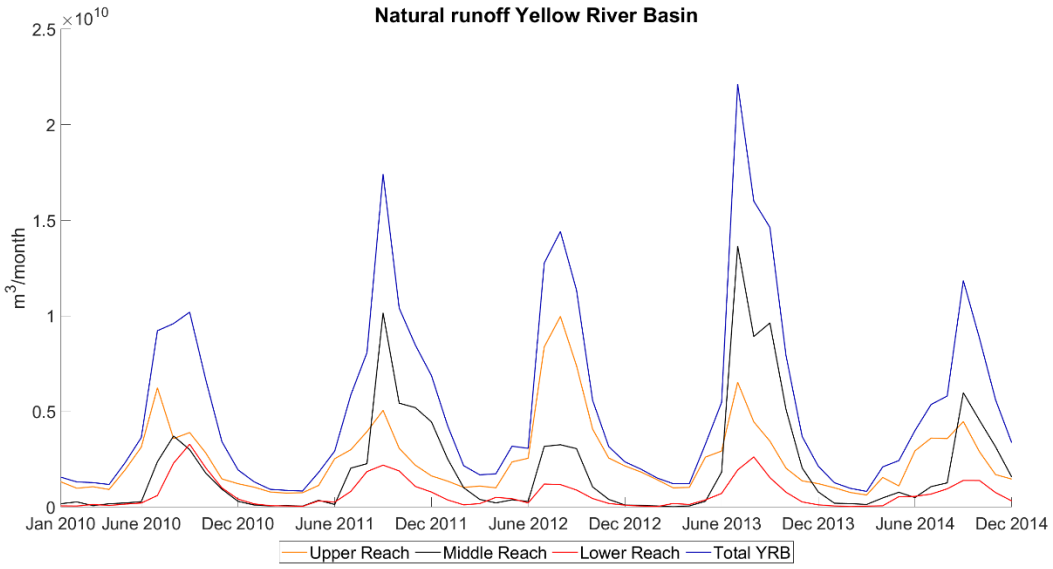

FIGURE 20: NATURAL RUNOFF PER REACH AND FOR THE ENTIRE BASIN.

The Upper and the Middle Reaches are considerably larger than the Lower Reach. In order to say something more meaningful about the natural runoff in the reaches, the areal average monthly precipitation and natural runoff are displayed in Figure 21. The natural runoff generation is expected to be the largest in the Source Region, the area upstream of Lanzhou. This component was added to the graphs to compare the natural runoff in the other areas. The graph for the Upper Reach still includes the Source Region. This implies that the other part of the Upper Reach does not have a large contribution to the natural runoff.

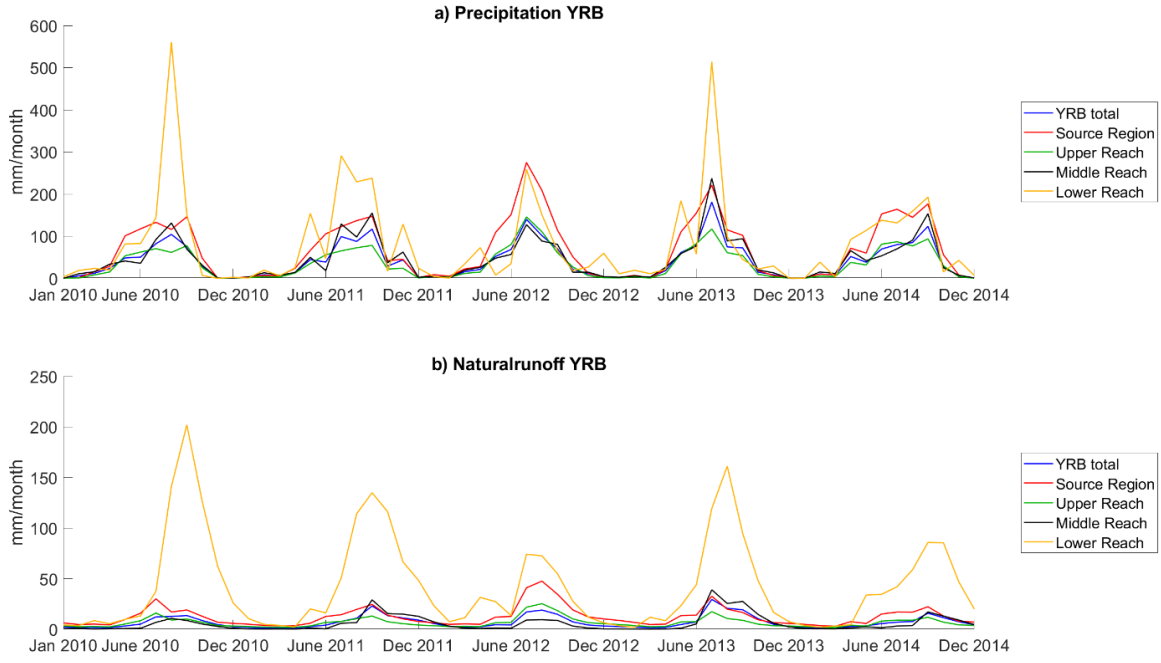

FIGURE 21: A) PRECIPITATION AND B) NATURAL RUNOFF PER REACH OF THE YRB AS AREAL AVERAGE BASED ON THE SURFACE AREA, WHERE SOURCE REGION IS THE AREA UPSTREAM OF LANZHOU IN MM/MONTH.

The precipitation graphs confirm that the year is divided into a wet and dry period. The natural runoff follows that division. In general, the precipitation peaks in the Lower Reach are relatively largest. The peaks in the natural runoff for the Lower Reach are relatively even larger. That indicates that a larger part of

precipitation becomes natural runoff in the Lower Reach than in the other reaches because the relative difference is larger. This is a curious result. This result is supported by the average monthly natural runoff in mm maps in Appendix F. The maps show that the values of Lower Reach, represented by sub-catchment 18, are among the largest if not the largest for every month even during the dry months. During the dry months of the year, the precipitation approaches zero for all areas. The natural runoff in the Upper Reach but mainly in the Source Region during those months appears to be more important than during the rest of the year. This corresponds with the findings from the absolute contributions. The reason for the increased relative importance of the Source Region during the dry months is the significant snowmelt process in the area (Zhang et al., 2008). The relative importance of snowmelt in the Source Region increases during the months there is little precipitation in the basin. This is why the areal average and absolute natural runoff of the Upper Reach and Source Region never approach zero during dry months.

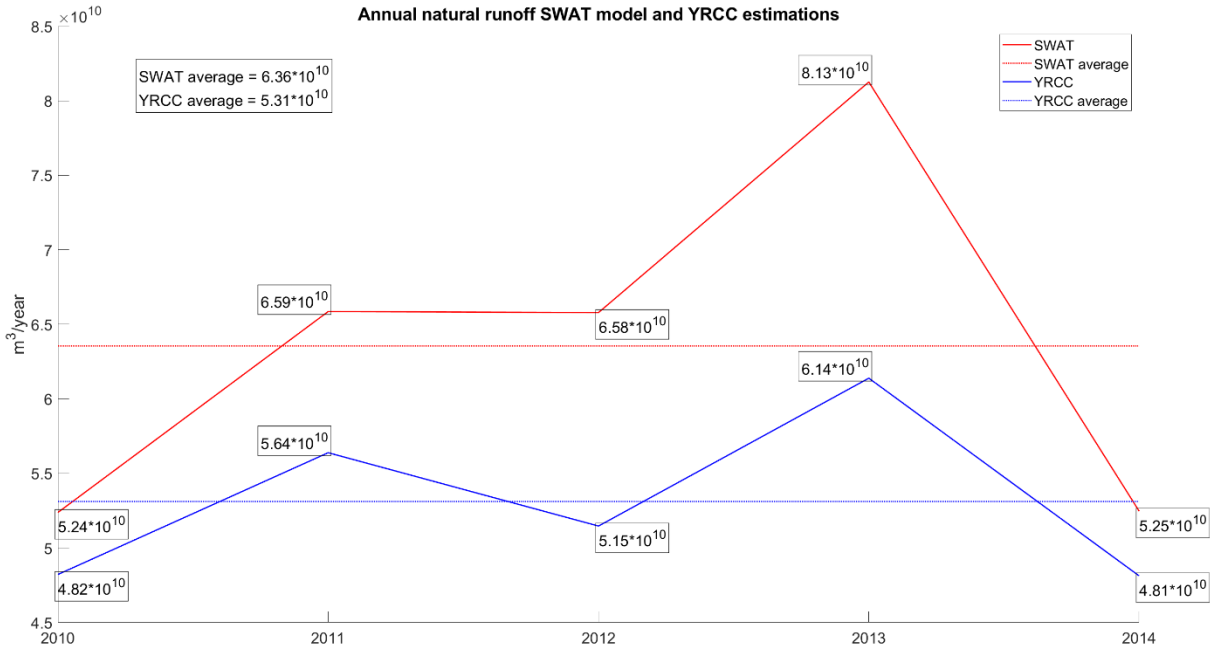

FIGURE 22: ESTIMATED ANNUAL NATURAL RUNOFF YRB ACCORDING TO SWAT AND THE YRCC (YRCC, 2015).

Figure 22 shows the comparison of the annual natural runoff from SWAT with the estimations by the YRCC from 2010 to 2014.The YRCC estimations are systematically smaller than the natural runoff computed by the SWAT model for the same period. However, the graphs exhibit a similar pattern over the years. The YRCC estimates the natural runoff by assuming the actual streamflow (Q_{act}) and adjust it for total surface water withdrawal (W_{total}) and reservoir storage change (ΔS), see Equation 20 (Li et al., 2001). Here the surface water withdrawal is the amount of water that is withdrawn from surface water in the YRB and is not completely equal to the BWF of the basin. The difference between methods could cause the systematical difference between the two methods.

$$RO_{nat} = Q_{act} + W_{total} + \Delta S \tag{20}$$

3.2. Blue water availability

The blue water availability result for the two EFR methods are displayed in Figure 23. The PRE method is more precautious and reserves 80% of the natural runoff for the environment. The VMF method reserves 60, 45, or 30% of the natural runoff for the environment depending on the flow season, either low, medium, or high flow. July to September comprises the high flow season, December to April the low flow season, and May, June, and October the medium flow season. The smaller percentage of natural runoff reserved for the environment in the VMF method results in a larger BWA than for the PRE method. This becomes clear during the high flow season, where the VMF line is relatively larger than during the other months of the year. This can be explained by the fact that the EFR percentage for the VMF method is relatively smaller than the 80% for the PRE method during the high flow season. This is in line with the assumption of this method based on the distinction of flow seasons.

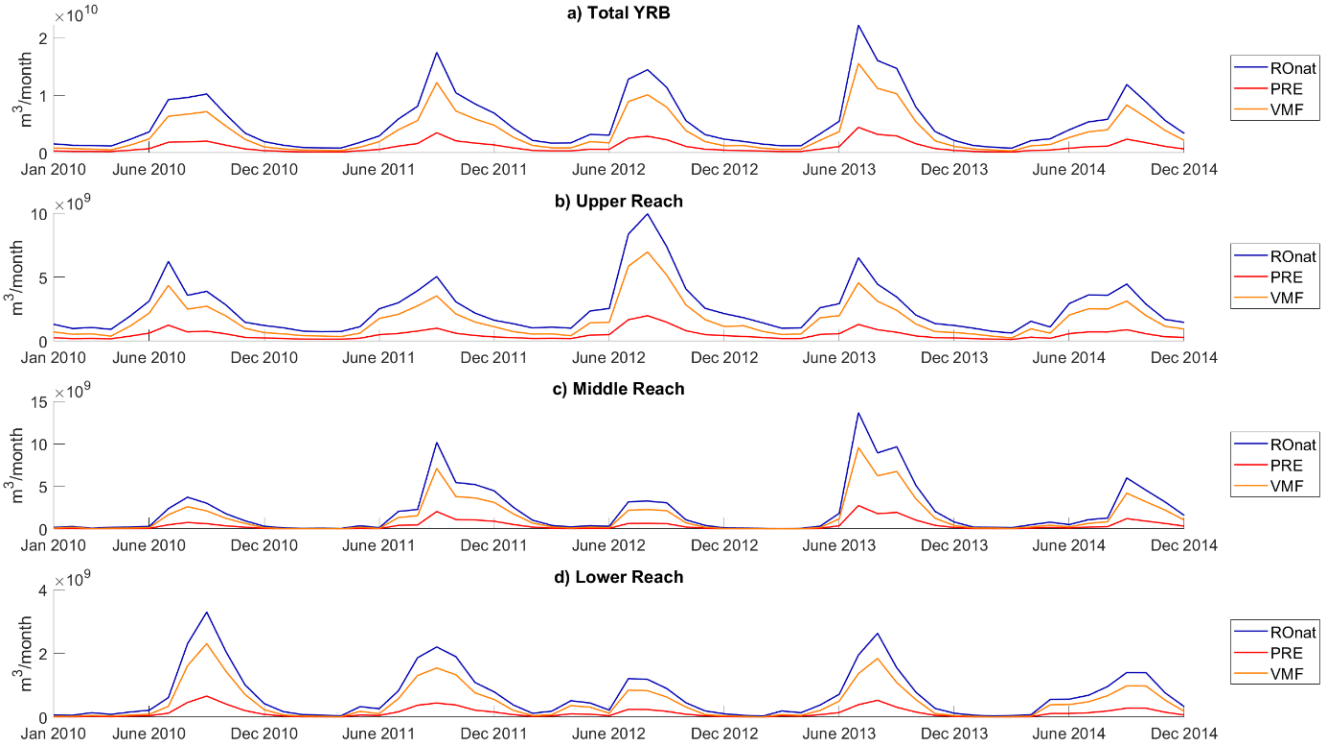

FIGURE 23: BLUE WATER AVAILABILITY AS A PART OF THE NATURAL RUNOFF, RONAT, ACCORDING TO THE PRESUMPTIVE STANDARD APPROACH (PRE) AND THE VARIABLE MONTHLY FLOW METHOD (VMF) FOR THE A) ENTIRE BASIN B) UPPER REACH C) MIDDLE REACH D) LOWER REACH.

3.3. Blue water footprint caps

The blue water footprint cap results for the four scenarios and both EFR methods are displayed in this paragraph. First, the default scenario in 3.3.1. Second the reservoir scenario in 3.3.2. Third the population-based scenario in 3.3.3. And fourth the demand-based scenario in 3.3.4.

Showing the results for 31 sub-catchments causes a lack of overview. Therefore, five representative sub-catchments are chosen to show the results for the BWF caps, indicated by the black boxes in Figure 24. Sub-catchment 31 is the most upstream sub-catchment with a large generation of blue water and a small population and demand and is located in the Upper Reach. Sub-catchment 17 has a small population and demand and is located in the Upper Reach and is included to show the effect of reservoir retention. Sub-catchment 2 has a relatively small population and a large demand, and experiences upstream reservoir operation. This sub-catchment is expected to show the difference in population- and demand-based BWF cap scenario and is located in at the end of the Upper Reach. Sub-catchment 23 represents the tributary sub-catchments and is located in the Middle Reach. Finally, sub-catchment 18 is the most downstream sub-catchment with a large population and demand and experiences upstream reservoir operation. This sub-catchment is expected to show the effect of the population- and demand-based scenarios. Sub-catchment 18 comprises the entire Lower Reach. Sub-catchment 18 is expected to benefit from the allocation principles that take other sub-catchments into account in BWF cap setting.

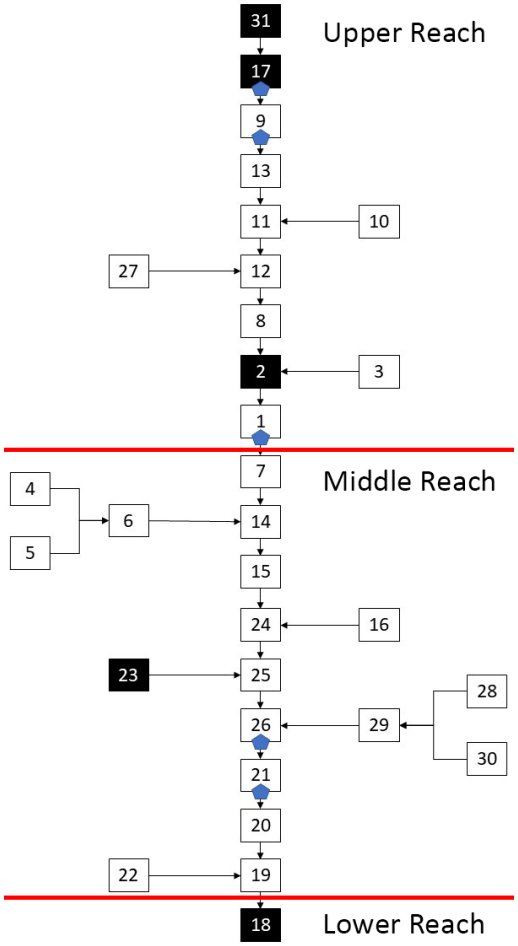

FIGURE 24: SCHEMATIZATION SUB-CATCHMENTS. BLACK BOXES REPRESENT THE FIVE REPRESENTATIVE SUB-CATCHMENTS. BLUE PENTAGONS ARE RESERVOIRS.

3.3.1. BWF cap default

Figure 25 shows the BWF cap decreases downstream and approaches zero in the dry months. This illustrates that this scenario favors upstream sub-catchments because there is less influence of blue water consumption on the BWF cap. The BWF caps follow the natural temporal and spatial variability of the BWA in combination with upstream blue water consumption. This results in a BWF cap that is close to the BWA without consumption for sub-catchments 31 and 17, because there is little consumption in that area. Further downstream, the BWF cap reduces during dry months due to intensive blue water consumption and a smaller BWA. In sub-catchment 18 this leads to a BWF cap that approaches or becomes zero. Tributary sub-catchment 23 depends completely on its local BWA. Therefore, the BWF caps have a comparable pattern to sub-catchment 31, because both sub-catchments have no sub-catchments upstream. The difference between the two EFR methods is obvious. Upstream they display a similar pattern, but downstream their patterns differ mainly during dry months. This is caused by the indirect effect the EFR methods have on the BWF cap. In addition to the direct effect on local BWA, they indirectly affect the BWF cap by the amount of water that flows from a sub-catchment to the next. Thereby they influence the available blue water in the system. The default BWF cap for every sub-catchment individually is given in Appendix G.

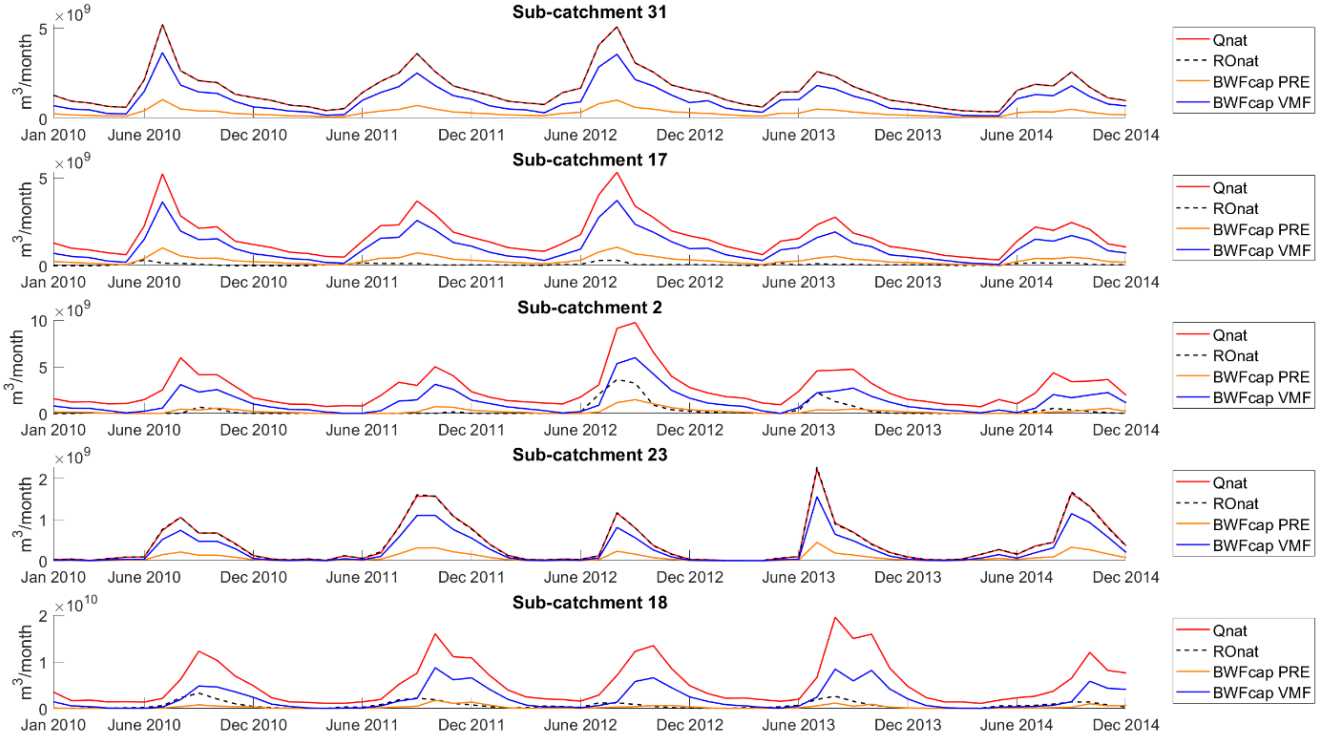

FIGURE 25: DEFAULT SCENARIO BWF CAPS FOR FIVE REPRESENTATIVE SUB-CATCHMENTS AND TWO EFR METHODS. Q_{nat} REPRESENTS THE STREAMFLOW UNDER NATURAL CONDITIONS AND RO_{nat} REPRESENTS THE AMOUNT OF GENERATED BLUE WATER THAT ADDS TO THE STREAMFLOW UNDER NATURAL CONDITIONS. SUB-CATCHMENT 31 IN UPPER REACH, 17 IN UPPER REACH AND CONTAINS A RESERVOIR, 2 IN END OF UPPER REACH, 23 TRIBUTARY IN MIDDLE REACH, AND 18 COMPRISES THE ENTIRE LOWER REACH.

3.3.2. BWF cap with reservoirs

The graphs in Figure 26 indicate that the highs and lows in the BWF caps are flattened in the reservoir scenario. Sub-catchment 31 and tributary sub-catchment 23 do not experience any influence from reservoirs. Reservoir retention can be distinguished in the BWF caps of sub-catchment 17. The months where the BWF caps do not follow the pattern of the natural streamflow are months when water is being retained. This mainly occurs during high flow months and is expressed as a drop in BWF cap. On some occasions, the BWF cap becomes zero indicating that the volume of retention is equal to or larger than the BWA. Hereby, the reservoirs can lead to water scarcity during wet months since there is little or no blue water available for consumption. The water scarcity in wet months corresponds with the findings by Zhuo et al. (2019). Reservoir retention affects downstream BWF caps as well. In comparison with the default BWF cap scenario, the BWF cap during wet months is smaller for sub-catchments located downstream of reservoirs, 2 and 18. The effect of reservoir release is present in the BWF caps of sub-catchment 2 and 18 during dry months. In sub-catchment 2 this results in the BWF caps to approach the natural streamflow during those months. A similar pattern applies to sub-catchment 18. The BWF caps are larger in the dry months than for the default scenario but do not approach the natural streamflow. The BWF caps in do still approach zero during the dry months due to the unlimited upstream consumption. The reservoir scenario BWF cap for every sub-catchment individually is given in Appendix H.

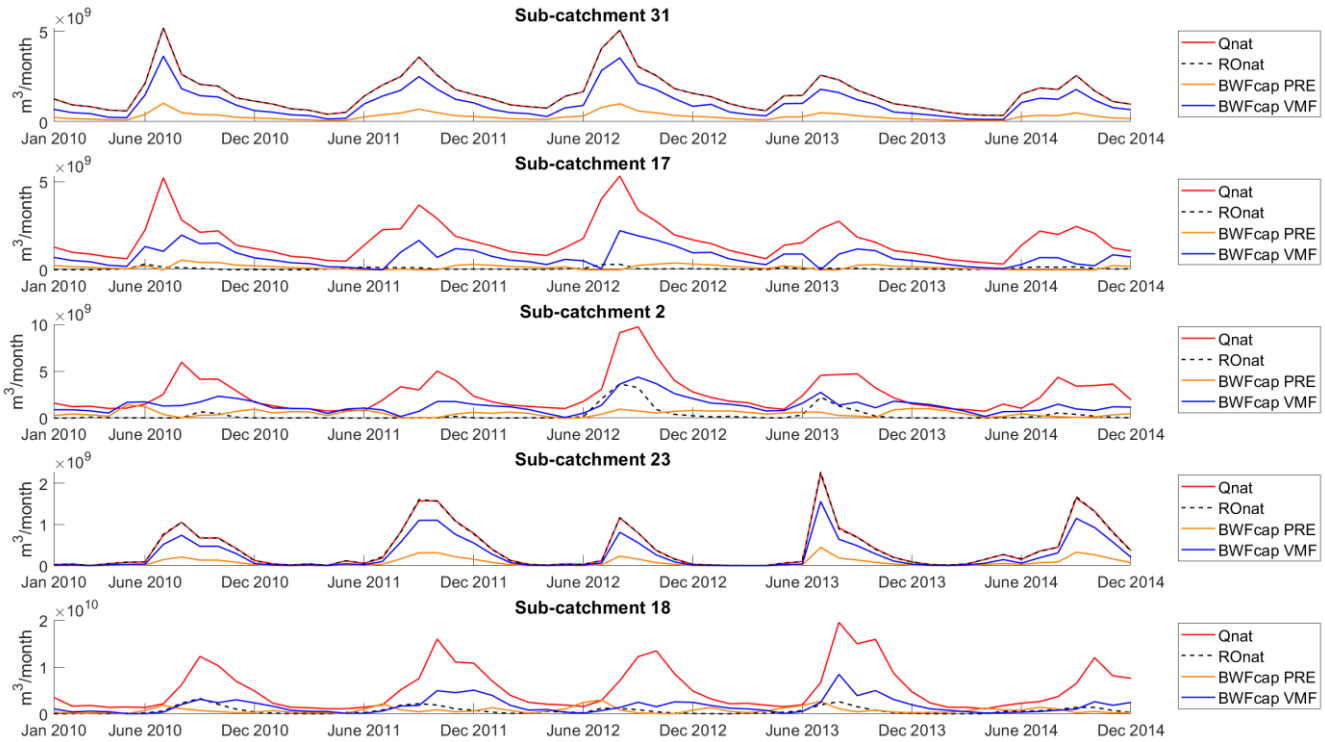

FIGURE 26: RESERVOIR SCENARIO BWF CAPS FOR FIVE REPRESENTATIVE SUB-CATCHMENTS AND TWO EFR METHODS. Q_{nat} REPRESENTS THE STREAMFLOW UNDER NATURAL CONDITIONS AND RO_{nat} REPRESENTS THE AMOUNT OF GENERATED BLUE WATER THAT ADDS TO THE STREAMFLOW UNDER NATURAL CONDITIONS. SUB-CATCHMENT 31 IN UPPER REACH, 17 IN UPPER REACH AND CONTAINS A RESERVOIR, 2 IN END OF UPPER REACH, 23 TRIBUTARY IN MIDDLE REACH, AND 18 COMPRISES THE ENTIRE LOWER REACH.

3.3.3. BWF cap population-based

The application of an allocation principle that takes other sub-catchments into account for BWF cap setting based on population leads the graphs in Figure 27. The effect of the allocation principle on upstream sub-catchments can be seen in the BWF caps of sub-catchment 31 and 17. The BWF caps decreases to such an extent that they are hardly visible compared to the natural streamflow. The decrease of the upstream BWF cap leads to a larger downstream BWF cap. This is mainly visible for the BWF caps of sub-catchment 18 during the low flow months. During these months, the BWF caps approach and even exceed the level of natural streamflow. The peaks in BWF caps during high flow months remain at the same level. The BWF caps in sub-catchment 2 decreases because, sub-catchments in the Middle and the Lower Reach are considered in BWF cap setting. This indicates that a large part of upstream blue water is reserved for this sub-catchment and that the population in this sub-catchment is relatively large. This corresponds with the population map in 2.3.3. Tributary sub-catchment 23 shows a decrease of the BWF caps as a result of the population-based allocation principle. These sub-catchments are the most upstream sub-catchment of the river system. Therefore, the allocation algorithm considers downstream sub-catchments in the BWF cap setting, causing the BWF cap to decrease compared to the previous scenarios. The BWF caps hardly changes during the wet months of the year because of the relatively large BWA and relatively small BWF. The population-based scenario BWF cap for every sub-catchment individually, is given in Appendix I.

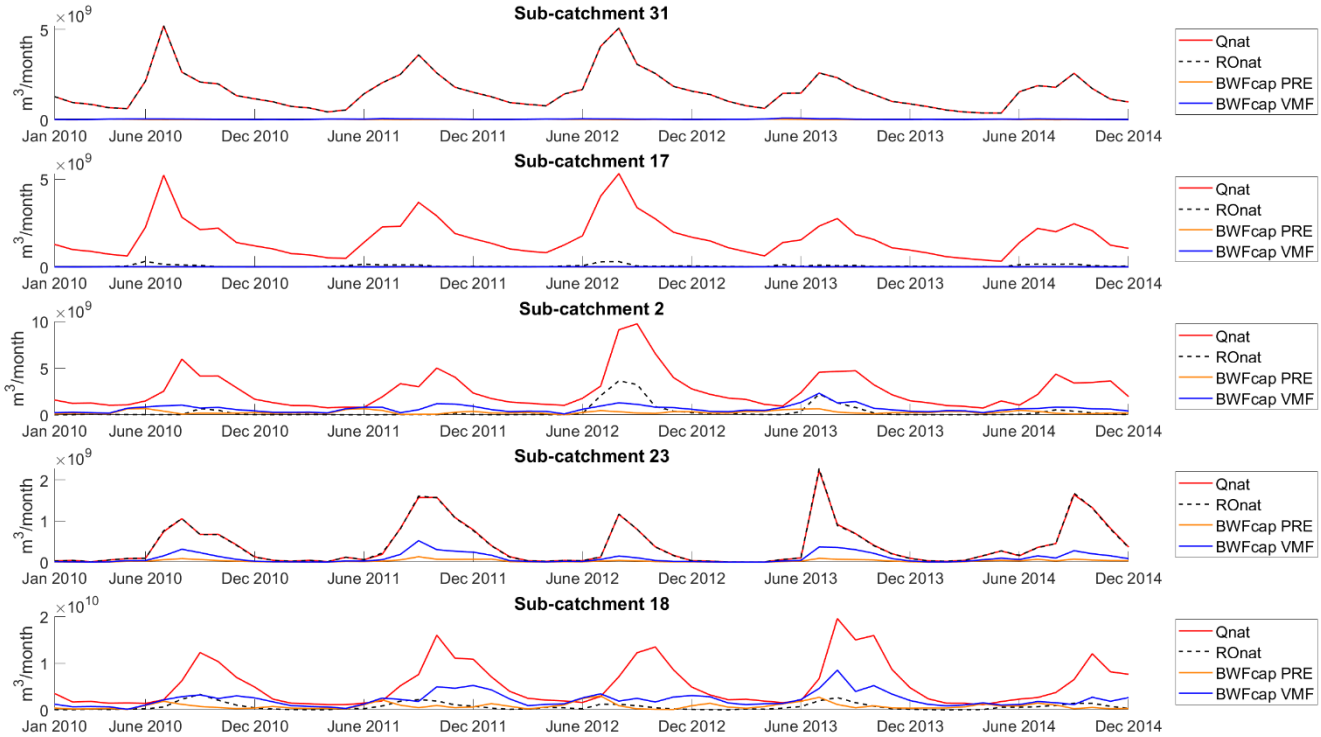

FIGURE 27: POPULATION-BASED SCENARIO BWF CAPS FOR FIVE REPRESENTATIVE SUB-CATCHMENTS AND TWO EFR METHODS. Q_{nat} REPRESENTS THE STREAMFLOW UNDER NATURAL CONDITIONS AND RO_{nat} REPRESENTS THE AMOUNT OF GENERATED BLUE WATER THAT ADDS TO THE STREAMFLOW UNDER NATURAL CONDITIONS. SUB-CATCHMENT 31 IN UPPER REACH, 17 IN UPPER REACH AND CONTAINS A RESERVOIR, 2 IN END OF UPPER REACH, 23 TRIBUTARY IN MIDDLE REACH, AND 18 COMPRISES THE ENTIRE LOWER REACH.

3.3.4. BWF cap demand-based

The BWF cap graphs in Figure 28 show a similar pattern as for the population-based scenario. The upstream BWF caps decrease and as a result, downstream BWF caps increase. The patterns of the population- and demand-based scenarios are expected to correspond, because the allocation principles applied only differ in the allocation factor employed. This difference is caused by the relative population and relative demand of a sub-catchment. This is visible in the BWF caps in sub-catchment 2 and 23, where the BWF caps are larger than in the population-based scenario implying that the relative demand is larger than the relative population. The BWF caps in the other sub-catchments appear to be the same. The demand-based scenario BWF cap for every sub-catchment individually is given in Appendix J.

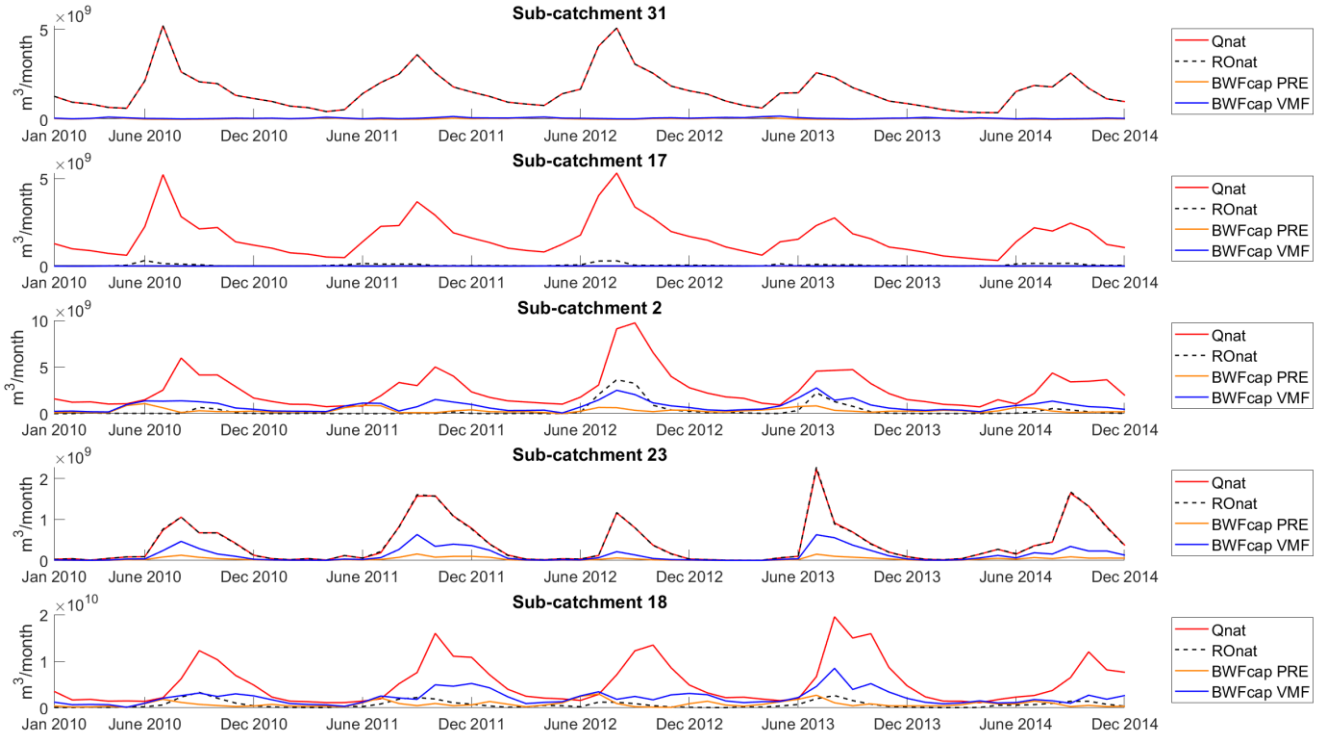

FIGURE 28: DEMAND-BASED SCENARIO BWF CAPS FOR FIVE REPRESENTATIVE SUB-CATCHMENTS AND TWO EFR METHODS. Q_{nat} REPRESENTS THE STREAMFLOW UNDER NATURAL CONDITIONS AND RO_{nat} REPRESENTS THE AMOUNT OF GENERATED BLUE WATER THAT ADDS TO THE STREAMFLOW UNDER NATURAL CONDITIONS. SUB-CATCHMENT 31 IN UPPER REACH, 17 IN UPPER REACH AND CONTAINS A RESERVOIR, 2 IN END OF UPPER REACH, 23 TRIBUTARY IN MIDDLE REACH, AND 18 COMPRISES THE ENTIRE LOWER REACH.

3.4. Water scarcity

In this paragraph, the temporal variability of blue water scarcity is displayed first as the time series of the BWF cap according to the four scenarios versus the time series of the actual BWF. Second, the spatial component of the water scarcity is expressed in average seasonal water scarcity maps. The BWF caps to express the water scarcity in this paragraph are calculated according to the VMF method. The BWF caps are presented according to the VMF method. This method is more sophisticated, includes the distinction in flow season which is proven to be essential, and the PRE method could be considered too precautious (Pastor et al., 2014; Zhuo et al., 2016). The results for the BWF caps based on the PRE method are given in Appendix K and L for the temporal distribution and spatial distribution, respectively.

The areal average water scarcity for the 31 sub-catchments from 2010 to 2014 per scenario and the decrease compared to the default scenario are given in Table 9. The water scarcity values are remarkably large for both EFR and the four BWF cap scenarios. This is caused by the water scarcity values in the tributary sub-catchments. During the dry months of the year, the generated natural runoff can be negligible in some tributary sub-catchments. Any BWF during those months results in extremely large water scarcity values, leading to these large areal average values. Including reservoirs for the calculation of water scarcity causes the largest decrease in water scarcity. The application of the population- and demand-based allocation principle on the situation with reservoirs causes the water scarcity to decrease further with the lowest values for the demand-based scenario. Furthermore, the effect of the EFR methods on the water scarcity is as expected based on percentages used for EFR.

TABLE 9: AREAL AVERAGE WATER SCARCITY PER SCENARIO.

	Areal average water scarcity [-]	Decrease from default [%]
VMF		
Default scenario	42.3	-
Reservoir scenario	38.5	9
Population scenario	36.9	12
Demand scenario	36.6	13
PRE		
Default scenario	171.3	-
Reservoir scenario	93.8	45
Population scenario	87.2	49
Demand scenario	82.3	52

3.4.1. Temporal distribution

The four calculated BWF caps and the actual BWF for the five representative sub-catchments using the VMF method are displayed in Figure 29. The BWF cap and the actual BWF are compared to observe the effect of the alternative BWF cap scenarios on the possible exceedance of BWF cap by the actual BWF. An overview of all four BWF cap scenarios according to both the VMF and PRE EFR method in combination with the actual BWF for every sub-catchment individually is given in Appendix K.

The exceedance and non-exceedance of the BWF caps in the default scenario display the difference between upstream and downstream, and between the dry and wet periods. The BWF cap largely exceeds the actual BWF for sub-catchment 31 and 17, whereas downstream the actual BWF regularly exceeds the BWF cap. There are two sides to this exceedance further downstream. First, upstream there is little blue water consumption and large blue water generation. Further downstream, this is not the case and the

opposite is true. Second, the natural variability of the BWF cap does not match the variability of the actual BWF.

The reservoir BWF cap scenario mitigates the regional differences of the BWF caps. The five reservoirs are located all over the mainstream of the Upper and the Middle Reach. Their location enables an equal distribution of the available blue water over the sub-catchments. In addition, the reservoirs partly deal with the mismatch in timing between BWF cap and actual BWF. In general, the high values from the default BWF cap are flattened, and in return, more blue water is available in dry periods to better match the actual BWF. However, there are still some upstream and downstream differences in BWF cap exceedance due to the use-what-is-there-principle and the resulting unlimited upstream consumption. Tributary sub-catchments are not affected by reservoirs. Therefore, their BWF caps and the possible exceedance remain the same.

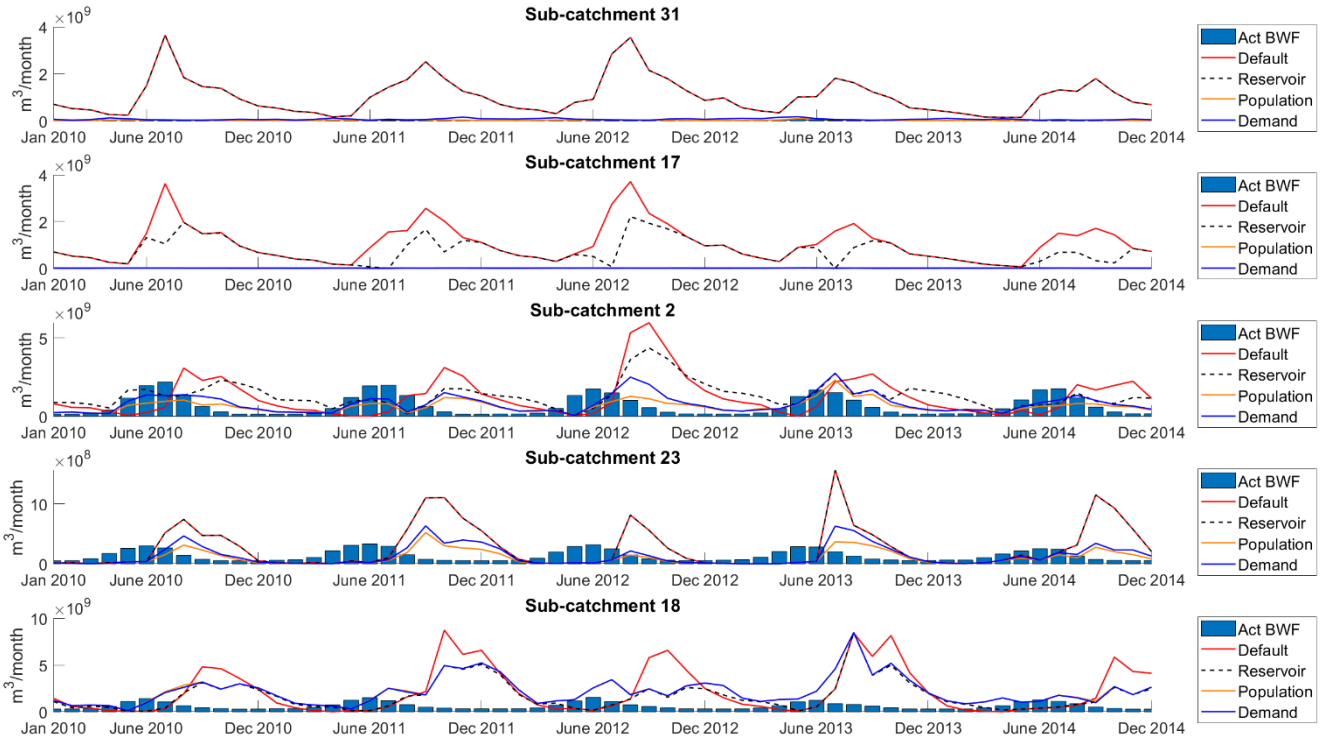

FIGURE 29: THE FOUR ALTERNATIVE BWF CAPS (BASED ON VMF), AND THE ACTUAL BWF (ACT BWF), FOR THE FIVE REPRESENTATIVE SUB-CATCHMENTS. SIMILAR GRAPHS FOR ALL SUB-CATCHMENTS AND PRE ARE INCLUDED IN APPENDIX J. SUB-CATCHMENT 31 IN UPPER REACH, 17 IN UPPER REACH AND CONTAINS A RESERVOIR, 2 IN END OF UPPER REACH, 23 TRIBUTARY IN MIDDLE REACH, AND 18 COMPRISES THE ENTIRE LOWER REACH.

The population-based BWF cap scenario alleviates the upstream and downstream differences further. In this scenario highs and lows are less prominently present in the BWF caps of the sub-catchments. The BWF caps for the default and reservoir scenario are considerably larger than the population-based BWF cap in sub-catchment 31 and 17. A more detailed analysis of the population-based BWF caps in sub-catchment 31 and 17 is given under Figure 30. The population-based BWF cap graph for sub-catchment 2 in Figure 29, shows that the number of months the actual BWF exceeds the BWF cap in sub-catchment 2 decreases compared to the default scenario. However, it remains at the same level compared to the reservoir scenario. The level of exceedance increases from the reservoir to the population-based scenario, because BWF cap setting in sub-catchment 2 considers downstream sub-catchments. Tributary sub-catchment 23 reserves water from the default BWF for the population-based BWF cap for downstream sub-catchments. However, the major cause for exceedance of the BWF cap is the mismatch between BWA and actual BWF.

The main beneficiary in case of these five representative sub-catchments is sub-catchment 18. During dry months, the actual BWF does not exceed the BWF cap or at least the level of exceedance decreases.

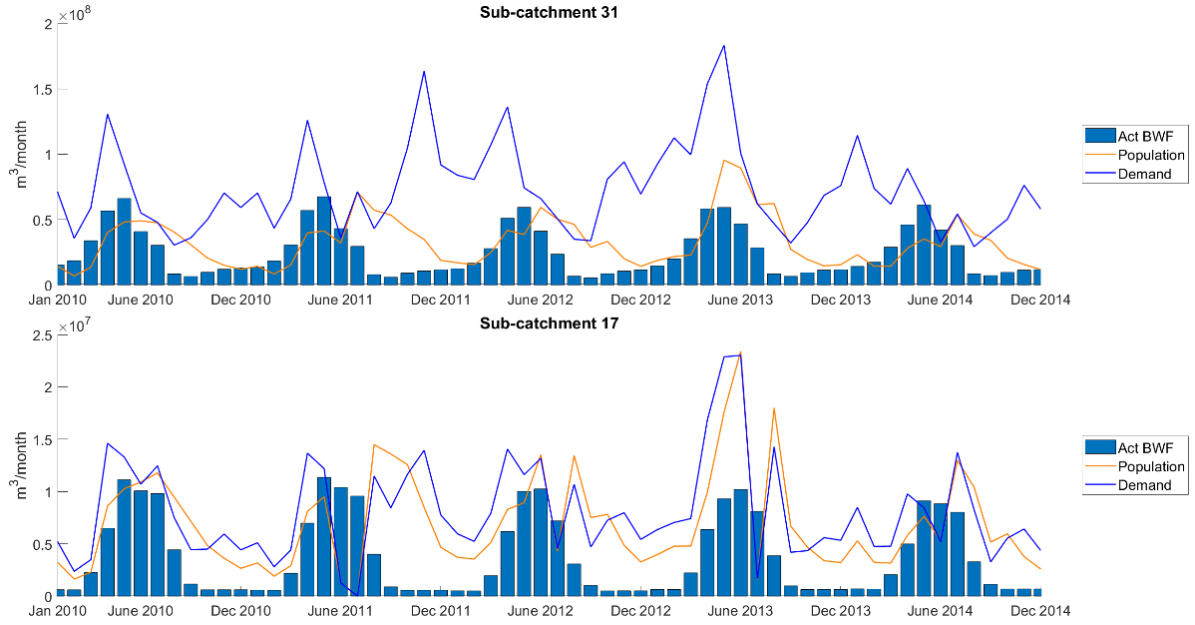

FIGURE 30: BWF CAP POPULATION- AND DEMAND-BASED SCENARIOS FOR SUB-CATCHMENT 31 AND 17 ACCORDING TO THE VMF METHOD.

Figure 30 shows the BWF cap for the population-based scenario in sub-catchment 31 and 17. The BWF cap in sub-catchment 31 decreases to such an extent that the little blue water consumption there is, exceeds the BWF cap for a few months each year. The BWF cap in sub-catchment 17 displays a few exceedances as well, but these exceedances can be attributed to reservoir retention rather than the reservation of blue water for downstream sub-catchments.

The findings for the demand-based scenario are similar to the population-based findings. However, the demand-based scenario appears to be a better match for the actual BWF. The graphs in Figure 30 show that the BWF cap in sub-catchment 31 is less often exceeded and the BWF cap corresponds more with the actual BWF in sub-catchment 17. In addition, the graphs in Figure 29 show the BWF cap better matches the actual BWF of sub-catchment 2 and 23 as well. This implies that the relative demand is larger than the relative population in those four sub-catchments. The BWF cap for sub-catchment 18 corresponds with the population-based BWF cap, because the relative population and relative demand are large for this sub-catchment. However, the timing component of the BWF cap and the actual BWF remains an issue. A reason for the mismatch in timing for the demand-based scenario could be that the past BWF data for the BWF cap setting are different from the BWF data for the study period. Figure 31 rejects this claim because it shows that the pattern of actual BWF has not changed over the two periods. An explanation for the difference between the timing of BWF cap and actual BWF, is the fact that the timing of BWA is not influenced by allocation principles. The timing is determined by the natural variability of BWA and the operation of reservoirs. The two scenarios only determine how available blue water is allocated over the 31 sub-catchments. To adjust the timing of BWA and BWF cap the operation of reservoirs could be adjusted. However, the operation of reservoirs cannot be based on adjusting the timing of BWA alone, because it depends on hydroelectricity generation, flood control, ice prevention, and sediment flushing as well (Zhuo et al., 2019).

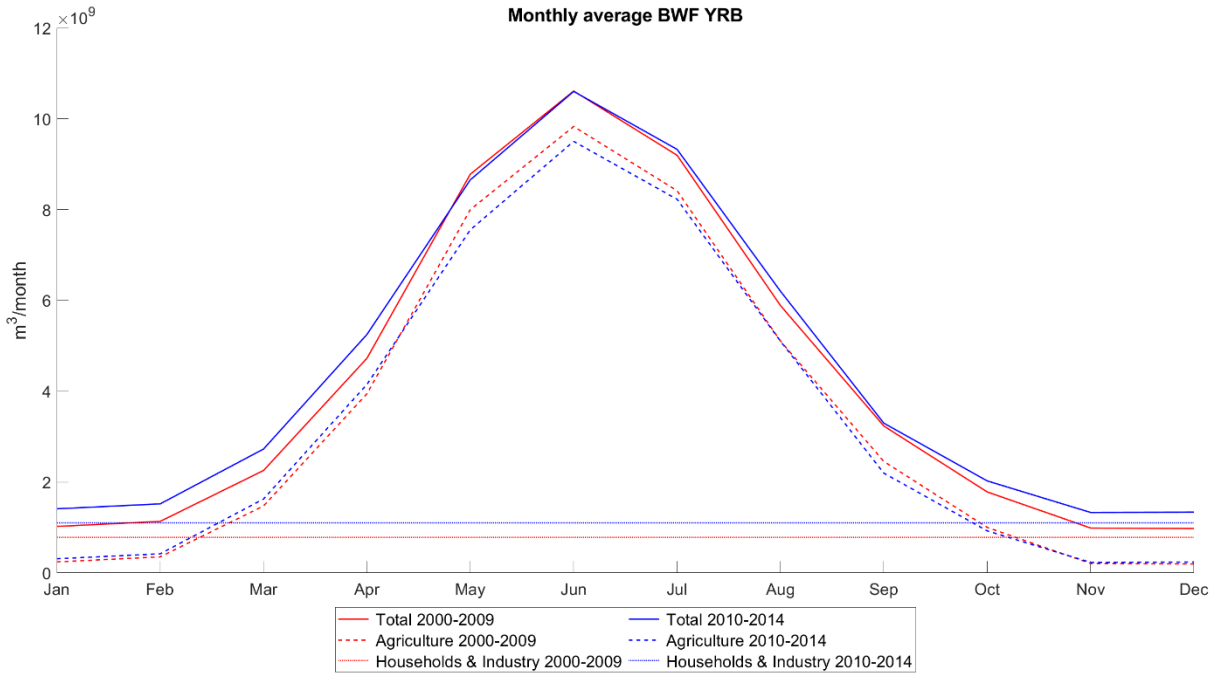

FIGURE 31: COMPARISON OF AVERAGE MONTHLY BWF FOR THE YRB BETWEEN 2000-2009 (RED) AND 2010-2014 (BLUE).

3.4.2. Spatial distribution

This section shows the effect of the four allocation scenarios on the spatial distribution of water scarcity. The presented water scarcity results are seasonal averages for 2010 – 2014.

Figure 32 illustrates the spatial distribution of water scarcity over the sub-catchment for spring. The default scenario shows the previously mentioned spatial differences between upstream and downstream sub-catchments. The reservoir scenario displays the effect of reservoirs on the temporal and spatial component of BWA. Additional blue water is released corresponding with the timing of the increasing BWF. This causes severe water scarcity to start further downstream compared to the default scenario. The effect of the spatial component on BWA is visible in the sub-catchments all the way downstream and is expressed as a decrease in water scarcity compared to the default scenario. The distribution of water scarcity is more equal for the population- and demand-based scenarios. Upstream reserved blue water leads to a local increase of water scarcity but causes a decrease in water scarcity downstream. A more equally distributed water scarcity indicates smaller extreme values, both high and low. This means that the regional differences in the severity of environmental damage due to blue water consumption decrease. The distribution of water

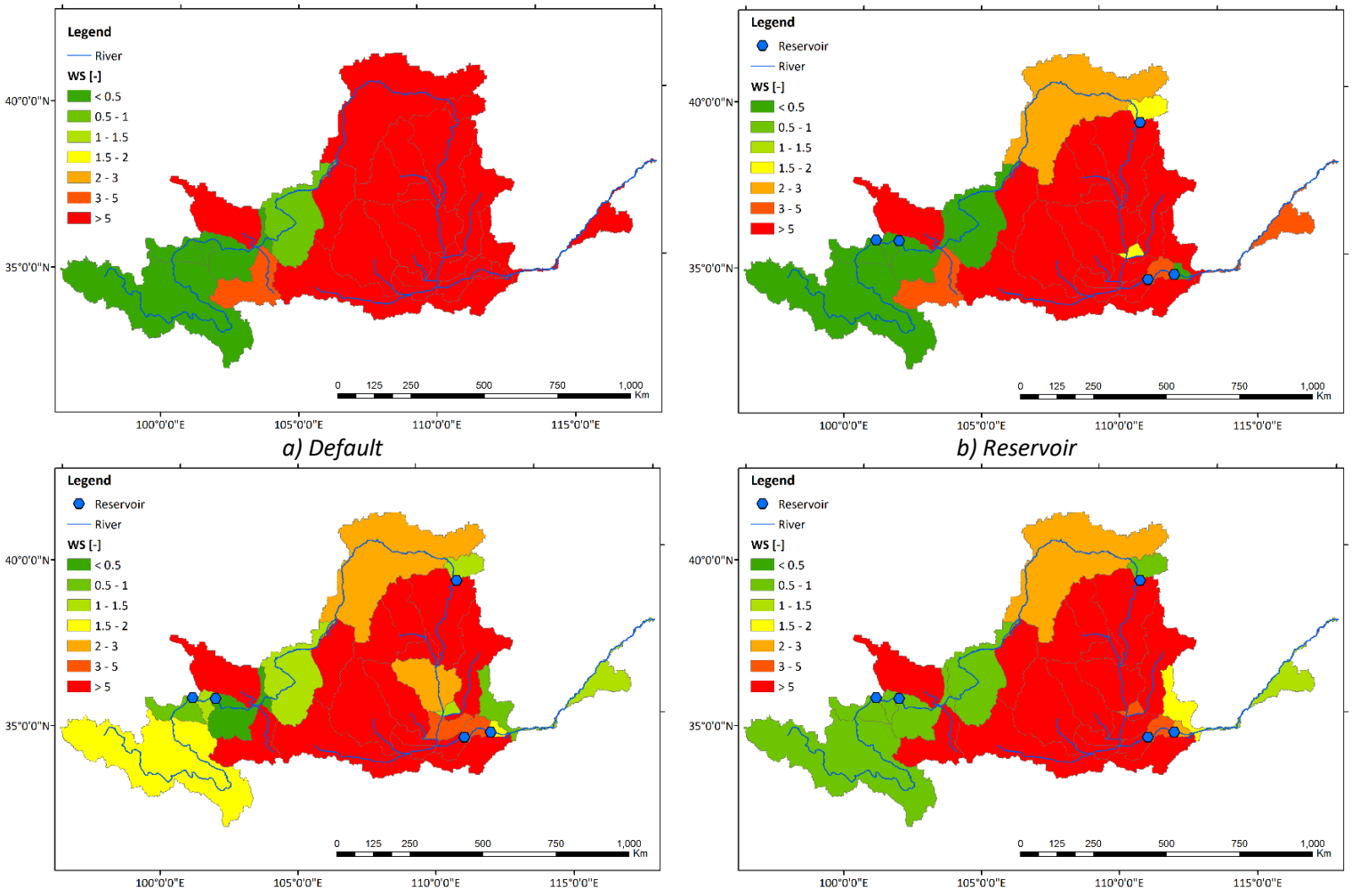

FIGURE 32: AVERAGE BLUE WATER SCARCITY SPRING (MARCH – MAY) PER SUB-CATCHMENT OF THE YRB (2010 – 2014) USING BWF CAPS ACCORDING TO A) DEFAULT SCENARIO, B) RESERVOIR SCENARIO, C) POPULATION-BASED SCENARIO, AND D) DEMAND-BASED SCENARIO USING VMF. THE CLASSES < 0.5 AND 0.5-1 INDICATE LOW, 1-1.5 MODERATE, 1.5-2 SIGNIFICANT, AND 2-3, 3-5 AND > 5 SEVERE WATER SCARCITY. FOR PRE RESULTS, SEE APPENDIX L.

scarcity is more equal for the demand-based scenario than for the population-based scenario. The maps of the two scenarios indicate that the BWF cap based on population show the mismatch of population and actual BWF. This is visible as the larger regional differences in water scarcity for the population-based scenario. In general, tributary sub-catchments experience severe water scarcity in spring, because they completely depend on local BWA. Finally, the water scarcity in spring is caused by the little generation of blue water and BWF. The former is the main cause of water scarcity. Appendix E shows the natural runoff in spring is still small, while Figure 31 indicates the BWF is increasing but has not reaches its peak yet.

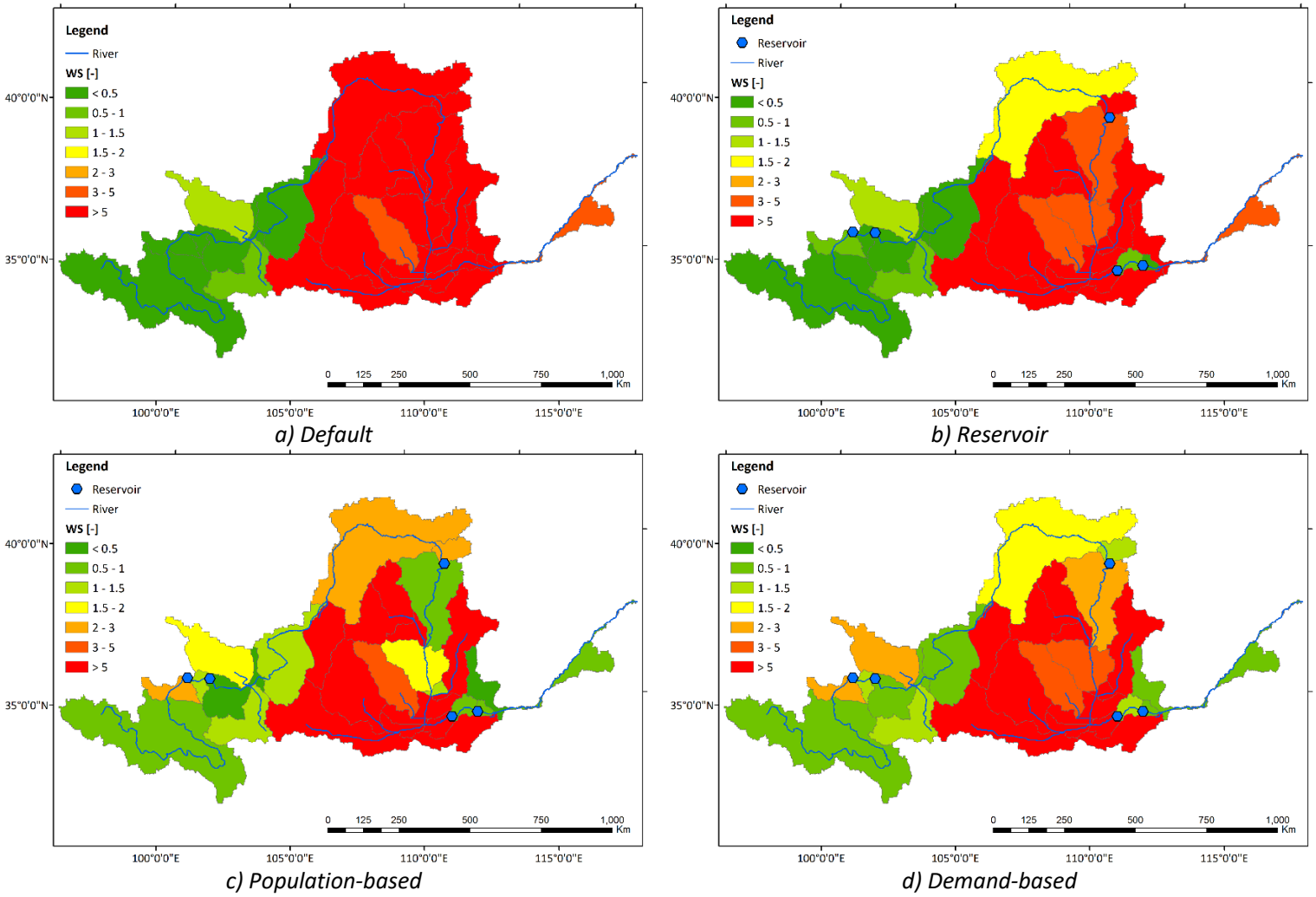

FIGURE 33: AVERAGE BLUE WATER SCARCITY SUMMER (JUNE – AUGUST) PER SUB-CATCHMENT OF THE YRB (2010 – 2014) USING BWF CAPS ACCORDING TO A) DEFAULT SCENARIO, B) RESERVOIR SCENARIO, C) POPULATION-BASED SCENARIO, AND D) DEMAND-BASED SCENARIO USING VMF. THE CLASSES < 0.5 AND 0.5-1 INDICATE LOW, 1-1.5 MODERATE, 1.5-2 SIGNIFICANT, AND 2-3, 3-5 AND > 5 SEVERE WATER SCARCITY. FOR PRE RESULTS, SEE APPENDIX L.

Figure 33 shows the average water scarcity results in summer. The summer water scarcity results are remarkably similar to the water scarcity results during spring. In general, the water scarcity values are lower in summer than in spring. This is caused by the larger generation of blue water than during spring, see Appendix E. This is visible as a decrease in water scarcity locally for the default scenario. The reservoir scenario alleviates a part of the water scarcity due to timing of BWA and location of reservoirs compared to the default scenario. The most upstream reservoir, Longyangxia, shows an increase in water scarcity due to reservoir retention. This is visible as an increase in water scarcity from the default to the reservoir scenario. In combination with blue water reservation in this sub-catchment for the population- and

demand-based scenarios, the retention causes severe water scarcity. The population and demand-based scenarios lead to a more equal distribution of water scarcity, where the distribution for the demand-based scenario is more equal. Tributary sub-catchments mainly experience extreme water scarcity in summer as well. However, during summer the water scarcity values are smaller due to the larger blue water generation. The large water scarcity in summer is mainly caused by a high BWF. The natural runoff is large, but simultaneously the BWF in the basin is at its peak.

The maps in Figure 34 illustrate that blue water scarcity in autumn is hardly present. The mainstream sub-catchments experience no water scarcity, whereas certain tributary sub-catchments show severe water scarcity. The effect on the four allocation scenarios on water scarcity is least present during this season. Even for the default scenario, there is little water scarcity present in the YRB. The population- and demand-based scenarios affect the water scarcity values for some of the tributary sub-catchments and cause them to increase. The overall decrease in blue water scarcity is attributed to the large generation of blue water and the decreasing BWF.

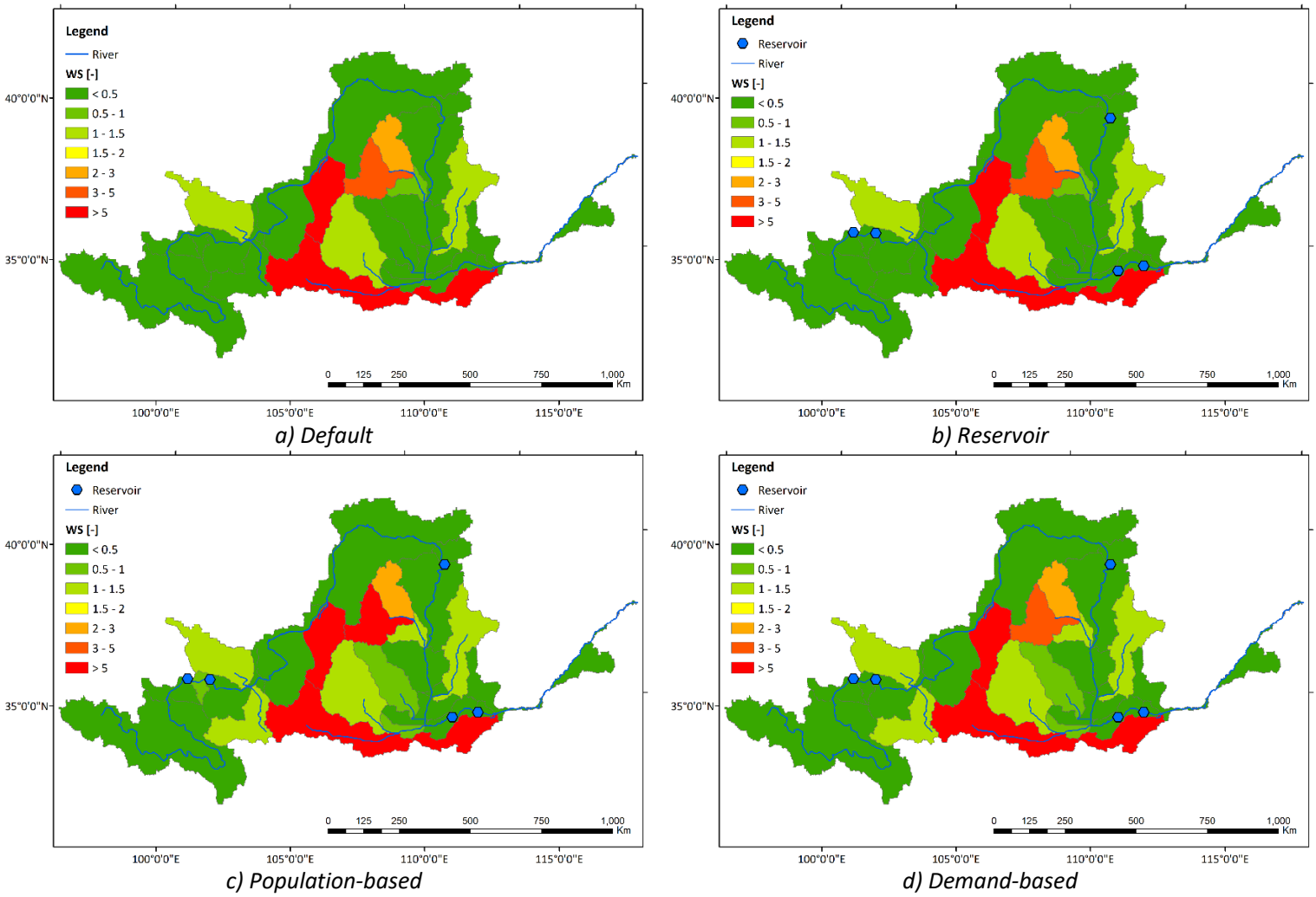

FIGURE 34: A BLUE WATER SCARCITY AUTUMN (SEPTEMBER – NOVEMBER) PER SUB-CATCHMENT OF THE YRB (2010 – 2014) USING BWF CAPS ACCORDING TO A) DEFAULT SCENARIO, B) RESERVOIR SCENARIO, C) POPULATION-BASED SCENARIO, AND D) DEMAND-BASED SCENARIO USING VMF. THE CLASSES < 0.5 AND 0.5-1 INDICATE LOW, 1-1.5 MODERATE, 1.5-2 SIGNIFICANT, AND 2-3, 3-5 AND > 5 SEVERE WATER SCARCITY. FOR PRE RESULTS SEE APPENDIX L.

Figure 35 shows the average water scarcity during winter. The spatial distribution differs not much among the four scenarios. The small BWF is the main reason for low water scarcity in the mainstream. However, compared to the results in autumn, there is more water scarcity in the tributary sub-catchments. This can be ascribed to the distribution of blue water generation in winter. The generation of blue water in the basin is smallest during winter and a large part is generated in the Source Region, see Appendix E. The sub-catchments in the mainstream benefit from this generated blue water. Since there is little blue water consumption indicate by the graphs in Figure 31, the generated blue water reaches the most downstream sub-catchment. The tributary sub-catchments do not benefit from this upstream blue water and depend on their little locally generated blue water for the small BWF in winter. Leading to severe water scarcity in the highest class (> 5).

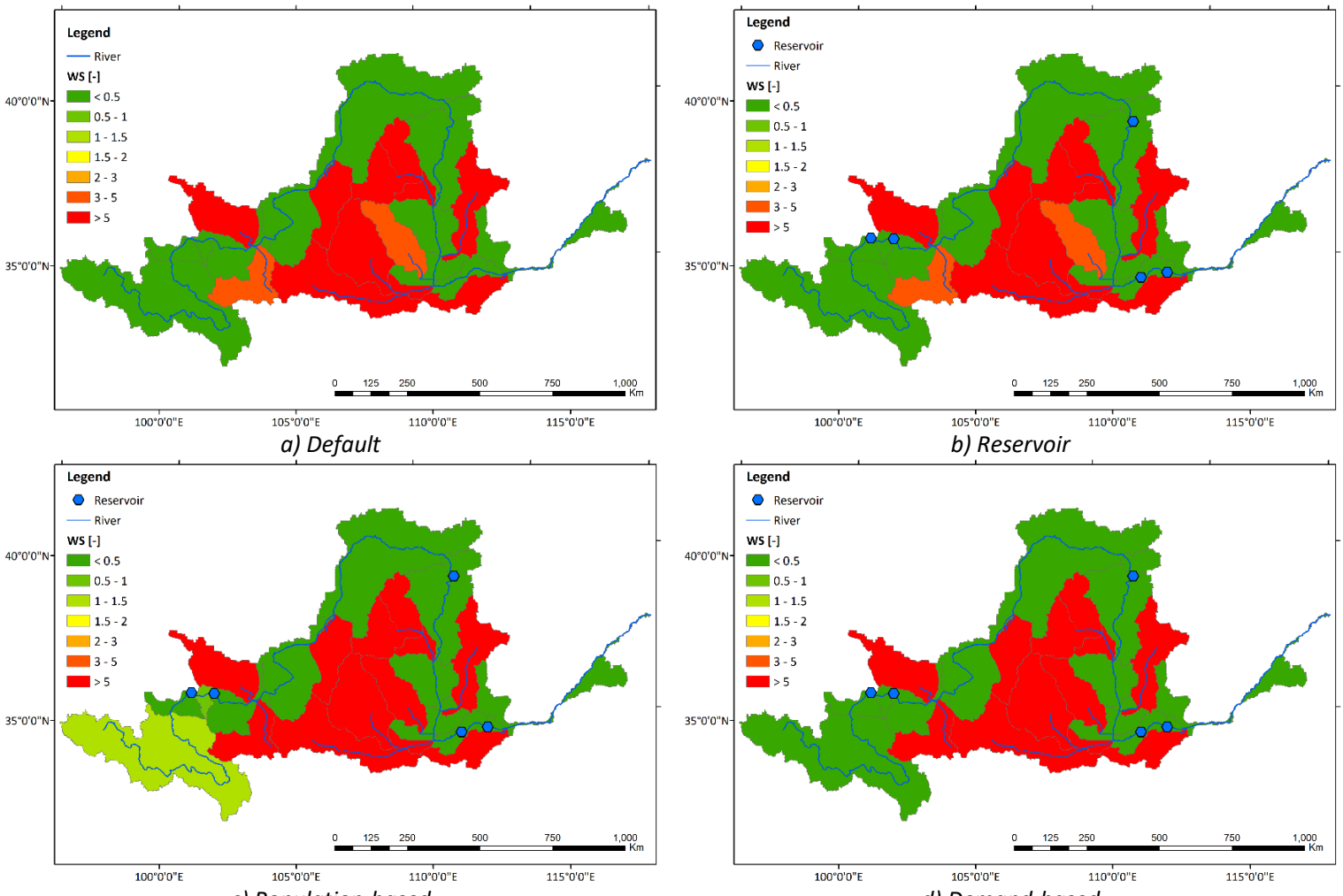

FIGURE 35: AVERAGE BLUE WATER SCARCITY WINTER (DECEMBER – FEBRUARY) PER SUB-CATCHMENT OF THE YRB (2010 – 2014) USING BWF CAPS ACCORDING TO A) DEFAULT SCENARIO, B) RESERVOIR SCENARIO, C) POPULATION-BASED SCENARIO, AND D) DEMAND-BASED SCENARIO USING VMF. THE CLASSES < 0.5 AND 0.5-1 INDICATE LOW, 1-1.5 MODERATE, 1.5-2 SIGNIFICANT, AND 2-3, 3-5 AND > 5 SEVERE WATER SCARCITY. FOR PRE RESULTS SEE APPENDIX L.

In all four seasons, the water scarcity in tributary sub-catchments increases between scenarios applying the use-what-is-there principle and the scenarios that consider other sub-catchments. This is a curious result. The results for the PRE EFR method in Appendix L, show a similar pattern as the results in this paragraph. The main difference is that the general water scarcity is larger for PRE than for VMF.

4. Discussion

In this chapter, the results from this study are compared with results from previous studies in 4.1. The limitations of the study are discussed in 4.2. Finally, the practical implications of the BWF cap are discussed in 4.3.

4.1. Comparison with previous studies

The average annual natural runoff estimated by SWAT in this study is within the reported range of the estimates in other studies of the YRB. Table 10 shows the comparison of the annual natural runoff between this study and other studies. The reconstructed method is a method similar to the one the YRCC uses as described in 3.1.2. Even though the annual average natural runoff in this study is larger than most of the averages from other studies, it is still within the range of reported studies.

TABLE 10: AVERAGE ANNUAL NATURAL RUNOFF FOR ENTIRE YRB COMPARED TO OTHER STUDIES.

Average annual natural runoff	Study	Period	Method
$5.31 * 10^{10}\ m^3$	YRCC	2010 – 2014	Reconstructed
$5.33 * 10^{10}\ m^3$	Wang et al. (2019b)	1956 – 2016	Reconstructed
$5.97 * 10^{10}\ m^3$	Cong et al. (2009)	2001 – 2005	Hydrological model
$6 * 10^{10}\ m^3$	Ran & Lu (2011)	1950 – 2009	Reconstructed
$6.12 * 10^{10}\ m^3$	Li & Yang (2004)	2000 – 2009	Reconstructed
$6.24 * 10^{10}\ m^3$	Yuan et al. (2018)	1986 – 2011	Hydrological model
$6.36 * 10^{10}\ m^3$	This study	2010 – 2014	Hydrological model
$7.31 * 10^{10}\ m^3$	Zhuo et al. (2019)	2002 – 2005	Hydrological model

Table 11 illustrates the difference between the distribution over the three reaches of this study and the initial expectations based on Zhuo et al. (2019) and Wang et al. (2019b). As mentioned in 3.1.2., the distribution of generated annual natural runoff over the three reaches does not comply with the expectations. The Lower Reach shows an exceptionally large natural runoff in mm per month compared to the Upper Reach, which is the largest contributor to the natural runoff. Although Wang et al. (2019b) show the Upper Reach generated relatively less and the Middle Reach a bit more compared to Zhuo et al. (2019), they both agree on the small contribution to the natural runoff of the Lower Reach.

TABLE 11: AVERAGE PERCENTAGE OF GENERATED ANNUAL NATURAL RUNOFF PER REACH.

	This study	Zhuo et al. (2019)	Wang et al. (2019b)
Upper Reach	50	67	60
Middle Reach	37	31	39
Lower Reach	13	2	1

The difference in percentages can be explained by the large precipitation events in the Lower Reach, but mainly by the fact that a larger part of this precipitation becomes natural runoff. The precipitation is relatively large in the Lower Reach compared to the other reaches, but this corresponds with other studies (Zhang et al., 2014; Yuan et al., 2017). The amount of this precipitation that becomes runoff is determined by SWAT. This is larger in the Lower Reach than in other reaches. The absolute average annual natural runoff per reach from this study is compared with studies by Zhuo et al. (2019) and Wang et al. (2019b). The comparison indicates that the natural runoff in the Upper Reach is comparable, the Middle Reach is slightly larger, and the Lower Reach considerably larger. The overestimation of the Lower Reach and, to a smaller extent of the Middle Reach, could be attributed to the partial calibration and validation of the SWAT

model. The the Middle and Lower Reach are not included in the calibration. The method of partial calibration and validation were based on the assumption that two-thirds of the annual natural runoff is generated in the area upstream of Lanzhou. Thereby, assuring the reliability of two-thirds of the natural runoff results. The different annual natural runoff distribution in this study could decrease the reliability of the natural runoff results. However, it should be kept in mind that the studies by Zhuo et al. (2019) and Wang et al. (2019b) were performed for a different study period and used other methods to estimate the natural runoff. Either an alternative hydrological model or the method of reconstructing the natural runoff.

To assure the robustness of results, the natural runoff of this study is altered according to the reported distribution. The natural runoff of the Upper and Middle Reach were considered to be 98% of the total average annual natural runoff. This amount is used to scale the natural runoff in the Lower Reach as 2% of the total. The alternative distribution is 57%, 41%, and 2% for the Upper, Middle and Lower Reach. The total annual natural runoff becomes $5.64 * 10^{10}\ m^3$. The distribution matches the reported distributions closer, and the natural runoff is within the reported range and closer to the YRCC estimations. The daily distribution of natural runoff from SWAT in the Lower Reach is used to recalculate the BWF caps and blue water scarcity. The overall findings of the study do not change. The use-what-is-there principle only affects the water scarcity in the Lower Reach. The water scarcity increases, because upstream sub-catchments do not consider the Lower Reach. Therefore, the effect of a smaller BWA locally, only affects the water scarcity in the Lower Reach. The population- and demand-based scenarios show a smaller increase in water scarcity in the Lower Reach since these principles consider all blue water in the system for BWF cap setting. The areal average water scarcity in the whole basin from 2010 to 2014 increases by 1.2, 0.9, 0.7, and 0.3% for the default, reservoir, population-based, and demand-based scenario, respectively. An allocation principle that considers all blue water in the system compensates for less blue water downstream by lowering the BWF cap in the whole basin. This leads to a smaller overall increase in areal average water scarcity than when the decrease in blue water is confined to one location and the corresponding larger local water scarcity.

The water scarcity findings correspond with other studies for the YRB by Zhuo et al. (2016) and Zhuo et al. (2019). The water scarcity results of PRE default scenario are compared with Zhuo et al. (2016) and Zhuo et al. (2019). Zhuo et al. (2016) calculated the water scarcity at a 5x5 arc min grid level. The spring (April) and summer (July) water scarcity results show a similar pattern of water scarcity and show a large part of the basin exhibits severe water scarcity. The water scarcity worsens from upstream to downstream, and the water scarcity decreases from spring to summer. Zhuo et al. (2019) divided the basin according to the three reaches. The basin experienced severe water scarcity for four months, moderate for one, and low for seven months per year. The number of months of severe water scarcity increased from upstream to downstream. The water scarcity results of the PRE reservoir scenario are compared with Zhuo et al. (2019). They calculated the water scarcity for the situation with reservoirs as well. The number of months the basin experienced severe water scarcity changed to severe water scarcity for three, significant for one, moderate for four, and low for four. The differences in water scarcity between the three reaches decreased compared to the situation with no reservoirs. These findings above correspond with the results of this study.

The EFRs are determined using the PRE and VMF methods which are both developed to protect the environment in and around rivers with no site-specific requirements (Richter et al., 2012; Pastor et al., 2014). There are considerable differences in the amount of water that should be reserved for the environment between the two EFR methods, and many more are methods available. In a perfect situation, the EFR is estimated based on onsite measurement of streamflow and the environment's response (Poff,

et al., 2010). For the YRB, an estimate of EFR was formulated by Yang et al. (2009b) based on classification and regionalization of the ecosystem, multiple ecological management objectives and spatial variability of the EFR. They reported an annual minimum EFR of 55% of the annual natural runoff. This value exceeds the annual average over all sub-catchment for VMF of 46% but is reasonably smaller than the 80% according to PRE. In general, literature agrees that BWA increases from the application of PRE to VMF as EFR method (Hogeboom et al., 2020; Sharma & Dutta, 2020). The BWF cap and water scarcity follow the trend of BWA and decrease from the application of PRE to VMF.

4.2. Limitations

The water scarcity for the tributary sub-catchments paints a picture of almost constant water scarcity in the highest category. However, this might be an exaggeration of the actual situation because more reservoirs are present than the five included in this study. This includes reservoirs in tributary sub-catchments as well. The five major and large reservoirs in this study account for 78% of the total storage capacity and the reservoirs in the tributary rivers account for 6% of the storage capacity (Ran & Lu, 2011). The reservoirs in tributary sub-catchments would mainly influence the local BWA instead of the BWA in mainstream sub-catchments due to the small storage capacity percentage compared to the mainstream reservoirs. However, as shown in 3.3. & 3.4., reservoirs substantially influence the timing of BWA and thereby water scarcity. This applies at a local level for tributary sub-catchments as well and could significantly alter the water scarcity in tributary sub-catchments.

The dependency on local BWA of tributary sub-catchments cause them to be prone to water scarcity. The population- and demand-based scenarios increase the water scarcity of tributary sub-catchments. According these scenarios the tributary sub-catchments are responsible for blue water in downstream sub-catchments, because the underlying allocation principles use the right to blue water to calculate the BWF cap. This implies that a tributary sub-catchment must reserve blue water for downstream, mainstream sub-catchments. Even though the tributary sub-catchment already experiences water scarcity itself for the reservoir scenario. In some cases, blue water from tributary sub-catchment is reserved for mainstream sub-catchments while the mainstream sub-catchments do not require this additional blue water. However, the reservation of the additional blue water leads to an increase in water scarcity in the tributary sub-catchments. This could be prevented by assigning the local BWA to the tributary sub-catchment and thus applying the use-what-is-there principle locally. However, this is not a general solution since the relationship between mainstream and tributary sub-catchment can be different in other basins. An additional component to the population- and demand-based allocation principle could be implemented. This additional component could include the actual BWF of a downstream sub-catchment or the effect on water scarcity of a certain allocation of blue water. The BWF for the first option determines if a downstream sub-catchment requires additional water from a tributary sub-catchment. This BWF is different from the BWF for the allocation factor in the demand-based allocation principle, because the latter BWF is past demand to determine the allocation factor. The second option for the additional component would determine the effect on water scarcity of a certain blue water distribution and allocate blue water to the sub-catchment that benefits most. This, in combination with the reservoirs, provides a more realistic representation of water scarcity in tributary sub-catchments.

Literature has not provided a value for the travel time of a sub-catchment or a value for the total travel time through the mainstream river channel. Therefore, the (total) travel time through the river channel of the sub-catchments cannot be compared. The travel time outcome from SWAT is directly used without validation in the BWF cap calculations. The travel time is an important component for the timing of the BWF

cap to match reality as closely as possible. The use of unvalidated travel time affects the reliability of the BWF caps' timing negatively. To assure the timing of BWF caps, the travel time should be validated.

The components in the demand-based allocation principle are not tailored for the YRB specifically and are therefore applicable to all basins. Simulation of the natural runoff is not limited to SWAT. Another hydrological model or the reconstruction of natural runoff could be used. However, SWAT is convenient for the delineation of sub-catchments. In addition, the reservoirs are implemented at the outlets of sub-catchments. The equations for the calculation of BWF caps in demand-based scenarios are based on this configuration. Therefore, SWAT is advised as the hydrological model for the BWF cap calculations according to this scenario. Furthermore, the EFR methods to estimate BWA are not limited to VMF and PRE. The findings in the study can be interpreted more broadly than the YRB. The effect of accounting for other sub-catchments in BWF cap setting has a clear effect on the water scarcity distribution in this basin. This distribution is not based on YRB specific characteristics other than population and demand. The effect on the water scarcity distribution will show in other basins as well, using their population and demand.

4.3. Practical implications of BWF cap

The BWF cap in this study is calculated monthly at sub-catchment level to deal with the temporal and spatial variability of BWA. However, bringing the BWF cap to practice as a policy instrument is not as straightforward as implementing these calculated BWF caps in this study. The BWF caps calculated in this study are based on previous data, e.g. meteorological and actual BWF data. To actively protect the environment, a BWF cap should be implemented as the future upper limit of consumption based on previous BWA and BWF. The inter- and intra-annual variability of BWA in the YRB as presented in 3.2. complicate BWF cap setting. Hogeboom et al. (2020) point out that choosing a certain BWA is a tradeoff between underutilization of the actual BWA and violating the EFR. On the one hand, if the actual BWA is larger than the chosen BWA, additional blue water is available that is not utilized. On the other hand, if the actual BWA is smaller than the chosen BWA, the EFR is violated in BWF cap setting. A balance between the two is achieved by taking the average BWA over several years. The threat of water scarcity in the YRB requires protection of the environment by setting a BWF cap. The potential underutilization of selecting a relatively small BWA may not be feasible for the YRB due to the large demand. A BWF cap that on average protects the environment is already a major improvement of the current situation and should be based on the average BWA over several years. The average BWA for the BWF cap should capture the effect of climate change. Climate change is an ongoing and gradual process, but abrupt climate change could occur within a few decades (IPCC, 2007; IPCC, 2018). In order to capture the intra- and inter-annual and the effect of climate change, the average BWA should be based on the previous BWA of a 15 to 20-year period.

The BWF cap setting should apply the demand-based allocation principle or an adjusted version of it to allocate the average BWA. The demand-based scenario showed the lowest water scarcity and the most equal spatial distribution over the sub-catchments of the four scenarios. The allocation based on past blue water demand matches the actual BWF best. However, this is only true if the pattern of past demand matches the pattern of actual BWF. Therefore, the allocation factor of demand should be updated each year to include the previous year in the allocation of the coming year. Instead of considering a long-term average like for blue water availability, the factor should be based on recent spatial patterns of demand to better match the actual demand. The average over five years includes the recent spatial pattern and excludes the possibility of a non-representative allocation factor based on a shorter period.

To increase the likelihood of enforcing BWF caps, they should be defined at administrative jurisdictions (Zhou et al., 2019). The administrative jurisdiction would know how much blue water is available for consumption and divide it over its users. Agreements between countries in a transboundary basin are required for the BWF cap setting to be successful. In fact, there are many more aspects that could influence BWF cap setting like existing legal and governance structures such as BWF permits that already have been issued (Hogeboom et al., 2020). However, the allocation algorithm itself is not hindered by boundaries and administrative jurisdictions. Therefore, it can be applied in all basins.

5. Conclusion and recommendations

In this chapter, the main findings and conclusion are presented in 5.1. The recommendation following from these findings and the discussion are displayed in 5.2.

5.1. Conclusion

The objective of this study was to examine the effect of defining alternative monthly BWF caps at sub-catchment level on the blue water scarcity for the YRB from 2010 – 2014. The BWF caps are based on four alternative allocation principles and two EFR methods.

The first of the four allocation principles, expressed as four scenarios, was the default allocation scenario. The effect of the other three allocation scenarios was compared with the default scenario. The scenario is based on the natural temporal and spatial variability with the application of the use-what-is-there principle. The second scenario included five major reservoirs and applied the same principle. The operation of the reservoirs changed the timing of BWA by retention and release. The location of reservoirs changed the spatial distribution of BWA. Thereby, the reservoirs changed the timing and spatial distribution of the BWF cap as well. The third and fourth scenario continued with the reservoirs and accounted for other sub-catchments in the BWF cap calculation. The BWF cap was calculated as a right to blue water by using either the relative population or blue water demand size, respectively. The BWA for allocation is determined using two EFR methods, VMF and PRE. The BWA was larger for VMF than for PRE because PRE is a more precautious method. This inversely affected the water scarcity.

The use-what-is-there principle favors upstream sub-catchments because they can consume all sustainable blue water present without considering downstream sub-catchments. This resulted in an increasing blue water scarcity from upstream to downstream, especially in dry seasons when the BWF is large. The addition of reservoirs in the second scenario caused a decrease in blue water scarcity and the difference of blue water scarcity between upstream and downstream sub-catchments due to their temporal and spatial influence on BWA.

However, the application of the use-what-is-there principle still leads to spatial differences in blue water scarcity, because a sub-catchment can consume all blue water that is sustainably available. The third and fourth scenarios allocate the available blue water more evenly over the sub-catchments, thereby decreasing the difference in blue water scarcity between sub-catchments. The other sub-catchments are taken into account by limiting the blue water consumption in some upstream sub-catchments, i.e. lowering the BWF cap. This enables an increase in BWF cap in other downstream sub-catchments. The scenario that considered the relative demand lead to lower overall blue water scarcity and the smallest differences between sub-catchments than the scenario that considered the relative population.

The timing of BWA is influenced by its natural temporal and spatial variability, and the operation of reservoirs. An allocation based on the use-what-is-there principle leads to large regional differences in BWF caps and water scarcity, increasing from upstream to downstream. An allocation principle that considers other sub-catchments mitigates regional differences between upstream and of the BWF caps and water scarcity. The allocation considering other sub-catchments and based on past demand shows the lowest water scarcity values and the most equal distribution of water scarcity if the pattern of past demand and actual demand correspond.

5.2. Recommendation

Based on the results of this study, it is recommended to carry out future research on BWF cap setting and blue water scarcity by continuing to include reservoirs. Reservoirs in tributary sub-catchments should be included in future research as well to obtain a more complete picture of water scarcity in these sub-catchments.

In some cases, the population- and demand-based scenarios lead to an increased water scarcity in tributary sub-catchments with respect to the default and reservoir scenarios. The allocation principle in the population- and demand-based scenarios calculates the right to the blue water of a sub-catchment to set the BWF cap irrespective to the needs of a sub-catchment. A future application of these allocation principles could include the needs of a sub-catchment as an addition to the calculation of the right to a certain amount of blue water. This could be implemented as a validation to check whether a downstream sub-catchment requires the reservation of upstream blue water. An alternative solution could be to check what sub-catchment would benefit more from the allocation of a certain amount of water.

For the implementation of the BWF cap, it is recommended to use the demand-based allocation principle based on the average BWA over a period from 15 to 20 years. The demand-based principle assumes that past demand matches the actual demand in the YRB. The allocation factor that is applied in this principle should be based on a 5-year period prior to the year of BWF cap setting, to capture the change and the most recent spatial distribution in demand. Furthermore, it is recommended to use VMF as EFR method. It is a sophisticated method that captures the natural variability in a river basin and has proven its worth in many types of basins around the world.

References

Abbaspour, K. C. (2015). *SWAT-CUP; SWAT Calibration and Uncertainty Programs.* Ewag: Swiss Federal Institute of Aquatic Science and Technology.

Arnold, J. G., Kiniry, J. R., Srinivasan, R., Williams, J. R., Haney, E. B., & Neitsch, S. L. (2011). *Input/Output Documentation Version 2012.* Temple, Texas: Texas Water Resource Insitute.

Arnold, J. G., Moriasi, D. N., Gassman, P. W., Abbaspour, K. C., White, M. J., Srinivasan, R., . . . Jha, M. K. (2012). SWAT: Model Use, Calibration, and Validation. *American Society of Agricultural and Biological Engineers, 55(4)*, 1491-1508.

Arnold, J. G., Srinivasan, R., Muttiah, R. S., & Williams, J. R. (1998). Large Area Hydrologic Modeling and Assessment Part I: Model Development. *Journal of the American Water Resources Association, 34(1)*, 73-89.

Brown, L. R. (2006). *Plan B 2.0: Rescuing a Planet Under Stress and a Civilization in Trouble.* London: W.W. Norton & Company.

Changming, L., & Shifeng, Z. (2002). Drying up of the Yellow River: it's impacts and countermeasures. *Mitigation and Adaptation Strategies for Global Change, 7,*, 203-214.

CNMIC. (2019). *Chinese National Meteorological Information Center.* Retrieved from http://data.cma.cn/site/index.html

Cong, Z., Yang, D., Gao, B., Yang, H., & Hu, H. (2009). Hydrological trend analysis in the Yellow River basin using a distributed hydrological model. *Water Resources Research, 45(7)*, 0043-1397.

Faramarzi, M., Abbaspour, K. C., Schulin, R., & Yang, H. (2009). Modelling blue and green water resources availability in Iran. *Hydrological Processes, 23*, 486-501.

Gassman, P. W., Reyes, M. R., Green, C. H., & Arnold, J. G. (2007). The Soil and Water Assessment Tool: Historical Development, Applications, and Future Research Directions. *American Society of Agricultural and Biological Engineers, 50(4)*, 1211-1250.

Gu, C., Mu, X., Gao, P., Zhao, G., & Sun, W. (2019). Changes in runoff and sediment load in three parts of the Yellow River Basin, in response to climate change and human activities. *Hydrological Processes, 33(4)*, 585-601.

Hao, F. H., Zhang, X. S., & Yang, Z. F. (2004). A distributed nonpoint-source pollution model: Calibration and validation in the Yellow River basin. *Journal of Environmental Sciences, 16(4)*, 646-650.

Hoekstra, A. Y. (2013). *The Water Footprint of Modern Consumer Society.* Abingdon & New York: Earthscan & Routledge.

Hoekstra, A. Y. (2014). Sustainable, efficient, and equitable water use: the three pillars under wise water allocation. *WIREs Water, 1*, 31-40.

Hoekstra, A. Y., Chapagain, A. K., Aldaya, M. M., & Mekonnen, M. M. (2011). *The water footprint assessment manual - setting the global standard.*

Hoekstra, A. Y., Mekonnen, M. M., Chapagain, A. K., Mathews, R. E., & Richter, B. D. (2012). Global Monthly Water Scarcity: Blue Water Footprints versus Blue Water Availability. *PLoS ONE, 7(2)*, 1-9.

Hogeboom, R. J., De Bruin, D., Schyns, J. F., Krol, M. S., & Hoekstra, A. Y. (2020). Capping Human Water Footprints in the World's River Basins. *Earth's Future, 8*.

Hua, Y., & Cui, B. (2018). Environmental flows and its satisfaction degree forecasting in the Yellow River. *Ecological Indicators, 92*, 207-220.

HWSD. (2009). *Harmonized World Soil Database.* Retrieved from http://westdc.westgis.ac.cn/

IPCC. (2007). *Climate Change 2007: The Physical Science Basis.* New York: Cambridge University Press.

IPCC. (2018). *Global warming of 1.5 °C.* Switzerland: Intergovernmental Panel on Climate Change.

Jiang, S.-h., Zhou, M., Ren, L.-l., Cheng, X.-r., & Zhang, P.-j. (2016). Evaluation of latest TMPA and CMORPH satellite precipitation products over the Yellow River Basin. *Water Science and Engineering, 9(2)*, 87-96.

Karimi, S. S., Yasi, M., & Eslamian, S. (2012). Use of hydrological methods for assessment of environmental flow in a river reach. *International Journal of Environmental Science and Technology, 9(3)*, 549-558.

Krause, P., Boyle, D. P., & Bäse, F. (2005). Comparison of different efficiency criteria for hydrological model assessment . *Advances in Geosciences*, 89-97.

Li, C. H., & Yang, Z. F. (2004). Division assessment of natural runoff in the Yellow River basin. *Journal of Beijing Normal University (Natural Science), 40(4), in Chinese*, 548-553.

Li, D., Jiang, X.-h., Wang, Y., & Li, H. (2001). Analysis of Calculation of Natural Runoff in the Yellow River Basin. *Yellow River, 23(2)*, 35-38.

Li, L., Hao, Z.-C., Wang, J.-H., Wang, Z.-H., & Yu, Z.-B. (2008). Impact of Future Climate Change on Runoff in the Head Region of the Yellow River. *Journal of Hydraulic Engineering, 13* , 347-354.

Liu, J., & Savenije , H. H. (2008). Food consumption patterns and their effect on water requirement in China. *Hydrology and Earth System Science, 12*, 887-898.

Liu, L., Liu, Z., Ren, X., Fischer, T., & Xu, Y. (2011). Hydrological impacts of climate change in the Yellow River Basin for the 21st century using hydrological model and statistical downscaling model. *Quaternary International, 244*, 211-220.

Liu, Q., Zifeng, Y., & Baoshan, C. (2008). Spatial and temporal variability of annual precipitation during 1961-2006 in Yellow River Basin, China. *Journal of Hydrology, 361*, 330-338.

McCuen, R. H., Knight, Z., & Cutter, A. G. (2006). Evaluation of the Nash-Sutcliffe Efficiency Index. *Journal of Hydrological Engineering, 11*, 597-602.

Mekonnen, M. M., & Hoekstra, A. Y. (2016). Four billion people facing severe water scarcity. *Science Advances, 2*.

Moriasi, D. N., Arnold, J. G., Van Liew, M. W., Bingner, R. L., Harmel, R. D., & Veith, T. L. (2007). Model Evaluation Guidelines for Systematic Quantification of Accuracy in Watershed Simulations. *American Society if Agricultural and Biological Engineers, 50(3)*, 885-900.

MWR. (2019). *Chinese Ministry of Water Resources real-time regimen water database.* Retrieved from http://xxfb.mwr.cn/ssIndex.html

Neitsch, S. L., Arnold, J. G., Kiniry, J. R., & Williams, J. R. (2011). *Soil and Water Assessment Tool Theoretical Documentation Version 2009.* Temple, Texas: Grassland, Soil and Water Research Laboratory - Agriculture Research Service & Blackland Research Ceter - Texas Agricultural Experiment Station.

Neitsch, S. L., Arnold, J. G., Kiniry, J. R., Srinivasan, R., & Williams, J. R. (2004). *Soil and Water Assessment Tool Input/Output File Documentation Version 2005.* Temple, Texas: Grassland, Soil and Water Research Laboratory Agriculture Research Service & Blackland Research Ceter Texas Agricultural Experiment Station.

Parikh, M., & Parekh, F. (2019). Hydrological Modelling of Deo River Sub-Basin using SWAT Model and Performance Evaluation using SWAT-CUP. *International Journal of Innovative Technology and Exploring Engineering (IJITEE), 8(12)*, 2890-2896.

Pastor, A. V., Ludwig, F., Biemans, H., Hoff, H., & Kabat, P. (2014). Accounting for environmental flow requirements in global water assessments. *Hydrology and Earth Systems Sciences, 18 (12)*, 5041-5059.

Poff, L. N., Richter, B. D., Arthington, A. H., Bunn, S. E., Naiman, R. J., Kendy, E., . . . Warner, A. (2010). The ecological limits of hydrological alteration (ELOHA): a new framework for developing regional environmental flow standards. *Freshwater Biology, 55*, 147-170.

Postel, S. L. (1999). *Pillar of Sand - Can the irrigation miracle last?* New York: W. W. Norton & Company Ltd.

Postel, S. L. (2000). Entering an era of water scarcity: the challenge ahead. *Ecological Applications*, 941-948.

Ran, L., & Lu, X. X. (2011). Delineation of reservoirs using remote sensing and their storage estimate: an example of the Yellow River Basin, China. *Hydrological Processes, 26*, 1215-1229.

REDCP. (2010). *Chinese Academy of Sciences, Resource and Environment Data Cloud Platform.* Retrieved from http://www.resdc.cn/

REDCP. (2015). *Chinese Academy of Sciences, Resource and Environment Data Cloud Platform.* Retrieved from http://www.resdc.cn/Login.aspx

Richter, B. D., Davis, M. M., Apse, C., & Konrad, C. (2012). A presumptive standard for environmental flow protection. *River Research and Application,*.

Richter, B. D., Warner, A. T., Meyer, J. L., & Lutz, K. (2006). A collaborative and adaptive process for developing environmental flow recommendations. *River Research and application, 22*, 297-318.

Roos, M. D. (1991). Proceedings of The Western Snow Conference; Trend of decreasing snowmelt runoff in northern California. *Trend of decreasing snowmelt runoff in northern California* (pp. 29-36). Juneau: California Department of Water Resources.

Sharma, U., & Dutta, V. (2020). Establishing environmental flows for intermittent tropical rivers: Why hydrological methods are not adequate? *International Journal Science and Technology, 17*, 2949-2966.

Smakhtin, V., Revenga, C., & Döll, P. (2004). A Pilot Global Assessment of Environmental Water Requirements and Scarcity. *Water International, 29(3)*, 307-317.

Tang, Q., Oki, T., Kanae, S., & Hu, H. (2008a). Hydrological cycle changes in the Yellow River Basin during the last half of the 20th century. *Journal of Climate, 21*, 1790-1806.

Tang, Q., Oki, T., Kanae, S., & Hu, H. (2008b). A Spatial Analysis of hydro-climatic and vegetation condition trends in the Yellow River basin. *Hydrological Processes*, 451-458.

United Nations. (2017). *World Population Prospects: key findings & advance tables (2017 revision).* New York: United Nations, Department of Economic and Social Affairs .

United Nations. (2019). *World Economic Situation and Prospects 2019.* New York: United Nations.

USGS. (2019). *United States Geological Survey.* Retrieved from https://hydrosheds.cr.usgs.gov/

Van der Zaag, P., Seyam, I. M., & Savenije, H. H. (2002). Towards measurable criteria for the equitable sharing of international water resources. *Water Policy, 4*, 19-32.

Veldkamp, T. I., Wada, Y., Aerts, J. C., Döll, P., Gosling, S. N., Liu, J., . . . Ward, P. J. (2017). Water scarcity hotspots travel downstream due to human interventions in the 20th and 21st century. *Nature Communications, 8*, 1-12.

Wang, W., Zhuo, L., Li, M., Liu, Y., & Wu, P. (2019a). The effect of development in water-saving irrigation techniques on spatial-temporal variations in crop water footprint and benchmarking. *Journal of Hydrology, 577*, 123916.

Wang, Y., Zhao, W., Wang, S., Feng, X., & Liu, Y. (2019b). Yellow River water rebalanced by human regulation. *Scientific Reports, 9*, 9707.

Wang, Z., Tian, J., & Feng, K. (2019c). Research on runoff simulation in Ningxia Section of the Yellow River basin based on improved SWAT model. *Applied Ecology and Environmental Research, 17(2)*, 3483-3497.

Wu, L., Liu, X., & Ma, X. (2018). Spatio-temporal temperature variations in the Chinese Yellow River Basin from 1981 to 2013. *Weather, 73*, 27-33.

Xie, P., Zhuo, L., Yang, X., Huang, H., Gao, X., & Wu, P. (2020). Spatio-temporal variations in blue and green water resources, water footprint and water scarcities in a large river basin: a case for the Yellow River Basin. *Journal of Hydrology, Manuscript submitted for publication*.

Xu, H., Taylor, R. G., & Xu, Y. (2011). Quantifying uncertainty in the impacts of climate change on river discharge in sub-catchments of the Yangtze and Yellow River Basins, China. *Hydrology and Earth System Sciences, 15*, 333-344.

Yang, D., Li, C., Hu, H., Lei, Z., Yang, S., Kusuda, T., . . . Musiake, K. (2004). Analysis of water resources variability in the Yellow River of China during the last half century using historical data. *Water Resources Research, 40*, W06502.

Yang, K., Ye, B., Zhou, D., Wu, B., Foken, T., Qin, J., & Zhou, Z. (2009a). *Response of hydrological cycle to recent climate changes in the Tibetan Plateau.*

Yang, Z. F., Sun, T., Cui, B. S., Chen, B., & Chen, G. Q. (2009b). Environmental flow requirements for integrated water resources allocation in the Yellow River Basin, China. *Communications in Nonlinear Science and Numerical Simulation, 14*, 2469-2481.

Yin, Y., Tang, Q., Liu, X., & Zhang, X. (2017). Water scarcity under various socio-economic pathways and its potential effect on food production in the Yellow River basin. *Hydrology and Earth System Sciences, 21*, 791-804.

YRCC. (2015). *Yellow River Water Resources Bulletin 2014.* Zhengzhou, China: Yellow River Conservancy Commission .

Yuan, X., Zhang, M., Linying, W., & Zhou, T. (2017). Understanding and seasonal forecasting of hydrological drought in the Anthropocene. *Hydrological Earth System Sciences, 21*, 5477-5492.

Yuan, Z., Yan, D., Yang, Z., Xu, J., Huo, J., Zhou, Y., & Zhang, C. (2018). Attribution assessment and projection of natural runoff change in the Yellow River Basin of China. *Mitigation and Adaptation Strategies for Global Change, 23*, 27 - 49.

Zang, C. F., Liu, J., Van der Velde, M., & Kraxner, F. (2012). Assessment of spatial and temporal patterns of green and blue water flows under natural conditions in inland river basins in Northwest China. *Hydrological and Earth System Sciences, 16*, 2859-2870.

Zhang, Q., Peng, J., Singh, V. P., Li, J., & Chen, Y. C. (2014). Spatio-temporal variations of precipitation in arid and semiarid regions of China: The Yellow River Basin as a case study. *Global and Planetary Change, 114*, 38-49.

Zhang, X., Srinivasan, R., Debele, B., & Hao, F. (2008). Runoff Simulation of the Headwaters of the Yellow River Using the SWAT Model with Three Snowmelt Algorithms. *Journal of the American Water Resource Association, 44(1)*, 48-61.

Zhou, X., Yang, Y., Sheng, Z., & Zhang, Y. (2019). Reconstruted natural runoff helps to quantify the relationship between upstream water use and downstream water scarcity in China's river basins. *Hydrology and Earth System Sciences, 23(5)*, 2491-2505.

Zhu, Z. P., Giordano, M., Cai, X. M., & Molden, D. (2004). The Yellow River basin: water accounting, water accounts and current issues. *Water International, 29(1)*, 2-10.

Zhuo, L., Hoekstra, A. Y., Wu, P., & Zhao, X. (2019). Monthly blue water footprint caps in a river basin to achieve sustainable water consumption: The role of reservoirs. *Science of the Total Environment, 650*, 891-899.

Zhuo, L., Mekonnen, M. M., Hoekstra, A. Y., & Wada, Y. (2016). Inter- and intra-annual variation of water footprint of crops and blue water scarcity in the Yellow River basin (1961-2009). *Advances in Water Resources, 87*, 29-41.

Appendices

Appendix A – Hydrologic operation SWAT

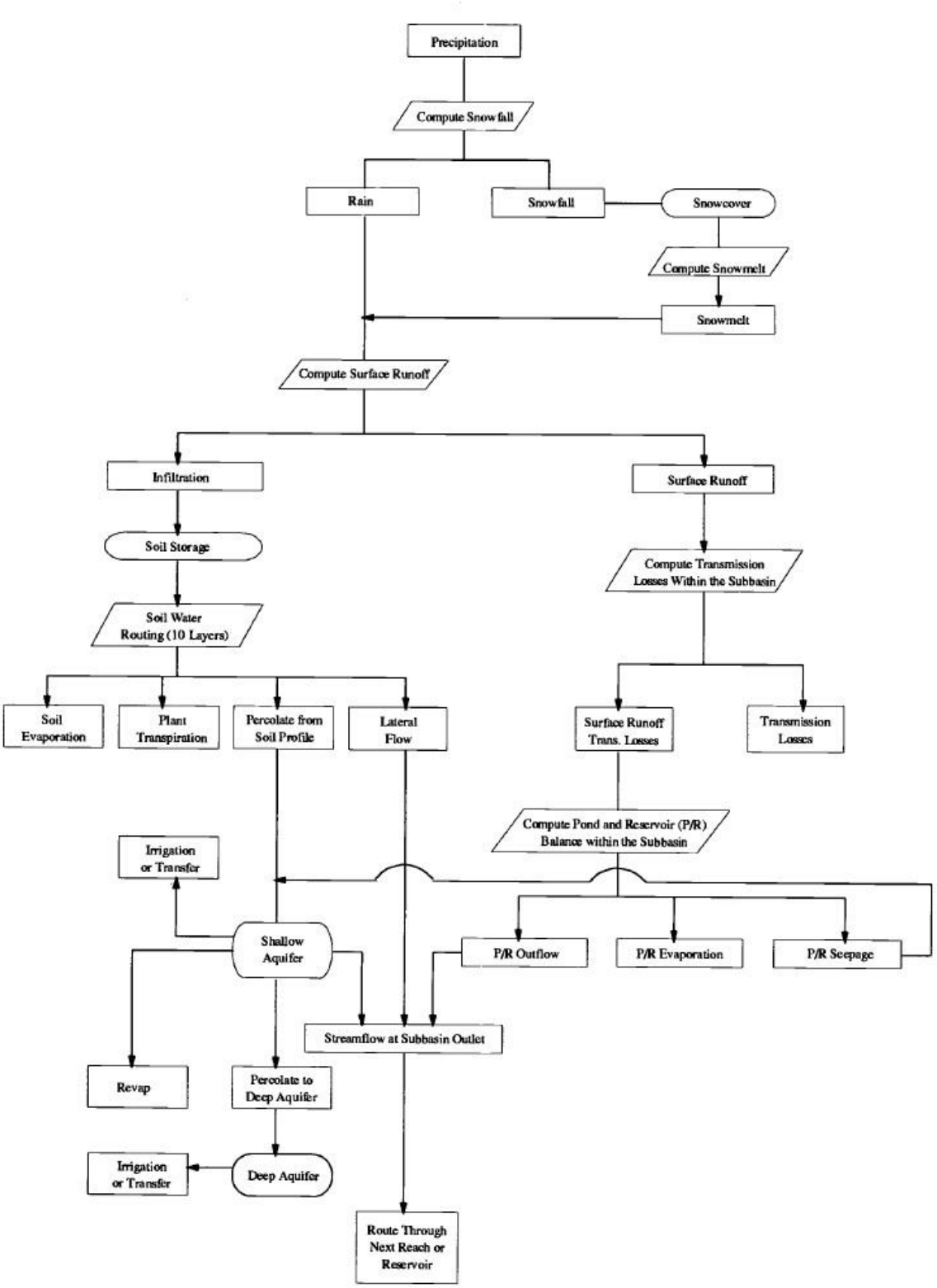

FIGURE 36: HYDROLOGIC FLOW CHART SWAT MODEL (ARNOLD ET AL., 1998).

Appendix B – Soil classes

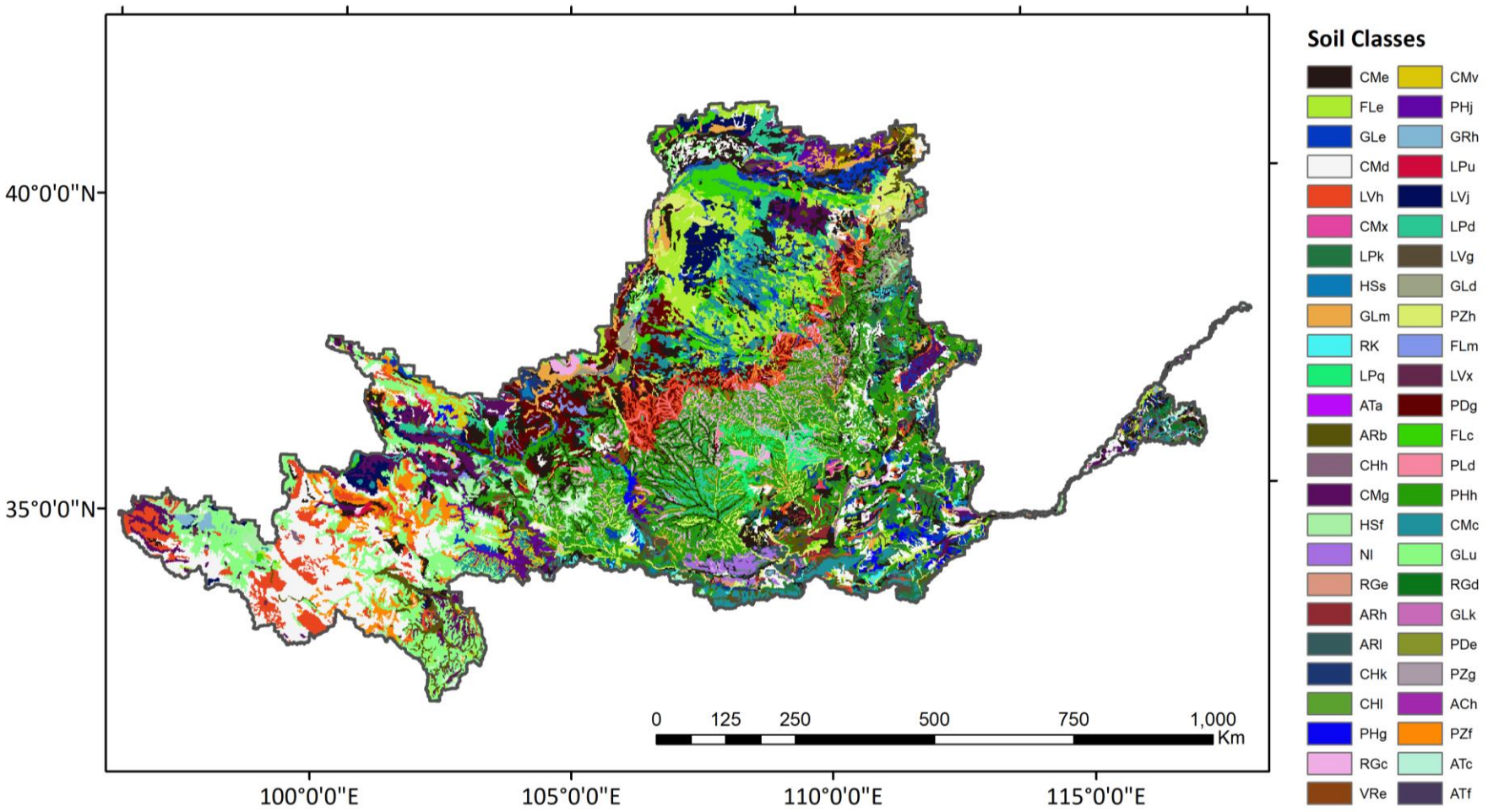

FIGURE 37: SOIL CLASSES YRB USED FOR HRU FORMATION (HWSD, 2009).

Appendix C – HRUs

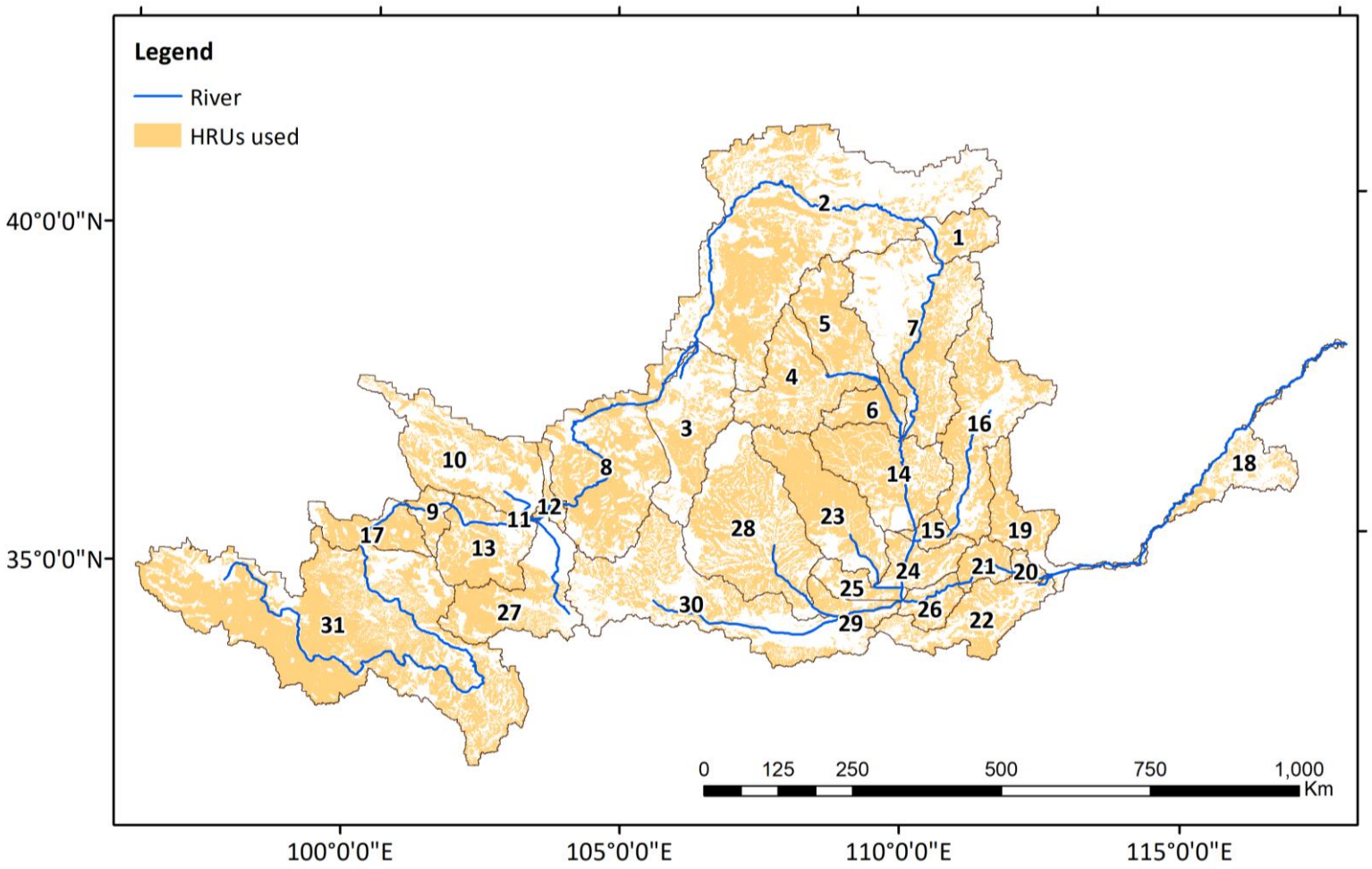

FIGURE 38: HRUS USED BY SWAT FOR THE SIMULATION OF NATURAL RUNOFF

Appendix D – Additional validation

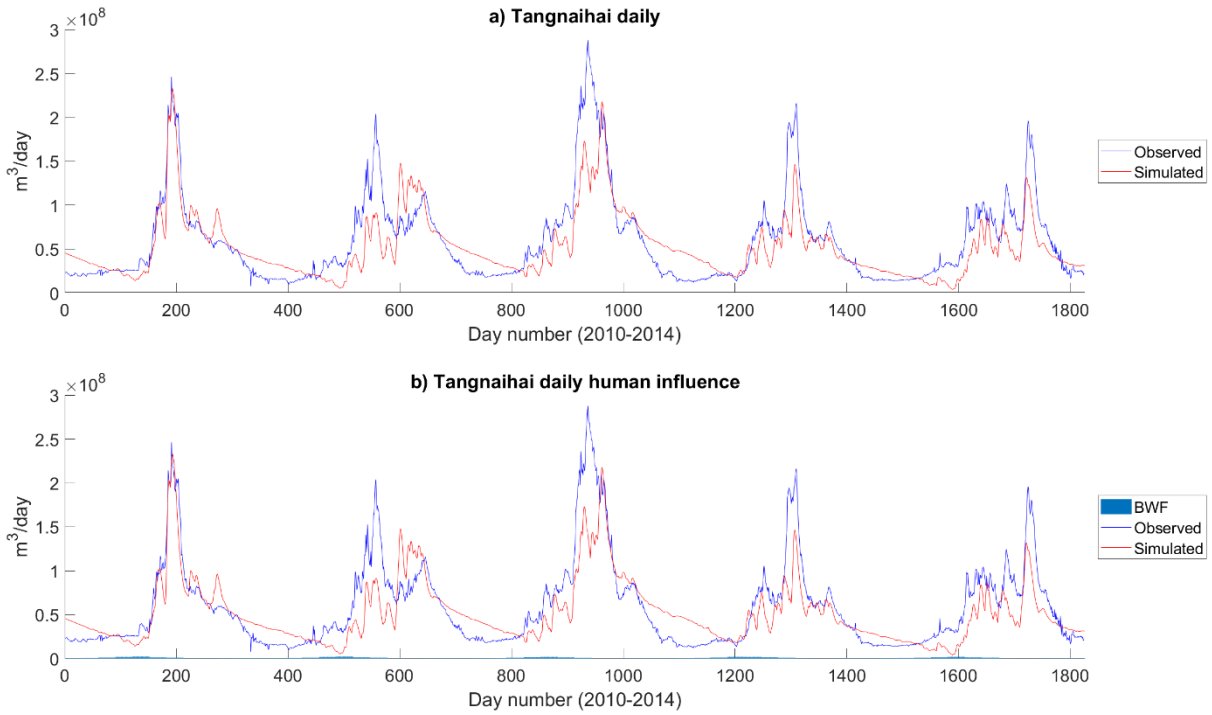

FIGURE 39: A) DAILY AND B) DAILY WITH HUMAN INFLUENCE AS BWF AND SIMULATED STREAMFLOW AT TANGNAIHAI.

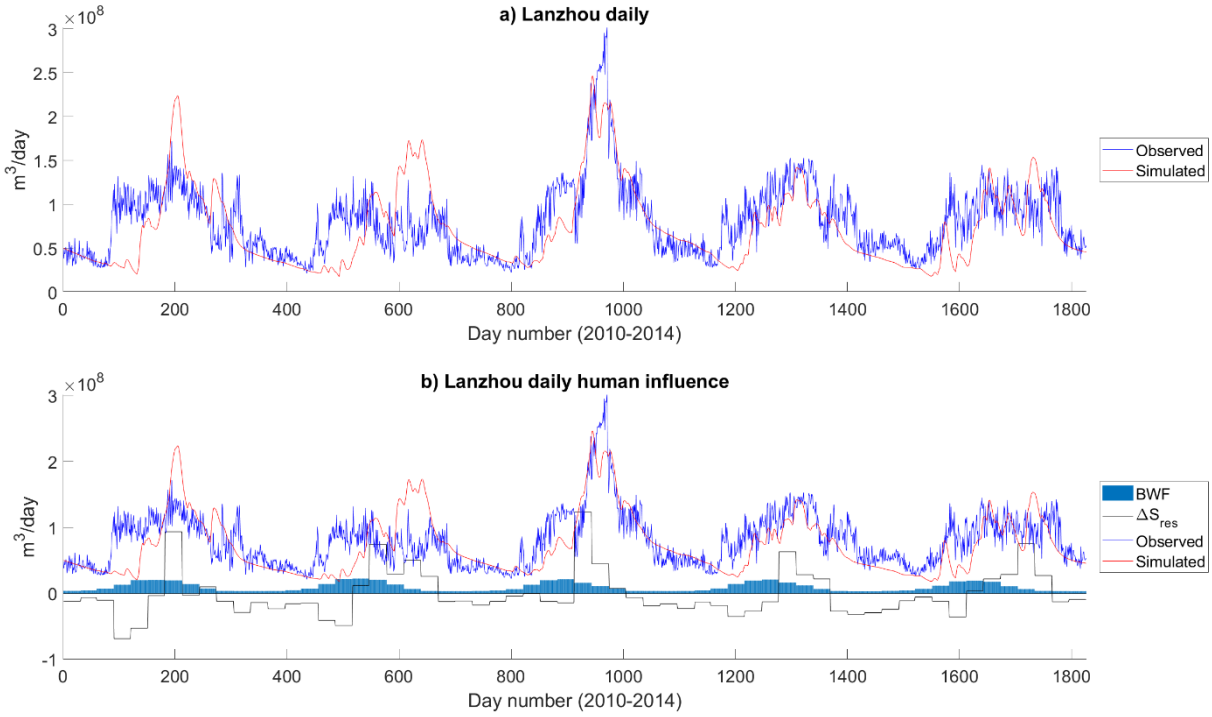

FIGURE 40: A) DAILY AND B) DAILY WITH HUMAN INFLUENCE AS BWF AND RESERVOIR STORAGE CHANGE (ΔS_{res}) AND SIMULATED STREAMFLOW AT LANZHOU.

Appendix E – Monthly average natural runoff

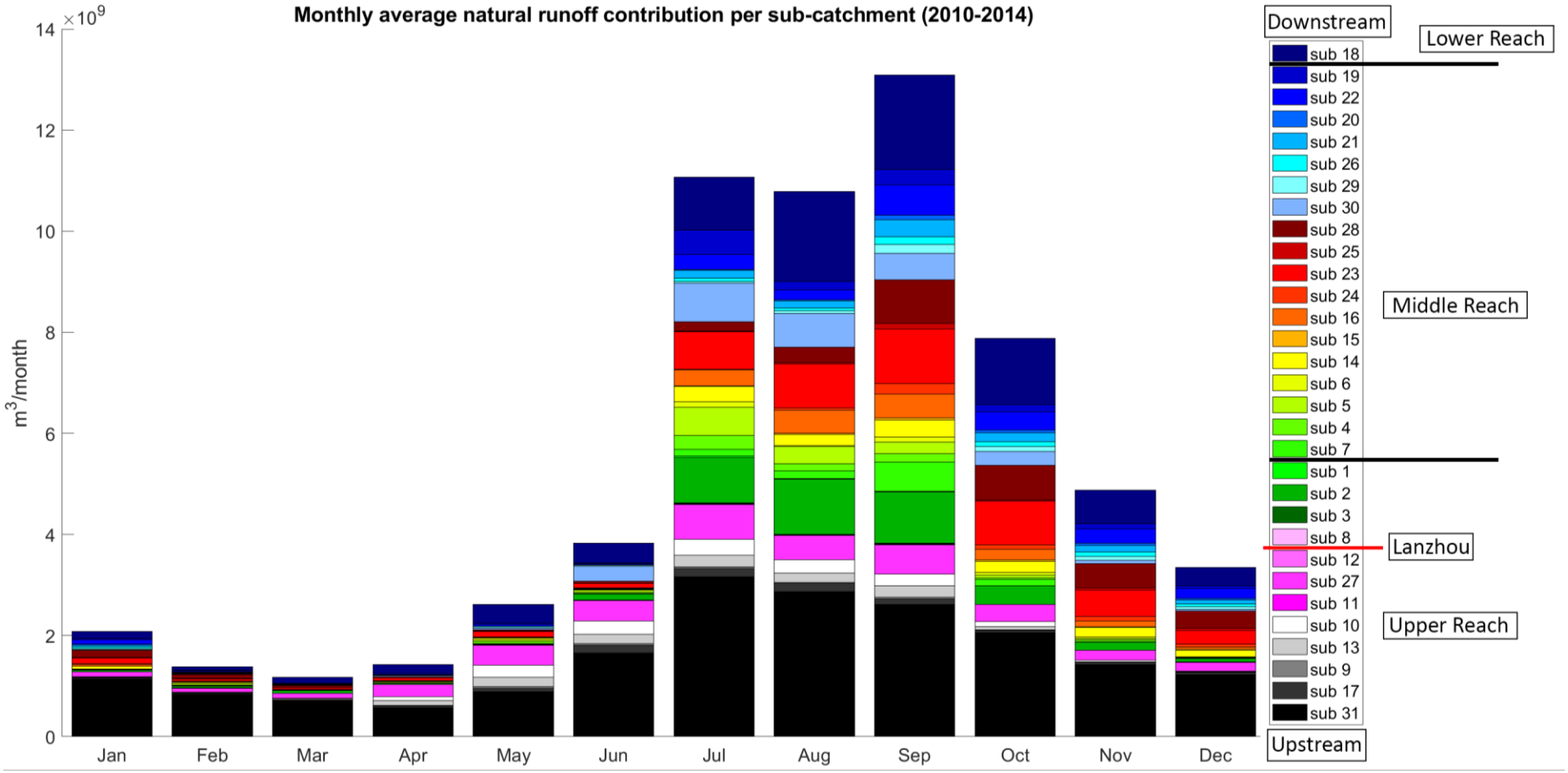

FIGURE 41: MONTHLY AVERAGE NATURAL RUNOFF CONTRIBUTION PER SUB-CATCHMENT FOR THE PERIOD 2010 – 2014 WITH IN THE RIGHT THE DIVISION OF THE THREE REACHES.

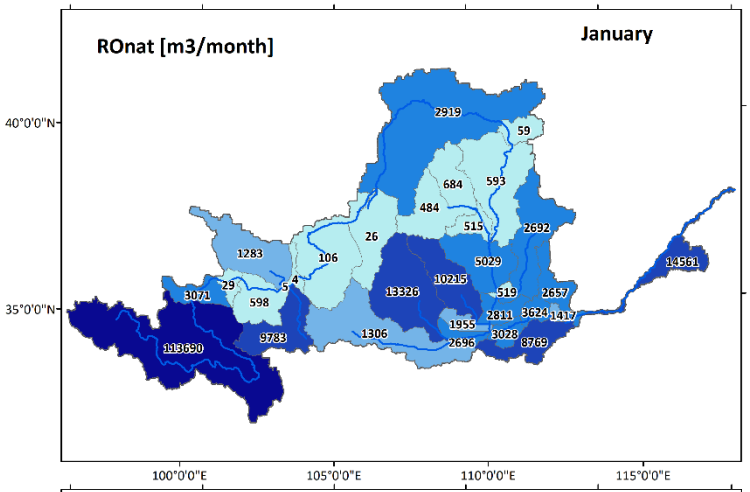
RONat [m3/month]
January
40°0'0"N
35°0'0"N
100°0'0"E
105°0'0"E
110°0'0"E
115°0'0"E
2919
59
684
593
484
515
2692
26
1283
106
5029
14561
29
4
10215
3071
598
13326
519
2657
2811
3624
1417
1955
9783
1306
3028
2696
8769
113690

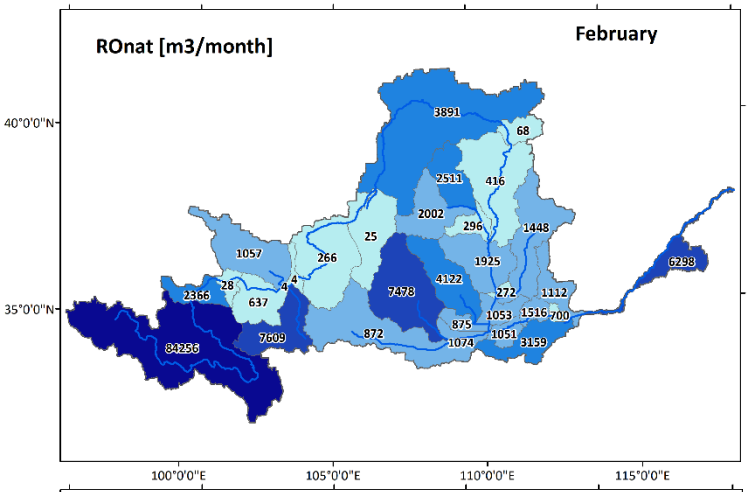
RONat [m3/month]
February
40°0'0"N
35°0'0"N
100°0'0"E
105°0'0"E
110°0'0"E
115°0'0"E
3891
68
2511
416
2002
296
1448
25
1057
266
1925
6298
28
4
4122
2366
637
7478
272
1112
1053
1516
700
875
1051
872
1074
3159
7609
84256

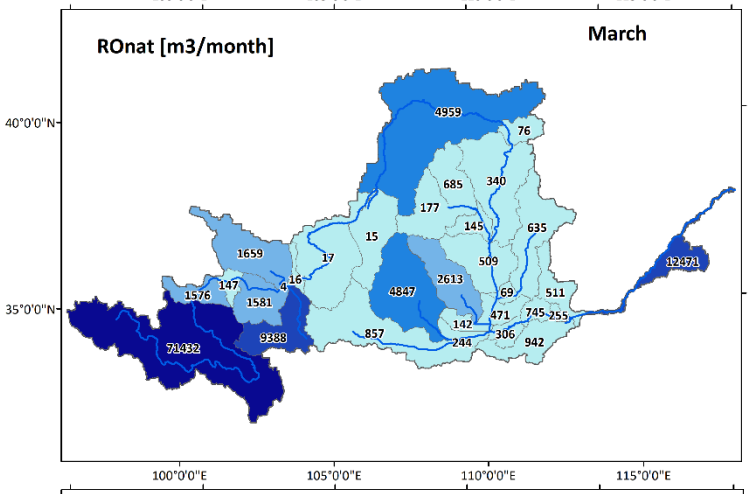
RONat [m3/month]
March
40°0'0"N
35°0'0"N
100°0'0"E
105°0'0"E
110°0'0"E
115°0'0"E
4959
76
685
340
177
145
635
15
1659
17
509
12471
16
147
4
2613
1576
1581
4847
69
511
471
745
255
142
9388
857
306
942
244
71432

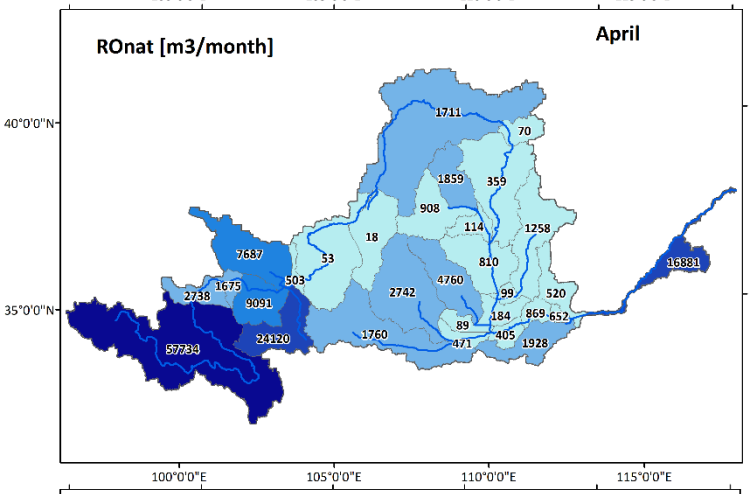
RONat [m3/month]
April
40°0'0"N
35°0'0"N
100°0'0"E
105°0'0"E
110°0'0"E
115°0'0"E
1711
70
1859
359
908
114
1258
18
7687
53
810
16881
1675
503
4760
2738
9091
2742
99
520
184
869
652
89
24120
1760
405
1928
471
97734

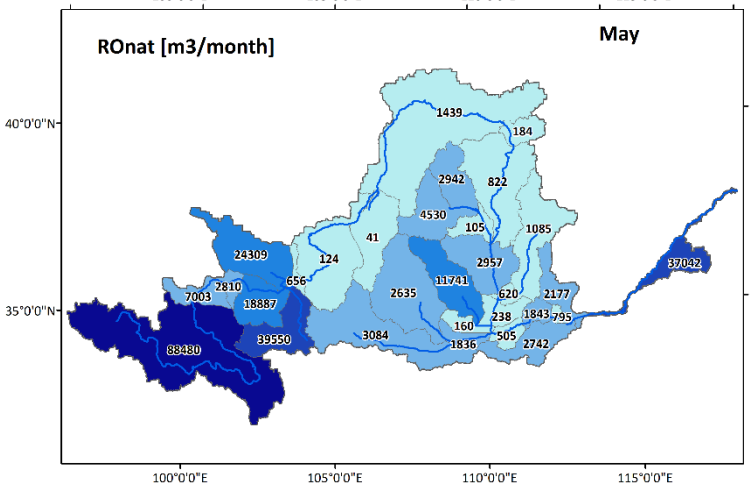
RONat [m3/month]
May
40°0'0"N
35°0'0"N
100°0'0"E
105°0'0"E
110°0'0"E
115°0'0"E
1439
184
2942
822
4530
105
1085
41
24309
124
2957
37042
656
11741
2810
2635
620
2177
7003
18887
160
238
1843
795
39550
3084
505
2742
1836
88480

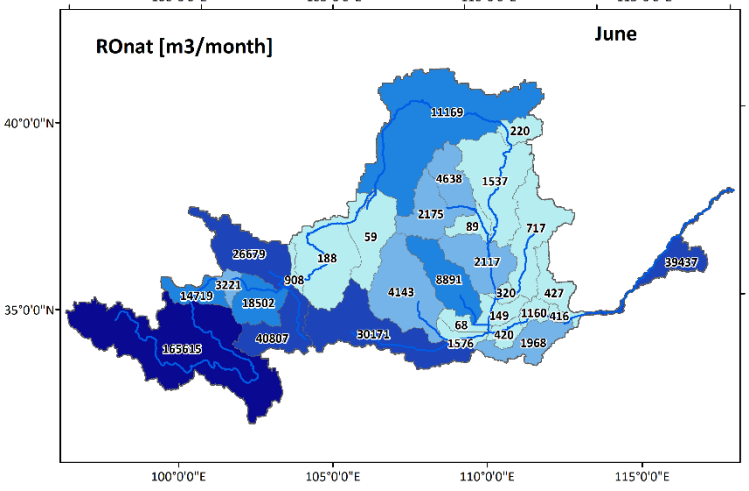
RONat [m3/month]
June
40°0'0"N
35°0'0"N
100°0'0"E
105°0'0"E
110°0'0"E
115°0'0"E
11169
220
4638
1537
2175
89
717
59
26679
188
2117
39437
3221
908
8891
14719
18502
4143
320
427
68
149
1160
416
40807
30171
420
1576
1968
165815

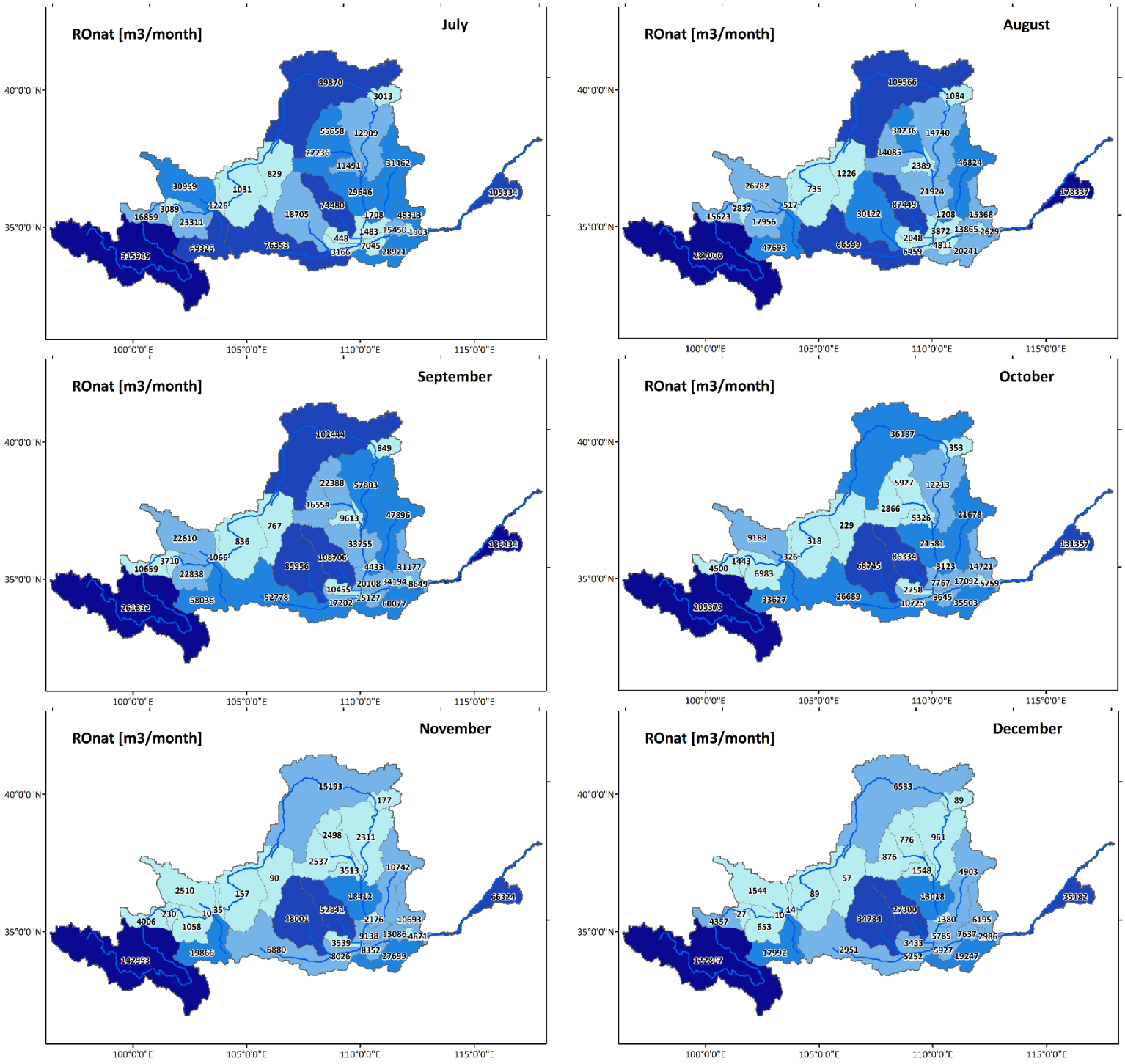

FIGURE 42: AVERAGE MONTHLY NATURAL RUNOFF PER SUB-CATCHMENT IN M3 PER MONTH (2010 – 2014).

Appendix F – Natural runoff in mm/month

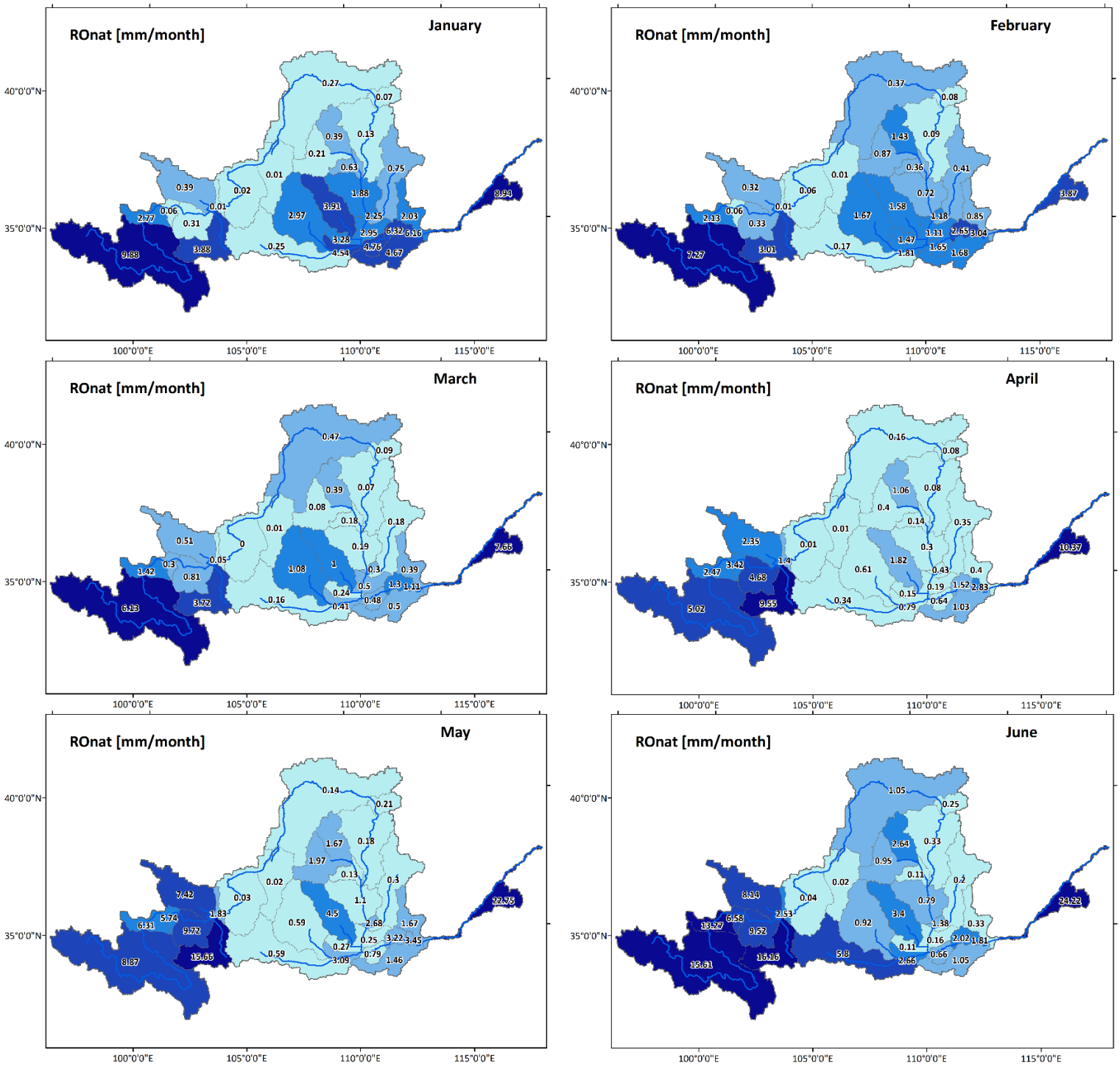

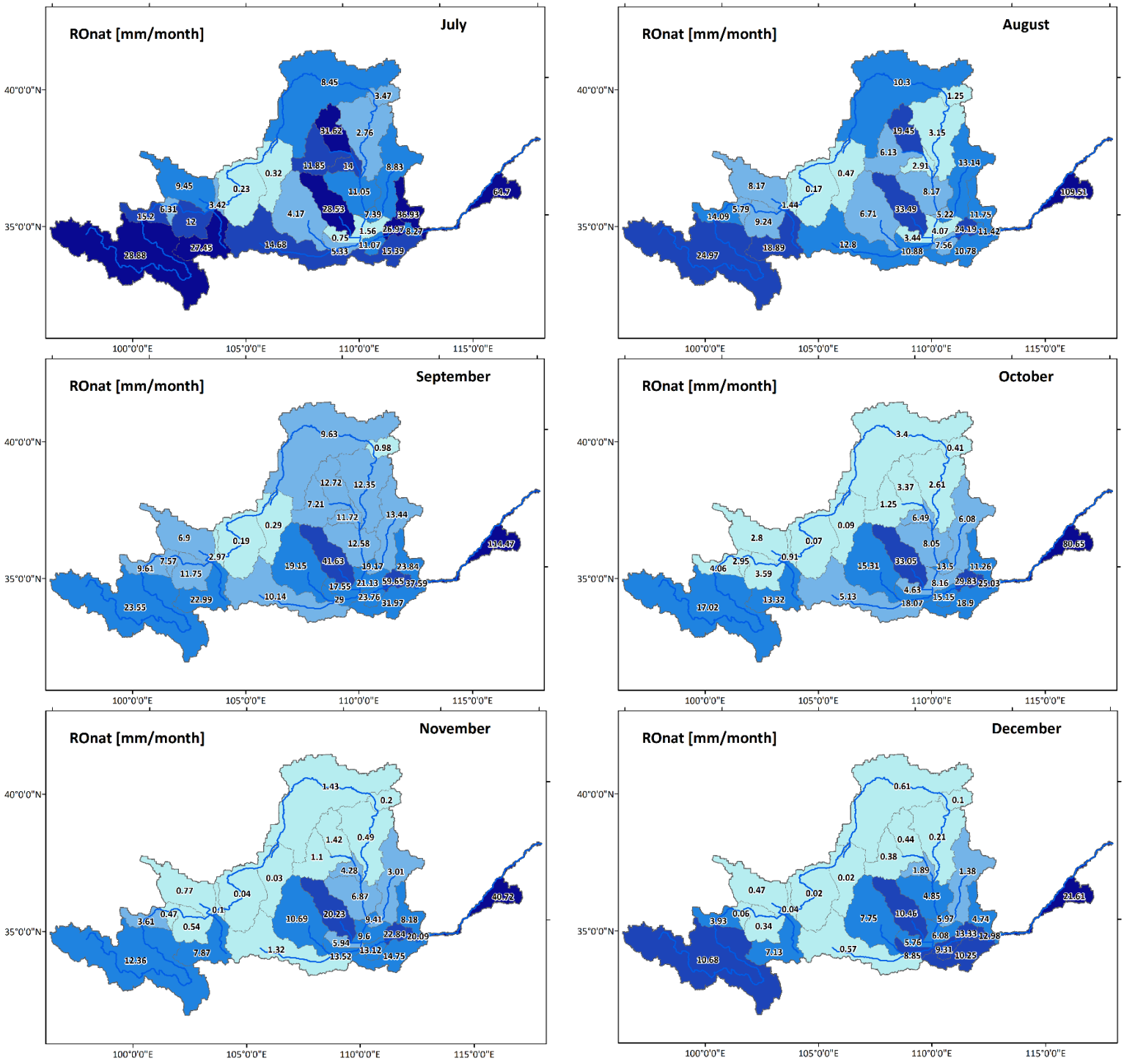

FIGURE 43: AVERAGE MONTHLY NATURAL RUNOFF PER SUB-CATCHMENT IN MM PER MONTH (2010 – 2014).

Appendix G – BWF cap default scenario

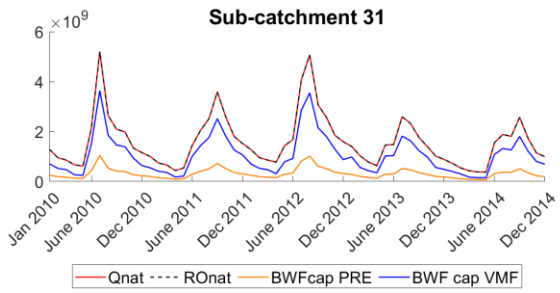

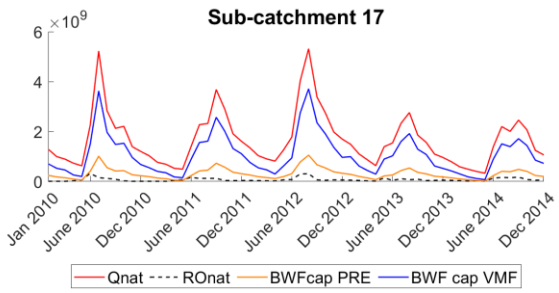

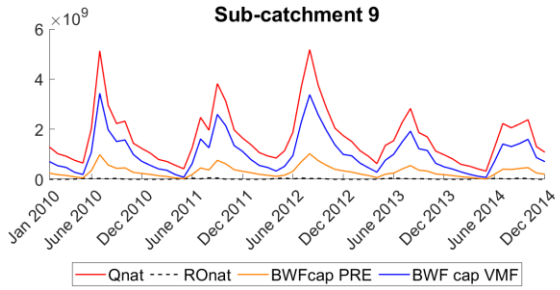

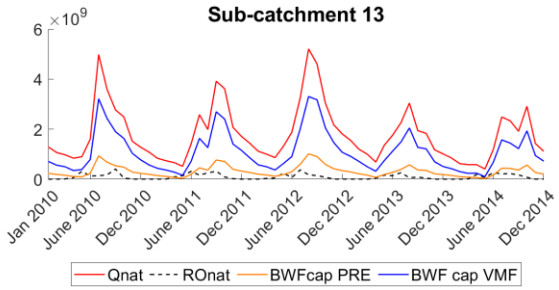

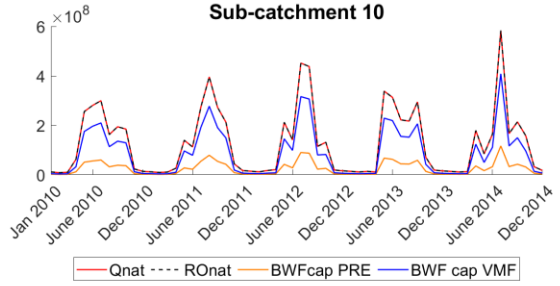

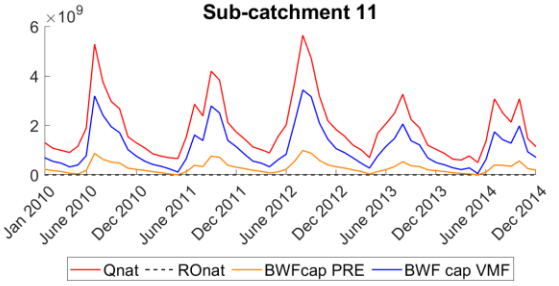

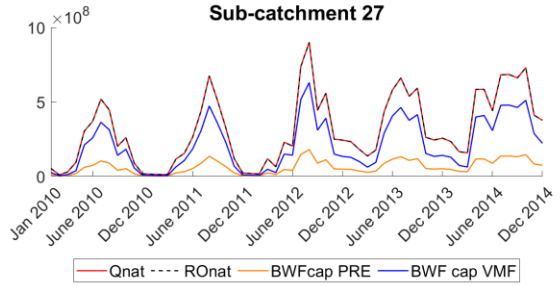

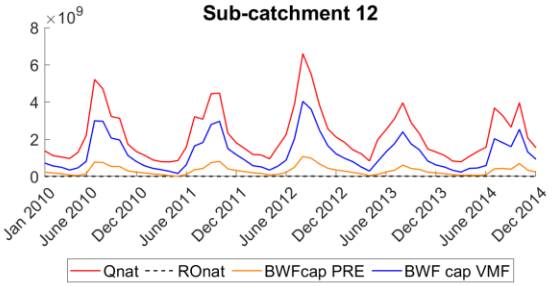

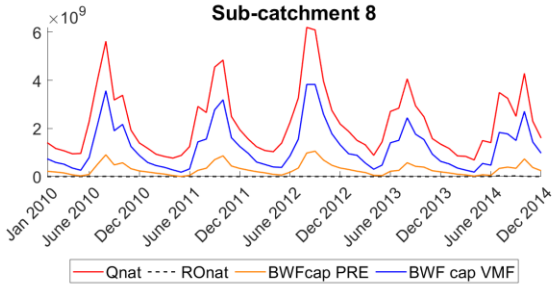
Sub-catchment 8
×10^9
6
4
2
0
Jan 2010
June 2010
Dec 2010
June 2011
Dec 2011
June 2012
Dec 2012
June 2013
Dec 2013
June 2014
Dec 2014
Qnat
ROnat
BWFcap PRE
BWF cap VMF

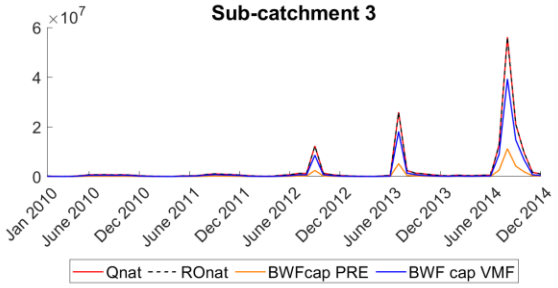
Sub-catchment 3
×10^7
6
4
2
0
Jan 2010
June 2010
Dec 2010
June 2011
Dec 2011
June 2012
Dec 2012
June 2013
Dec 2013
June 2014
Dec 2014
Qnat
ROnat
BWFcap PRE
BWF cap VMF

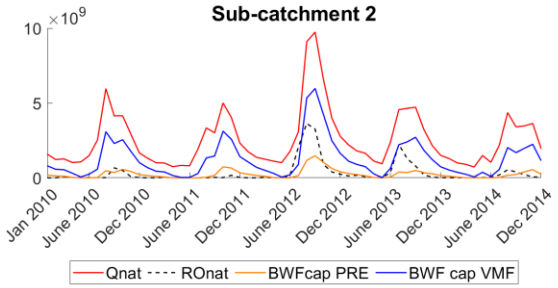
Sub-catchment 2
×10^9
10
5
0
Jan 2010
June 2010
Dec 2010
June 2011
Dec 2011
June 2012
Dec 2012
June 2013
Dec 2013
June 2014
Dec 2014
Qnat
ROnat
BWFcap PRE
BWF cap VMF

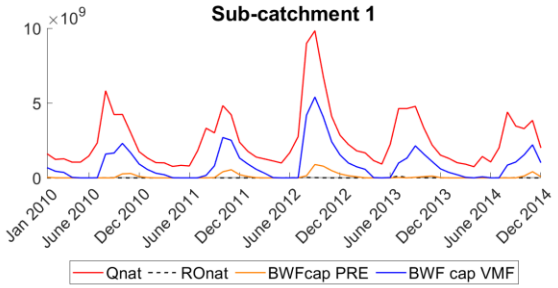
Sub-catchment 1
×10^9
10
5
0
Jan 2010
June 2010
Dec 2010
June 2011
Dec 2011
June 2012
Dec 2012
June 2013
Dec 2013
June 2014
Dec 2014
Qnat
ROnat
BWFcap PRE
BWF cap VMF

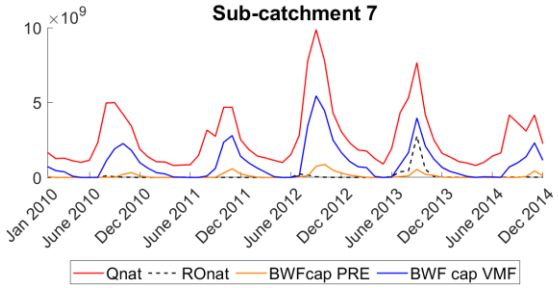
Sub-catchment 7
×10^9
10
5
0
Jan 2010
June 2010
Dec 2010
June 2011
Dec 2011
June 2012
Dec 2012
June 2013
Dec 2013
June 2014
Dec 2014
Qnat
ROnat
BWFcap PRE
BWF cap VMF

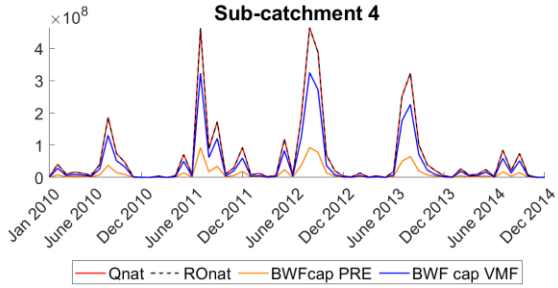
Sub-catchment 4
×10^8
4
3
2
1
0
Jan 2010
June 2010
Dec 2010
June 2011
Dec 2011
June 2012
Dec 2012
June 2013
Dec 2013
June 2014
Dec 2014
Qnat
ROnat
BWFcap PRE
BWF cap VMF

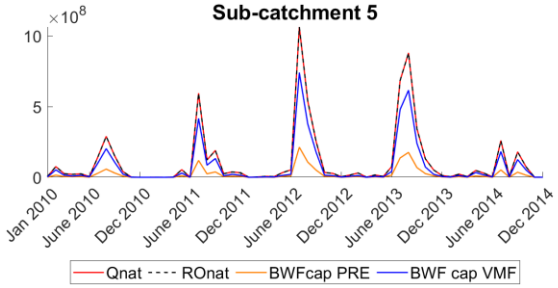
Sub-catchment 5
×10^8
10
5
0
Jan 2010
June 2010
Dec 2010
June 2011
Dec 2011
June 2012
Dec 2012
June 2013
Dec 2013
June 2014
Dec 2014
Qnat
ROnat
BWFcap PRE
BWF cap VMF

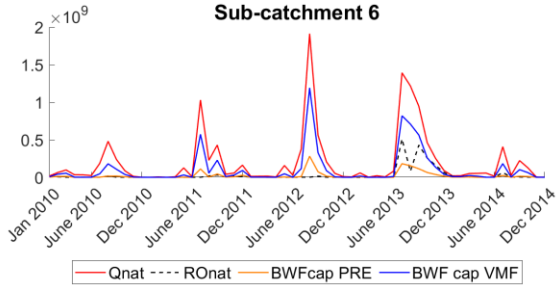
Sub-catchment 6
×10^9
2
1.5
1
0.5
0
Jan 2010
June 2010
Dec 2010
June 2011
Dec 2011
June 2012
Dec 2012
June 2013
Dec 2013
June 2014
Dec 2014
Qnat
ROnat
BWFcap PRE
BWF cap VMF

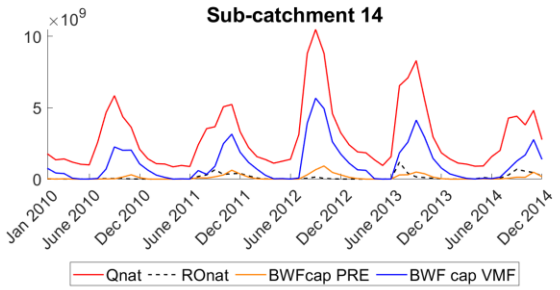
Sub-catchment 14
×10^9
10
5
0
Jan 2010
June 2010
Dec 2010
June 2011
Dec 2011
June 2012
Dec 2012
June 2013
Dec 2013
June 2014
Dec 2014
Qnat
ROnat
BWFcap PRE
BWF cap VMF

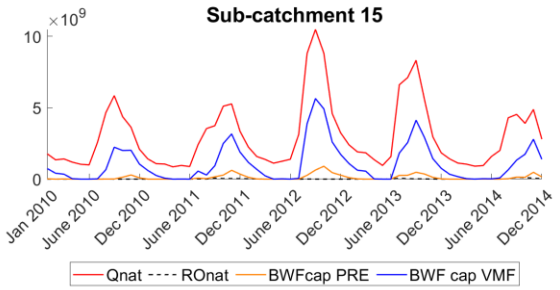
Sub-catchment 15
×10^9
10
5
0
Jan 2010
June 2010
Dec 2010
June 2011
Dec 2011
June 2012
Dec 2012
June 2013
Dec 2013
June 2014
Dec 2014
Qnat
ROnat
BWFcap PRE
BWF cap VMF

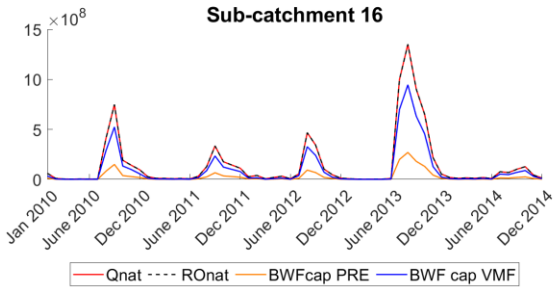
Sub-catchment 16
×10^8
15
10
5
0
Jan 2010
June 2010
Dec 2010
June 2011
Dec 2011
June 2012
Dec 2012
June 2013
Dec 2013
June 2014
Dec 2014
Qnat
ROnat
BWFcap PRE
BWF cap VMF

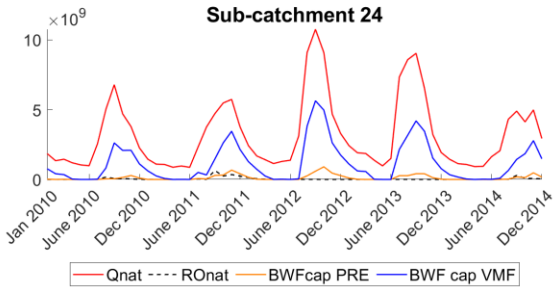
Sub-catchment 24
×10^9
10
5
0
Jan 2010
June 2010
Dec 2010
June 2011
Dec 2011
June 2012
Dec 2012
June 2013
Dec 2013
June 2014
Dec 2014
Qnat
ROnat
BWFcap PRE
BWF cap VMF

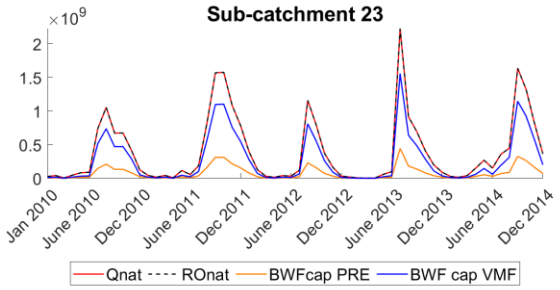
Sub-catchment 23
×10^9
2
1.5
1
0.5
0
Jan 2010
June 2010
Dec 2010
June 2011
Dec 2011
June 2012
Dec 2012
June 2013
Dec 2013
June 2014
Dec 2014
Qnat
ROnat
BWFcap PRE
BWF cap VMF

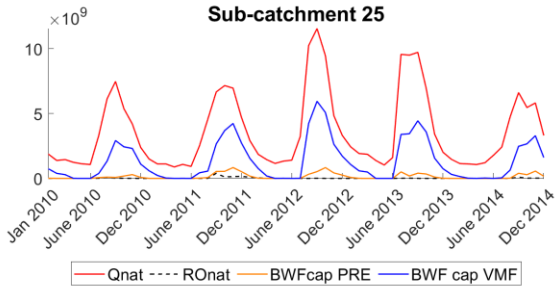
Sub-catchment 25
×10^9
10
5
0
Jan 2010
June 2010
Dec 2010
June 2011
Dec 2011
June 2012
Dec 2012
June 2013
Dec 2013
June 2014
Dec 2014
Qnat
ROnat
BWFcap PRE
BWF cap VMF

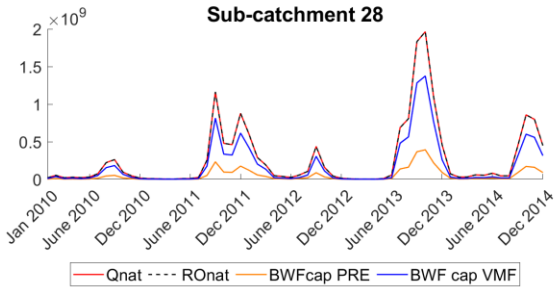
Sub-catchment 28
×10^9
2
1.5
1
0.5
0
Jan 2010
June 2010
Dec 2010
June 2011
Dec 2011
June 2012
Dec 2012
June 2013
Dec 2013
June 2014
Dec 2014
Qnat
ROnat
BWFcap PRE
BWF cap VMF

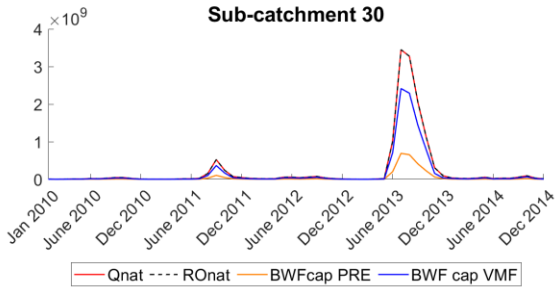
Sub-catchment 30
×10^9
4
3
2
1
0
Jan 2010
June 2010
Dec 2010
June 2011
Dec 2011
June 2012
Dec 2012
June 2013
Dec 2013
June 2014
Dec 2014
Qnat
ROnat
BWFcap PRE
BWF cap VMF

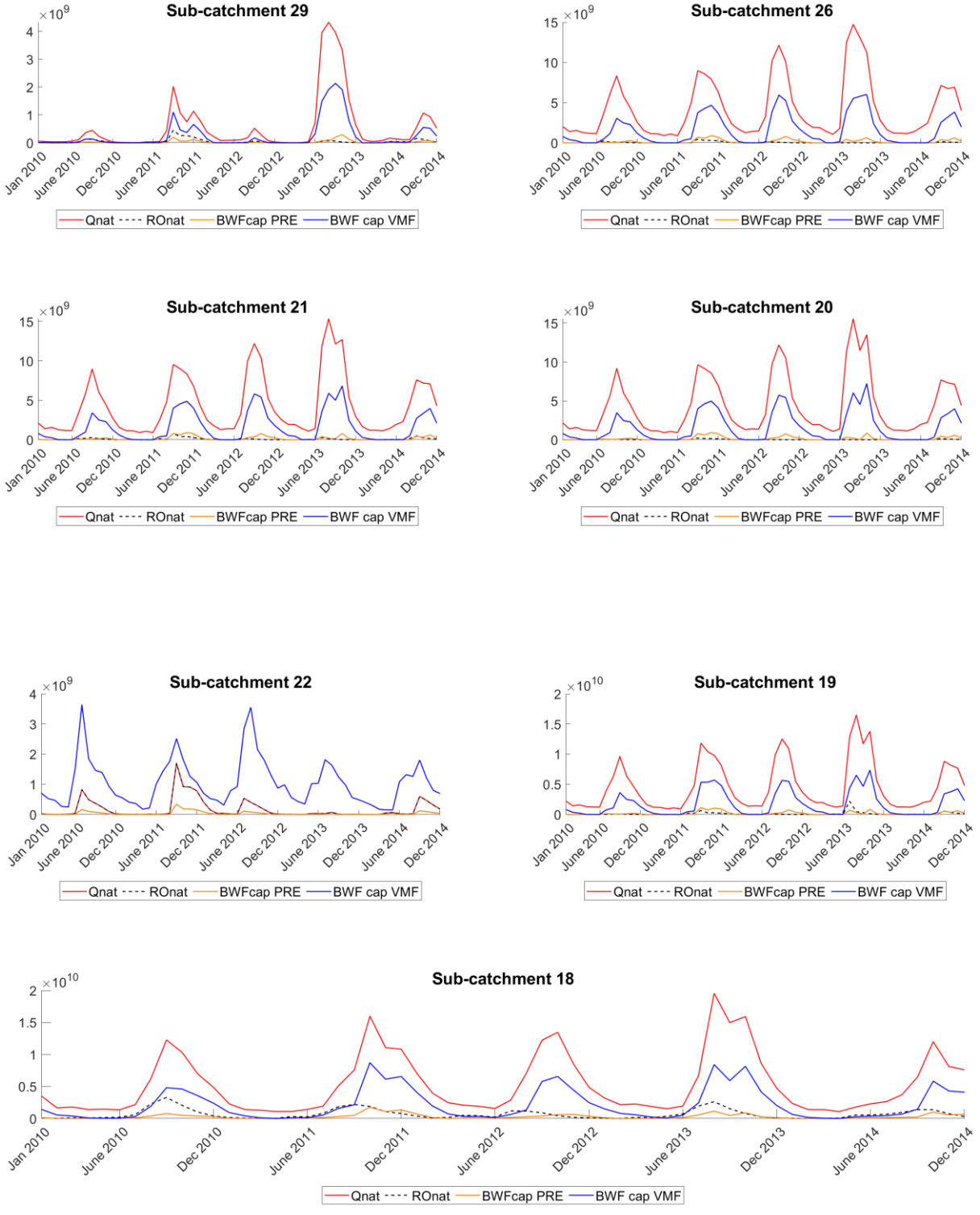

FIGURE 44: DEFAULT SCENARIO BWF CAP PER SUB-CATCHMENT INDIVIDUALLY FOR PRE AND VMF METHOD INCLUDING NATURAL STREAMFLOW (Q_{nat}) AND NATURAL RUNOFF (RO_{nat}).

Appendix H – BWF cap reservoir scenario

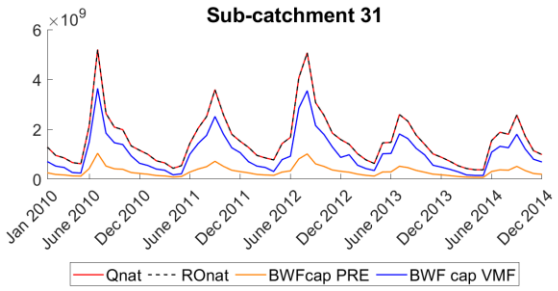

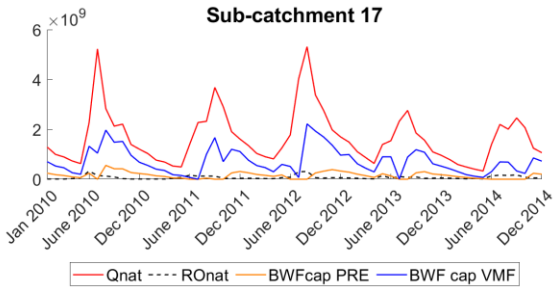

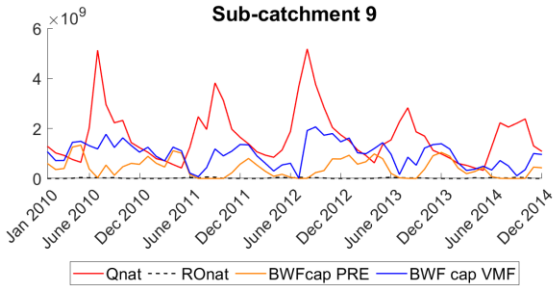

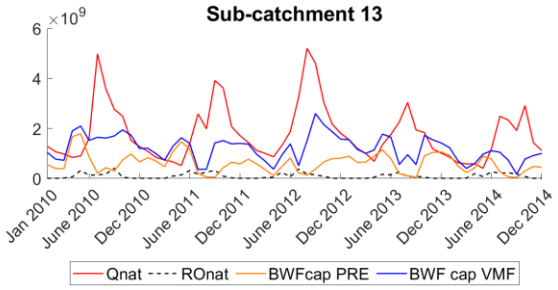

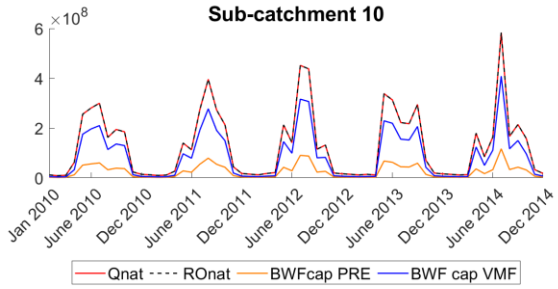

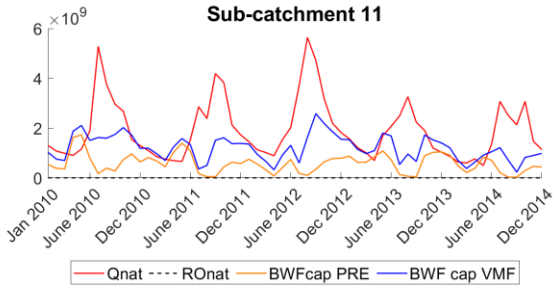

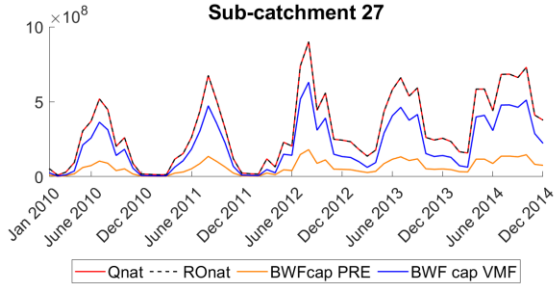

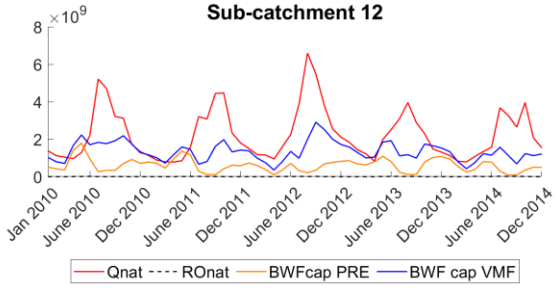

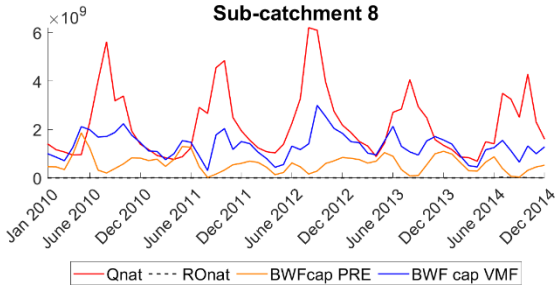
Sub-catchment 8
×10^9
6
4
2
0
Jan 2010
June 2010
Dec 2010
June 2011
Dec 2011
June 2012
Dec 2012
June 2013
Dec 2013
June 2014
Dec 2014
Qnat
ROnat
BWFcap PRE
BWF cap VMF

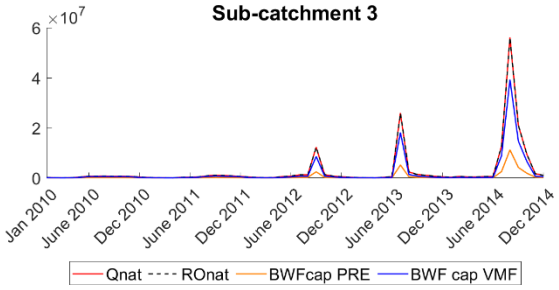
Sub-catchment 3
×10^7
6
4
2
0
Jan 2010
June 2010
Dec 2010
June 2011
Dec 2011
June 2012
Dec 2012
June 2013
Dec 2013
June 2014
Dec 2014
Qnat
ROnat
BWFcap PRE
BWF cap VMF

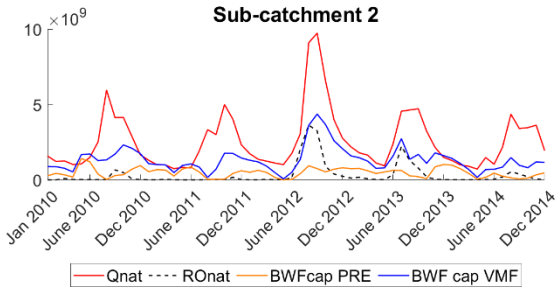
Sub-catchment 2
×10^9
10
5
0
Jan 2010
June 2010
Dec 2010
June 2011
Dec 2011
June 2012
Dec 2012
June 2013
Dec 2013
June 2014
Dec 2014
Qnat
ROnat
BWFcap PRE
BWF cap VMF

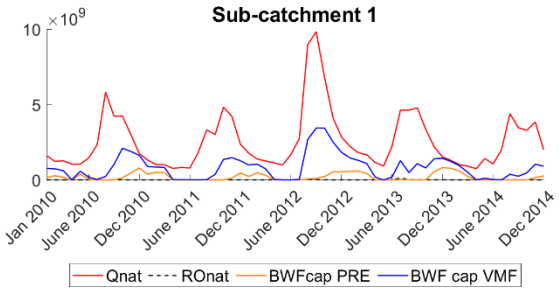
Sub-catchment 1
×10^9
10
5
0
Jan 2010
June 2010
Dec 2010
June 2011
Dec 2011
June 2012
Dec 2012
June 2013
Dec 2013
June 2014
Dec 2014
Qnat
ROnat
BWFcap PRE
BWF cap VMF

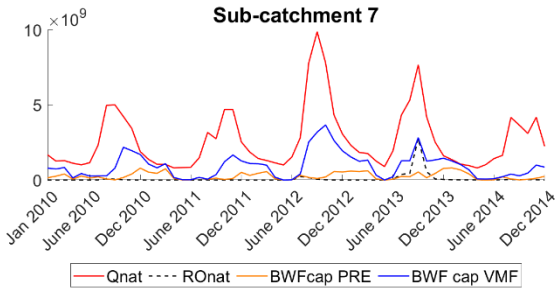
Sub-catchment 7
×10^9
10
5
0
Jan 2010
June 2010
Dec 2010
June 2011
Dec 2011
June 2012
Dec 2012
June 2013
Dec 2013
June 2014
Dec 2014
Qnat
ROnat
BWFcap PRE
BWF cap VMF

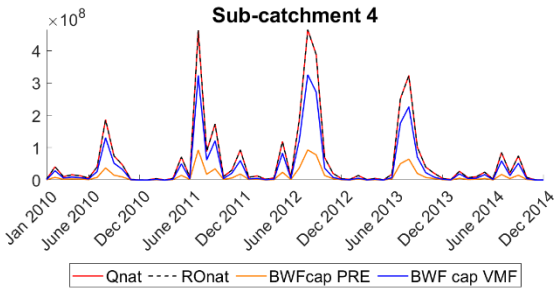
Sub-catchment 4
×10^8
4
3
2
1
0
Jan 2010
June 2010
Dec 2010
June 2011
Dec 2011
June 2012
Dec 2012
June 2013
Dec 2013
June 2014
Dec 2014
Qnat
ROnat
BWFcap PRE
BWF cap VMF

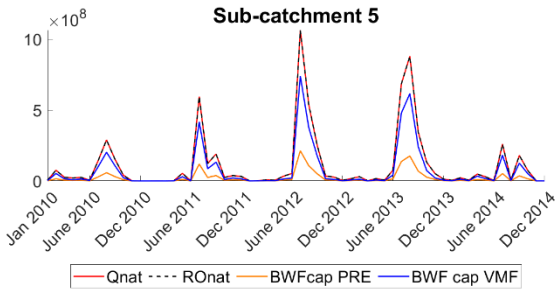
Sub-catchment 5
×10^8
10
5
0
Jan 2010
June 2010
Dec 2010
June 2011
Dec 2011
June 2012
Dec 2012
June 2013
Dec 2013
June 2014
Dec 2014
Qnat
ROnat
BWFcap PRE
BWF cap VMF

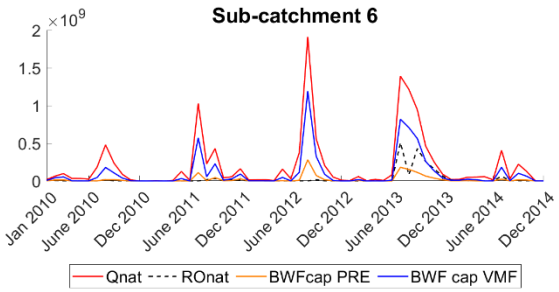
Sub-catchment 6
×10^9
2
1.5
1
0.5
0
Jan 2010
June 2010
Dec 2010
June 2011
Dec 2011
June 2012
Dec 2012
June 2013
Dec 2013
June 2014
Dec 2014
Qnat
ROnat
BWFcap PRE
BWF cap VMF

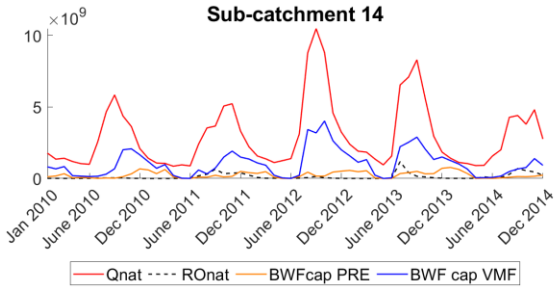
Sub-catchment 14
×10^9
10
5
0
Jan 2010
June 2010
Dec 2010
June 2011
Dec 2011
June 2012
Dec 2012
June 2013
Dec 2013
June 2014
Dec 2014
Qnat
ROnat
BWFcap PRE
BWF cap VMF

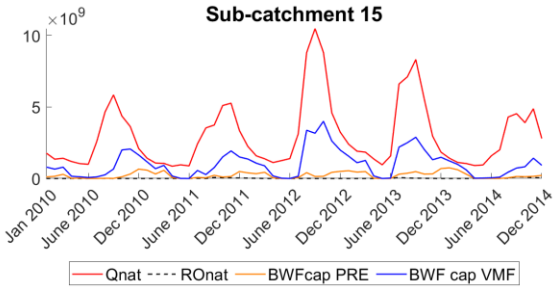
Sub-catchment 15
×10^9
10
5
0
Jan 2010
June 2010
Dec 2010
June 2011
Dec 2011
June 2012
Dec 2012
June 2013
Dec 2013
June 2014
Dec 2014
Qnat
ROnat
BWFcap PRE
BWF cap VMF

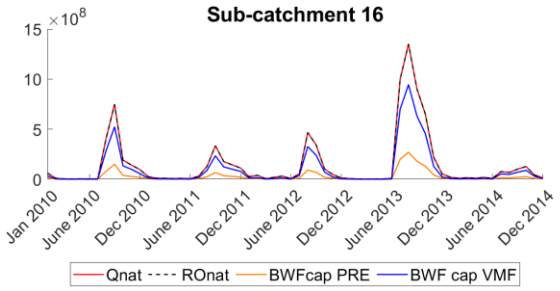
Sub-catchment 16
×10^8
15
10
5
0
Jan 2010
June 2010
Dec 2010
June 2011
Dec 2011
June 2012
Dec 2012
June 2013
Dec 2013
June 2014
Dec 2014
Qnat
ROnat
BWFcap PRE
BWF cap VMF

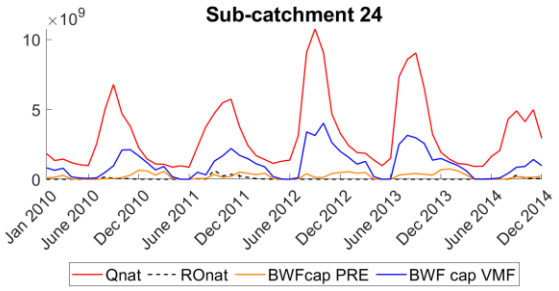
Sub-catchment 24
×10^9
10
5
0
Jan 2010
June 2010
Dec 2010
June 2011
Dec 2011
June 2012
Dec 2012
June 2013
Dec 2013
June 2014
Dec 2014
Qnat
ROnat
BWFcap PRE
BWF cap VMF

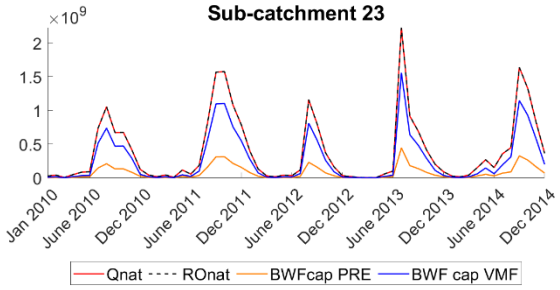
Sub-catchment 23
×10^9
2
1.5
1
0.5
0
Jan 2010
June 2010
Dec 2010
June 2011
Dec 2011
June 2012
Dec 2012
June 2013
Dec 2013
June 2014
Dec 2014
Qnat
ROnat
BWFcap PRE
BWF cap VMF

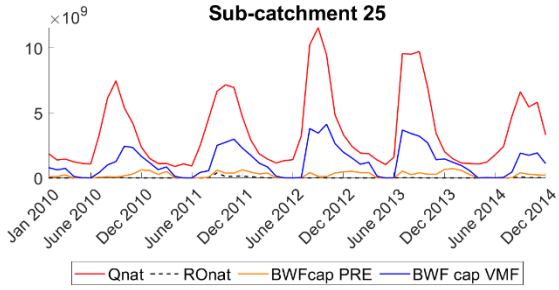
Sub-catchment 25
×10^9
10
5
0
Jan 2010
June 2010
Dec 2010
June 2011
Dec 2011
June 2012
Dec 2012
June 2013
Dec 2013
June 2014
Dec 2014
Qnat
ROnat
BWFcap PRE
BWF cap VMF

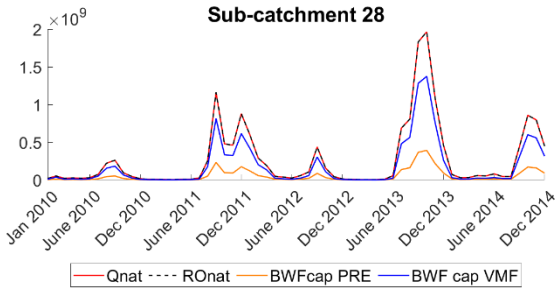
Sub-catchment 28
×10^9
2
1.5
1
0.5
0
Jan 2010
June 2010
Dec 2010
June 2011
Dec 2011
June 2012
Dec 2012
June 2013
Dec 2013
June 2014
Dec 2014
Qnat
ROnat
BWFcap PRE
BWF cap VMF

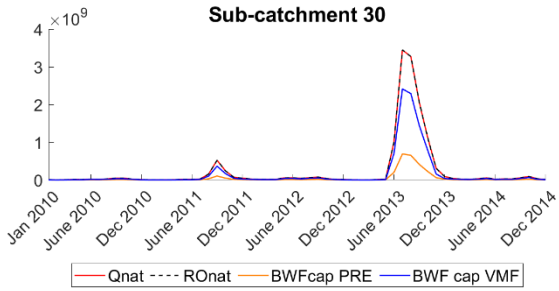
Sub-catchment 30
×10^9
4
3
2
1
0
Jan 2010
June 2010
Dec 2010
June 2011
Dec 2011
June 2012
Dec 2012
June 2013
Dec 2013
June 2014
Dec 2014
Qnat
ROnat
BWFcap PRE
BWF cap VMF

FIGURE 45: RESERVOIR SCENARIO BWF CAP PER SUB-CATCHMENT INDIVIDUALLY FOR PRE AND VMF METHOD INCLUDING NATURAL STREAMFLOW (Q_{nat}) AND NATURAL RUNOFF (RO_{nat}).

Appendix I – BWF cap population-based scenario

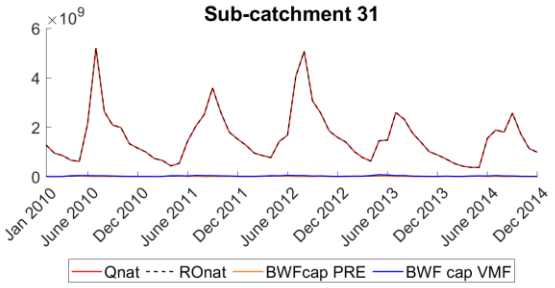

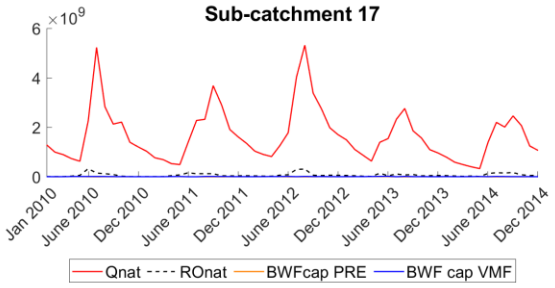

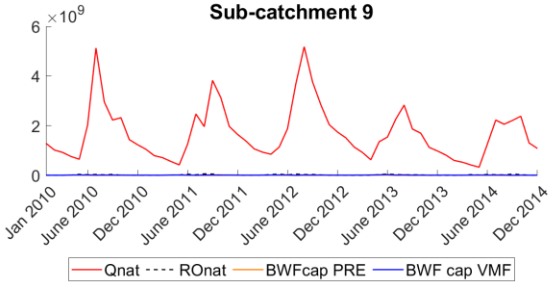

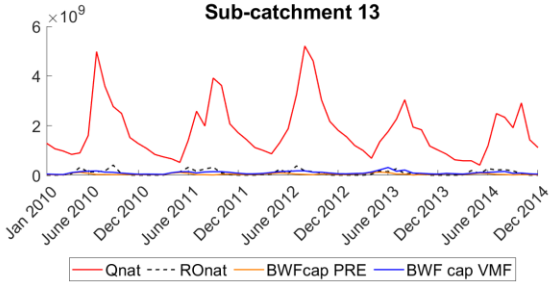

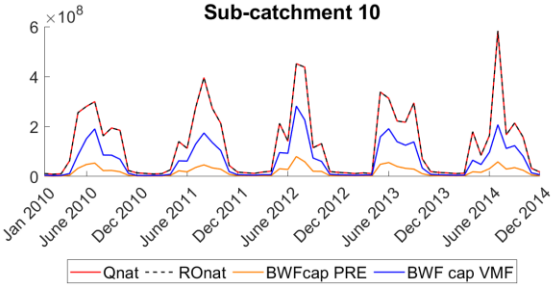

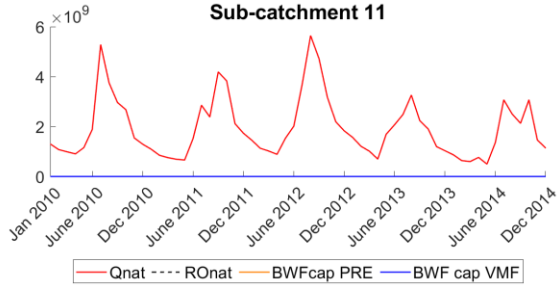

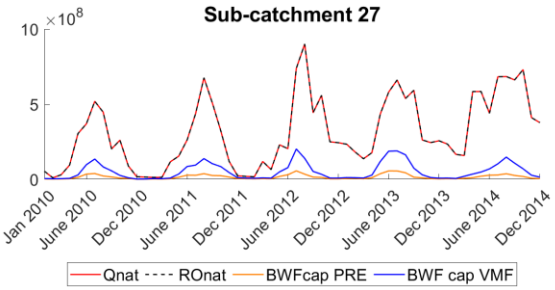

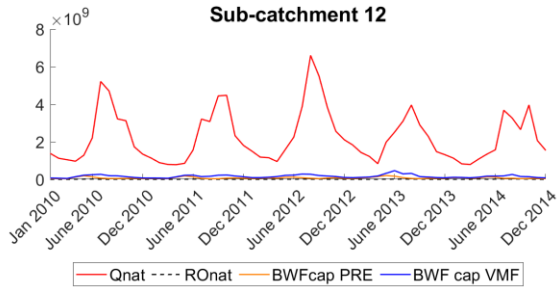

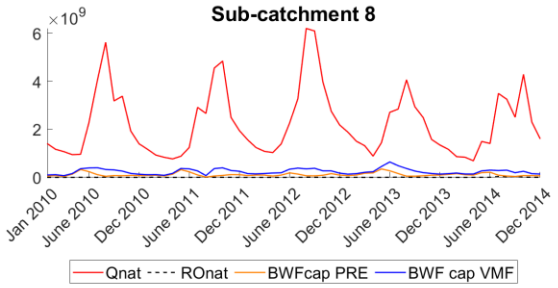
Sub-catchment 8
×10^9
6
4
2
0
Jan 2010
June 2010
Dec 2010
June 2011
Dec 2011
June 2012
Dec 2012
June 2013
Dec 2013
June 2014
Dec 2014
Qnat
ROnat
BWFcap PRE
BWF cap VMF

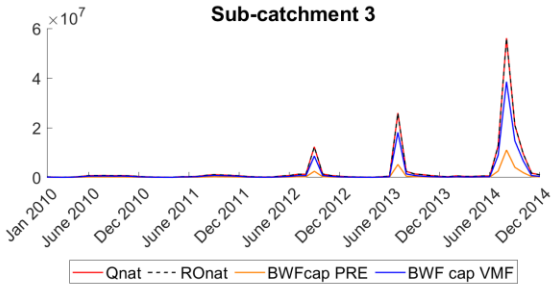
Sub-catchment 3
×10^7
6
4
2
0
Jan 2010
June 2010
Dec 2010
June 2011
Dec 2011
June 2012
Dec 2012
June 2013
Dec 2013
June 2014
Dec 2014
Qnat
ROnat
BWFcap PRE
BWF cap VMF

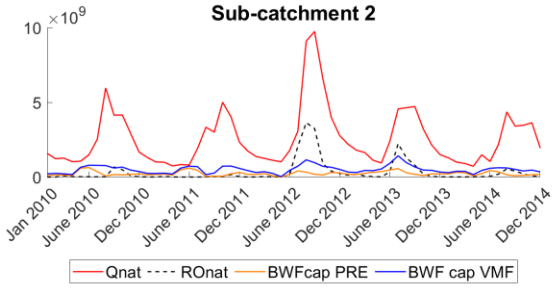
Sub-catchment 2
×10^9
10
5
0
Jan 2010
June 2010
Dec 2010
June 2011
Dec 2011
June 2012
Dec 2012
June 2013
Dec 2013
June 2014
Dec 2014
Qnat
ROnat
BWFcap PRE
BWF cap VMF

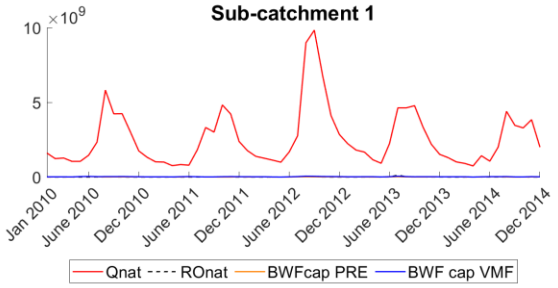
Sub-catchment 1
×10^9
10
5
0
Jan 2010
June 2010
Dec 2010
June 2011
Dec 2011
June 2012
Dec 2012
June 2013
Dec 2013
June 2014
Dec 2014
Qnat
ROnat
BWFcap PRE
BWF cap VMF

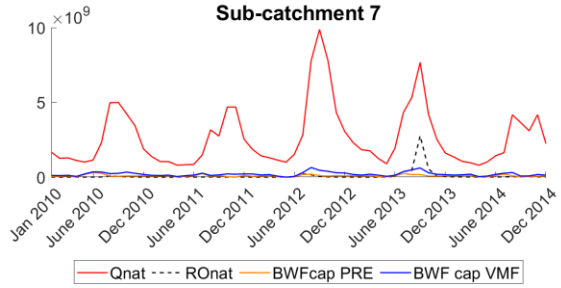
Sub-catchment 7
×10^9
10
5
0
Jan 2010
June 2010
Dec 2010
June 2011
Dec 2011
June 2012
Dec 2012
June 2013
Dec 2013
June 2014
Dec 2014
Qnat
ROnat
BWFcap PRE
BWF cap VMF

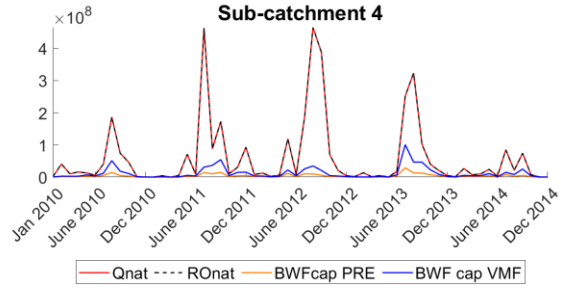
Sub-catchment 4
×10^8
4
3
2
1
0
Jan 2010
June 2010
Dec 2010
June 2011
Dec 2011
June 2012
Dec 2012
June 2013
Dec 2013
June 2014
Dec 2014
Qnat
ROnat
BWFcap PRE
BWF cap VMF

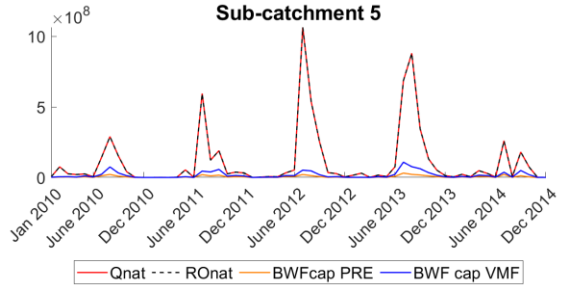
Sub-catchment 5
×10^8
10
5
0
Jan 2010
June 2010
Dec 2010
June 2011
Dec 2011
June 2012
Dec 2012
June 2013
Dec 2013
June 2014
Dec 2014
Qnat
ROnat
BWFcap PRE
BWF cap VMF

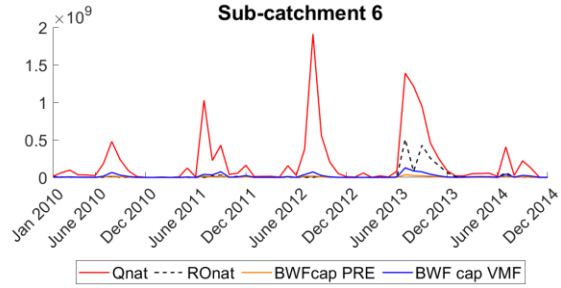
Sub-catchment 6
×10^9
2
1.5
1
0.5
0
Jan 2010
June 2010
Dec 2010
June 2011
Dec 2011
June 2012
Dec 2012
June 2013
Dec 2013
June 2014
Dec 2014
Qnat
ROnat
BWFcap PRE
BWF cap VMF

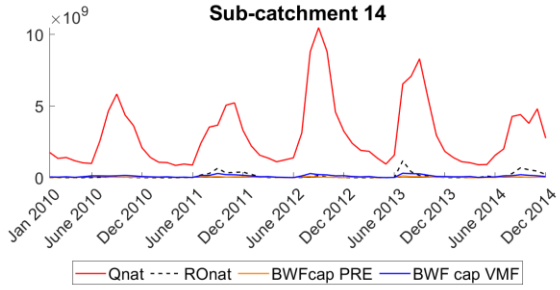
Sub-catchment 14
×10^9
10
5
0
Jan 2010
June 2010
Dec 2010
June 2011
Dec 2011
June 2012
Dec 2012
June 2013
Dec 2013
June 2014
Dec 2014
Qnat
ROnat
BWFcap PRE
BWF cap VMF

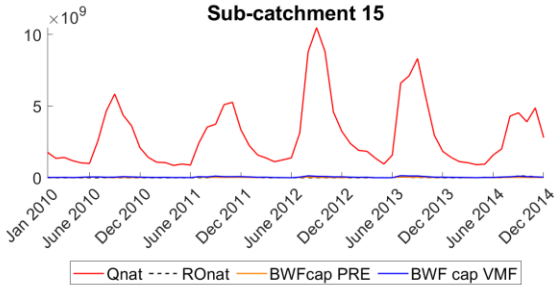
Sub-catchment 15
×10^9
10
5
0
Jan 2010
June 2010
Dec 2010
June 2011
Dec 2011
June 2012
Dec 2012
June 2013
Dec 2013
June 2014
Dec 2014
Qnat
ROnat
BWFcap PRE
BWF cap VMF

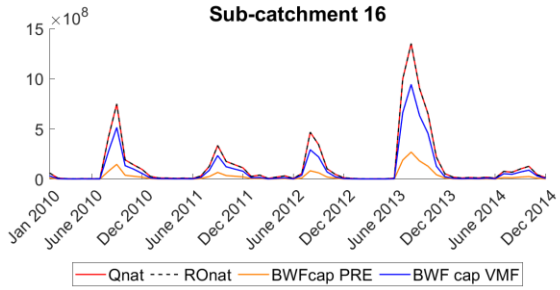
Sub-catchment 16
×10^8
15
10
5
0
Jan 2010
June 2010
Dec 2010
June 2011
Dec 2011
June 2012
Dec 2012
June 2013
Dec 2013
June 2014
Dec 2014
Qnat
ROnat
BWFcap PRE
BWF cap VMF

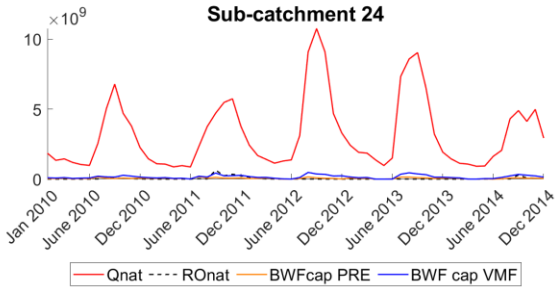
Sub-catchment 24
×10^9
10
5
0
Jan 2010
June 2010
Dec 2010
June 2011
Dec 2011
June 2012
Dec 2012
June 2013
Dec 2013
June 2014
Dec 2014
Qnat
ROnat
BWFcap PRE
BWF cap VMF

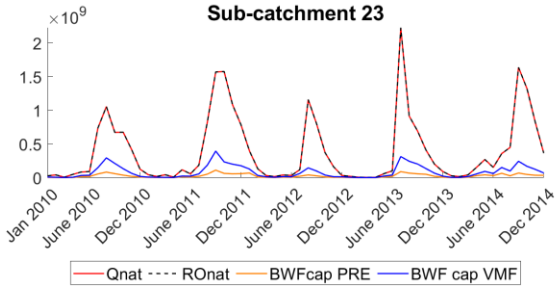
Sub-catchment 23
×10^9
2
1.5
1
0.5
0
Jan 2010
June 2010
Dec 2010
June 2011
Dec 2011
June 2012
Dec 2012
June 2013
Dec 2013
June 2014
Dec 2014
Qnat
ROnat
BWFcap PRE
BWF cap VMF

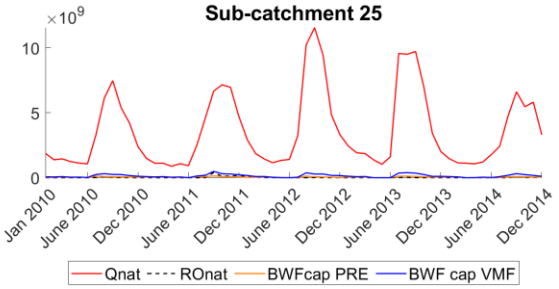
Sub-catchment 25
×10^9
10
5
0
Jan 2010
June 2010
Dec 2010
June 2011
Dec 2011
June 2012
Dec 2012
June 2013
Dec 2013
June 2014
Dec 2014
Qnat
ROnat
BWFcap PRE
BWF cap VMF

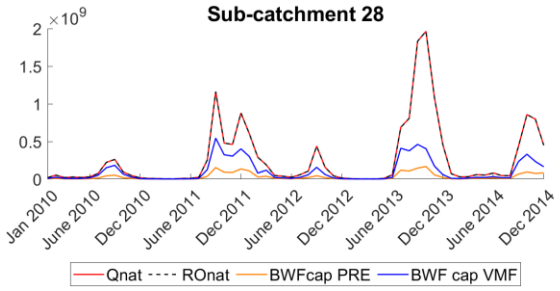
Sub-catchment 28
×10^9
2
1.5
1
0.5
0
Jan 2010
June 2010
Dec 2010
June 2011
Dec 2011
June 2012
Dec 2012
June 2013
Dec 2013
June 2014
Dec 2014
Qnat
ROnat
BWFcap PRE
BWF cap VMF

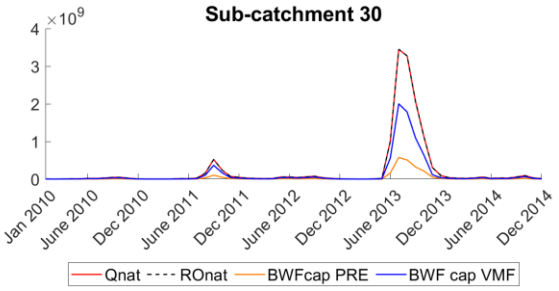
Sub-catchment 30
×10^9
4
3
2
1
0
Jan 2010
June 2010
Dec 2010
June 2011
Dec 2011
June 2012
Dec 2012
June 2013
Dec 2013
June 2014
Dec 2014
Qnat
ROnat
BWFcap PRE
BWF cap VMF

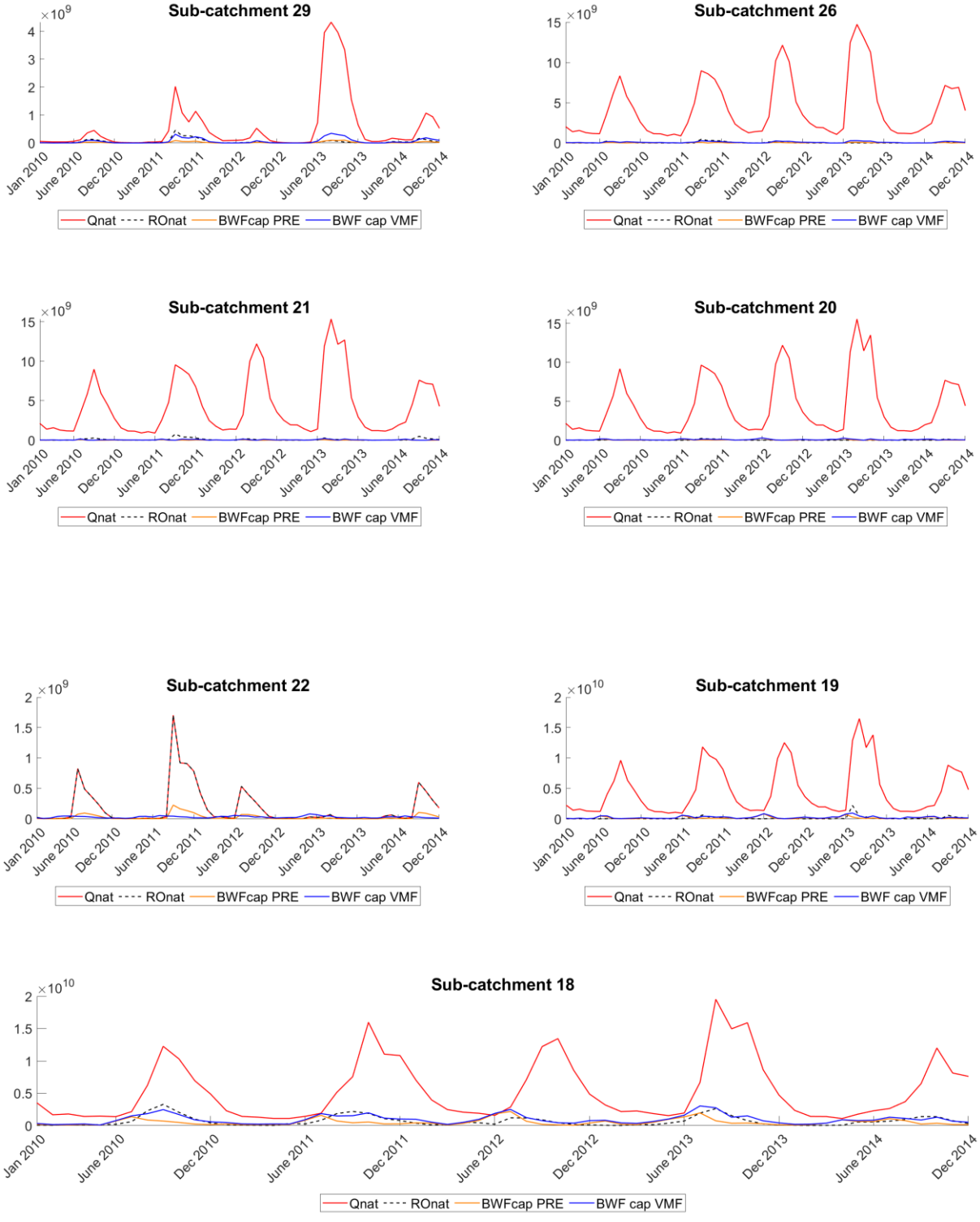

FIGURE 46: POPULATION-BASED SCENARIO BWF CAP PER SUB-CATCHMENT INDIVIDUALLY FOR PRE AND VMF METHOD INCLUDING NATURAL STREAMFLOW (Q_{nat}) AND NATURAL RUNOFF (RO_{nat}).

Appendix J – BWF cap demand-based scenario

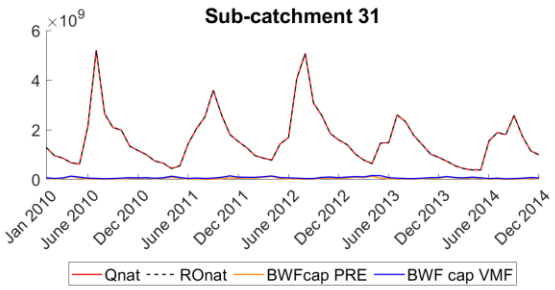

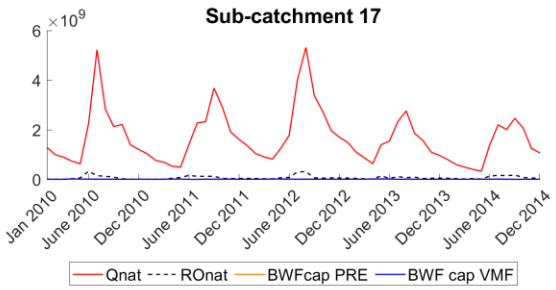

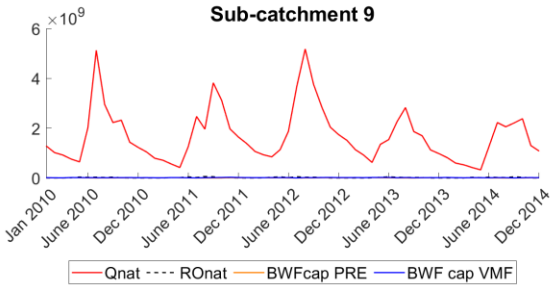

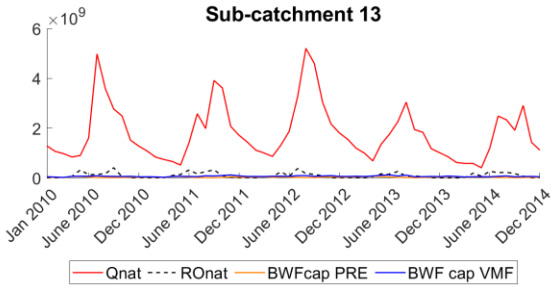

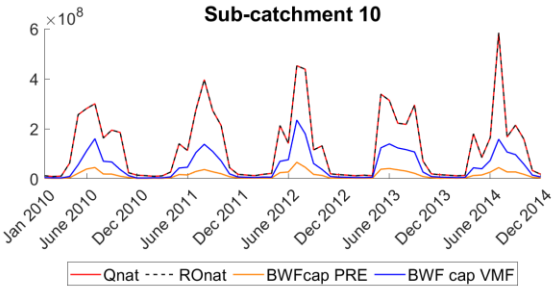

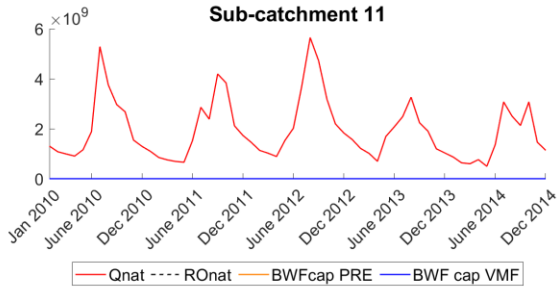

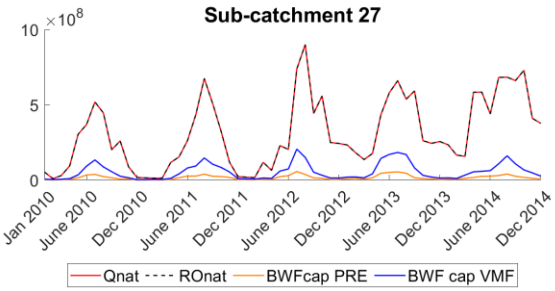

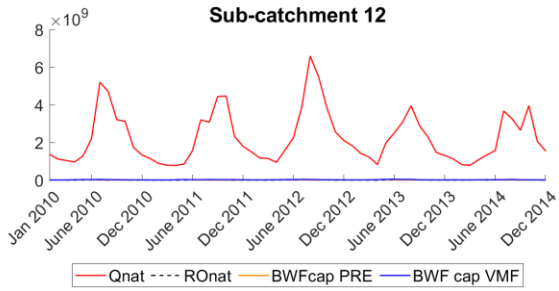

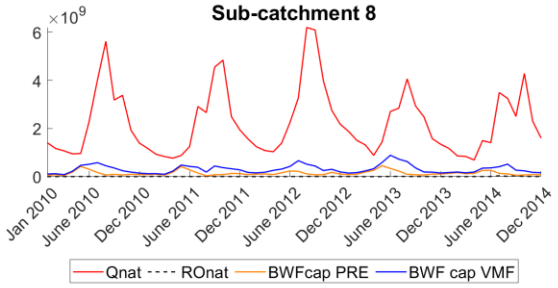
Sub-catchment 8
×10^9
6
4
2
0
Jan 2010
June 2010
Dec 2010
June 2011
Dec 2011
June 2012
Dec 2012
June 2013
Dec 2013
June 2014
Dec 2014
Qnat
ROnat
BWFcap PRE
BWF cap VMF

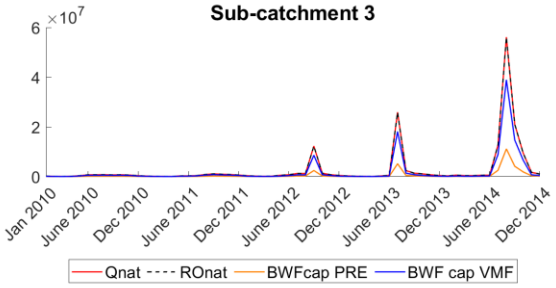
Sub-catchment 3
×10^7
6
4
2
0
Jan 2010
June 2010
Dec 2010
June 2011
Dec 2011
June 2012
Dec 2012
June 2013
Dec 2013
June 2014
Dec 2014
Qnat
ROnat
BWFcap PRE
BWF cap VMF

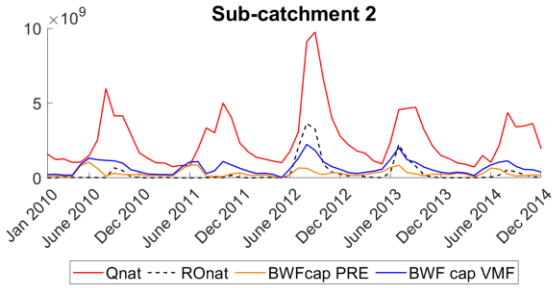
Sub-catchment 2
×10^9
10
5
0
Jan 2010
June 2010
Dec 2010
June 2011
Dec 2011
June 2012
Dec 2012
June 2013
Dec 2013
June 2014
Dec 2014
Qnat
ROnat
BWFcap PRE
BWF cap VMF

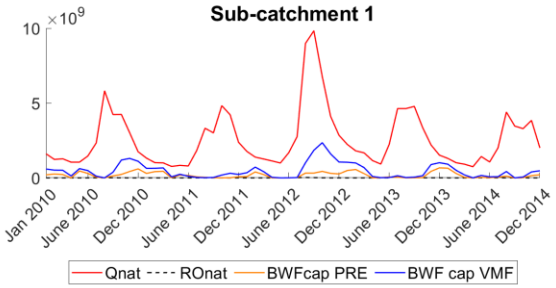
Sub-catchment 1
×10^9
10
5
0
Jan 2010
June 2010
Dec 2010
June 2011
Dec 2011
June 2012
Dec 2012
June 2013
Dec 2013
June 2014
Dec 2014
Qnat
ROnat
BWFcap PRE
BWF cap VMF

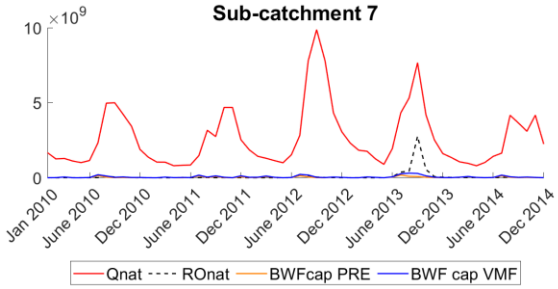
Sub-catchment 7
×10^9
10
5
0
Jan 2010
June 2010
Dec 2010
June 2011
Dec 2011
June 2012
Dec 2012
June 2013
Dec 2013
June 2014
Dec 2014
Qnat
ROnat
BWFcap PRE
BWF cap VMF

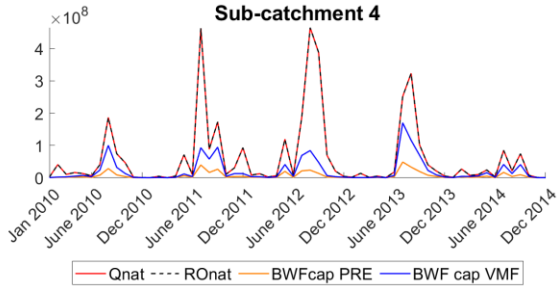
Sub-catchment 4
×10^8
4
3
2
1
0
Jan 2010
June 2010
Dec 2010
June 2011
Dec 2011
June 2012
Dec 2012
June 2013
Dec 2013
June 2014
Dec 2014
Qnat
ROnat
BWFcap PRE
BWF cap VMF

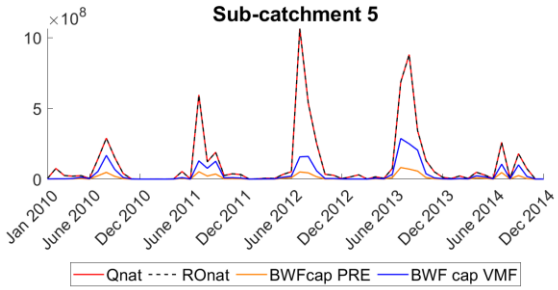
Sub-catchment 5
×10^8
10
5
0
Jan 2010
June 2010
Dec 2010
June 2011
Dec 2011
June 2012
Dec 2012
June 2013
Dec 2013
June 2014
Dec 2014
Qnat
ROnat
BWFcap PRE
BWF cap VMF

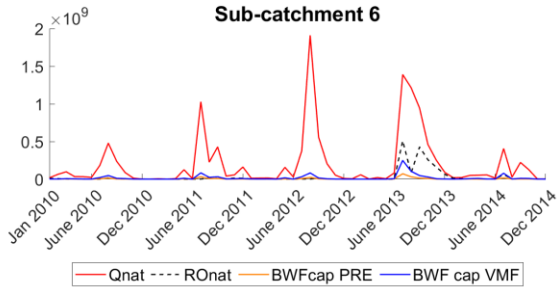
Sub-catchment 6
×10^9
2
1.5
1
0.5
0
Jan 2010
June 2010
Dec 2010
June 2011
Dec 2011
June 2012
Dec 2012
June 2013
Dec 2013
June 2014
Dec 2014
Qnat
ROnat
BWFcap PRE
BWF cap VMF

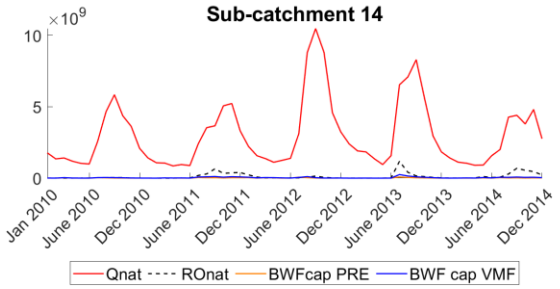
Sub-catchment 14
×10^9
10
5
0
Jan 2010
June 2010
Dec 2010
June 2011
Dec 2011
June 2012
Dec 2012
June 2013
Dec 2013
June 2014
Dec 2014
Qnat
ROnat
BWFcap PRE
BWF cap VMF

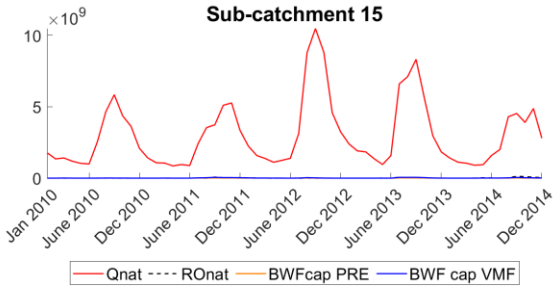
Sub-catchment 15
×10^9
10
5
0
Jan 2010
June 2010
Dec 2010
June 2011
Dec 2011
June 2012
Dec 2012
June 2013
Dec 2013
June 2014
Dec 2014
Qnat
ROnat
BWFcap PRE
BWF cap VMF

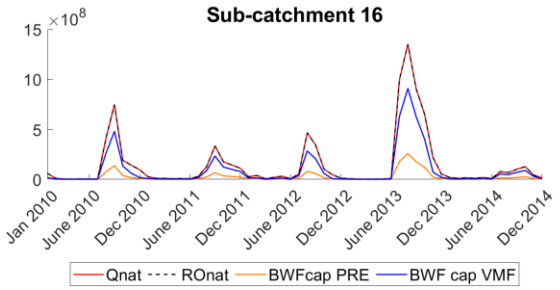
Sub-catchment 16
×10^8
15
10
5
0
Jan 2010
June 2010
Dec 2010
June 2011
Dec 2011
June 2012
Dec 2012
June 2013
Dec 2013
June 2014
Dec 2014
Qnat
ROnat
BWFcap PRE
BWF cap VMF

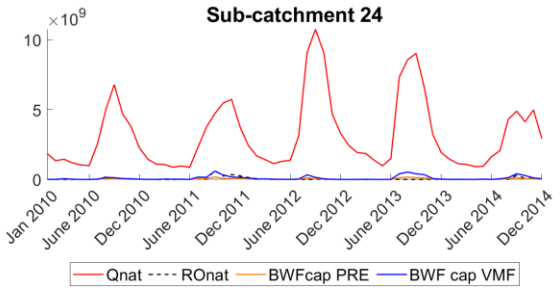
Sub-catchment 24
×10^9
10
5
0
Jan 2010
June 2010
Dec 2010
June 2011
Dec 2011
June 2012
Dec 2012
June 2013
Dec 2013
June 2014
Dec 2014
Qnat
ROnat
BWFcap PRE
BWF cap VMF

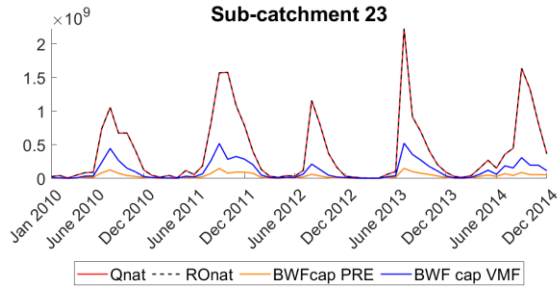
Sub-catchment 23
×10^9
2
1.5
1
0.5
0
Jan 2010
June 2010
Dec 2010
June 2011
Dec 2011
June 2012
Dec 2012
June 2013
Dec 2013
June 2014
Dec 2014
Qnat
ROnat
BWFcap PRE
BWF cap VMF

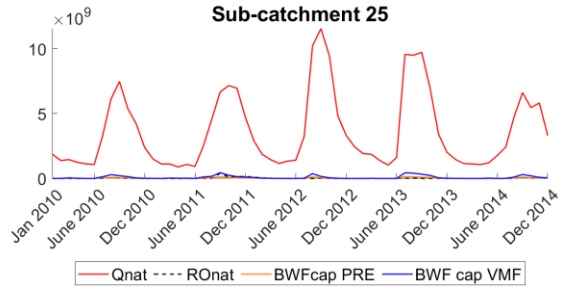
Sub-catchment 25
×10^9
10
5
0
Jan 2010
June 2010
Dec 2010
June 2011
Dec 2011
June 2012
Dec 2012
June 2013
Dec 2013
June 2014
Dec 2014
Qnat
ROnat
BWFcap PRE
BWF cap VMF

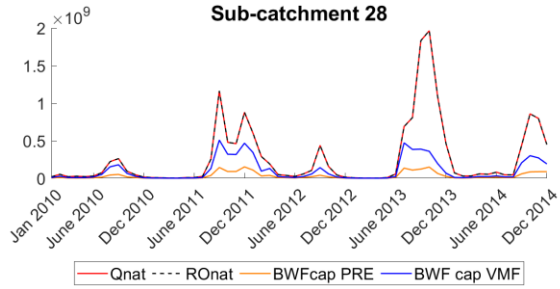
Sub-catchment 28
×10^9
2
1.5
1
0.5
0
Jan 2010
June 2010
Dec 2010
June 2011
Dec 2011
June 2012
Dec 2012
June 2013
Dec 2013
June 2014
Dec 2014
Qnat
ROnat
BWFcap PRE
BWF cap VMF

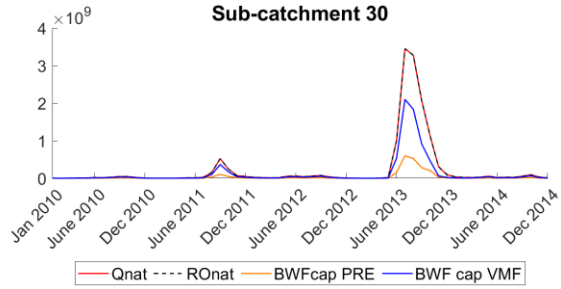
Sub-catchment 30
×10^9
4
3
2
1
0
Jan 2010
June 2010
Dec 2010
June 2011
Dec 2011
June 2012
Dec 2012
June 2013
Dec 2013
June 2014
Dec 2014
Qnat
ROnat
BWFcap PRE
BWF cap VMF

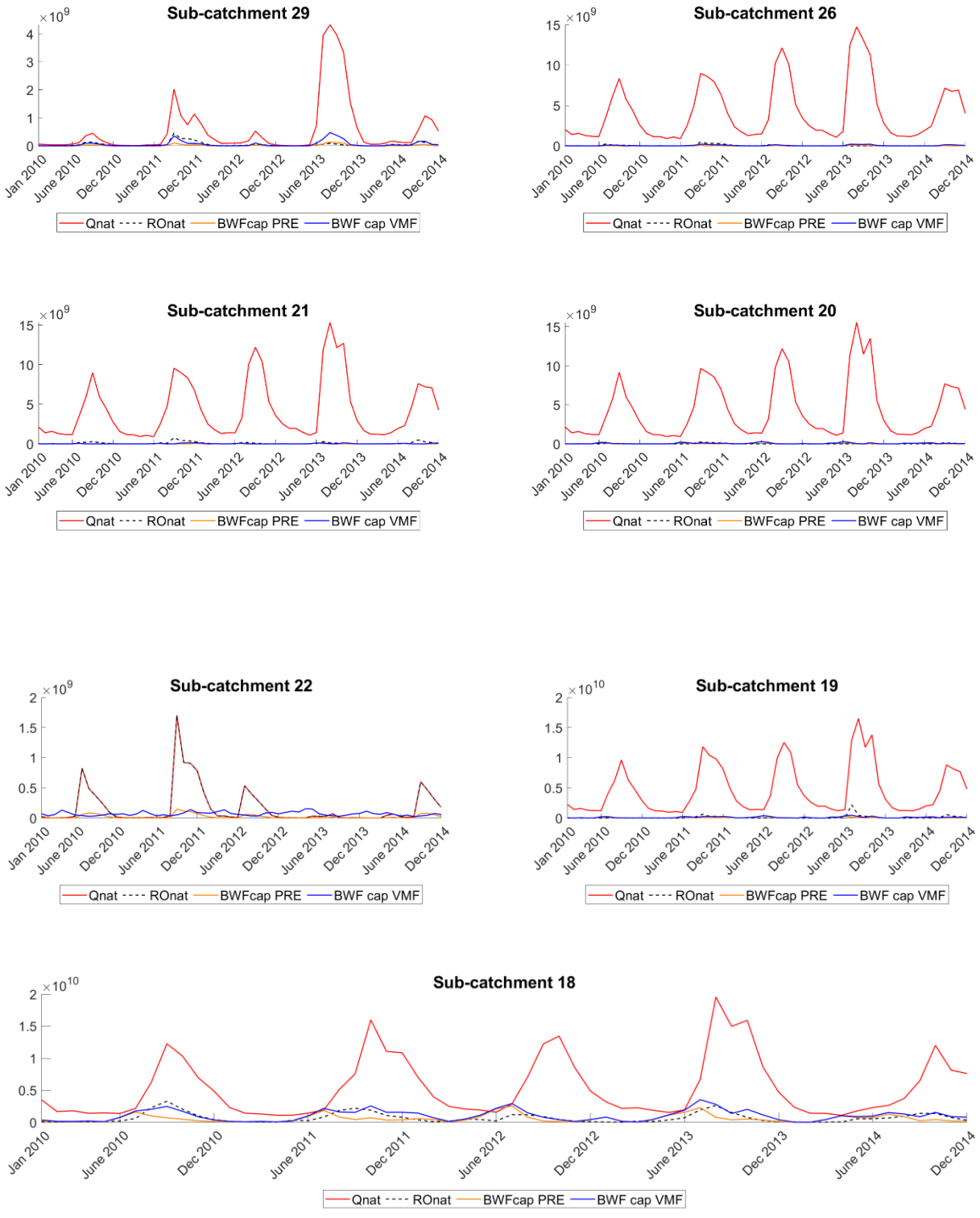

FIGURE 47: DEMAND-BASED SCENARIO BWF CAP PER SUB-CATCHMENT INDIVIDUALLY FOR PRE AND VMF METHOD INCLUDING NATURAL STREAMFLOW (Q_{nat}) AND NATURAL RUNOFF (RO_{nat}).

Appendix K – Temporal time series water scarcity

K.1. Variable monthly flow method

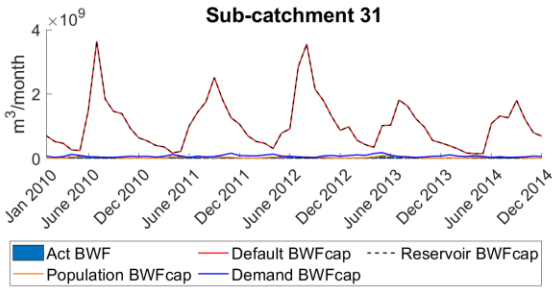

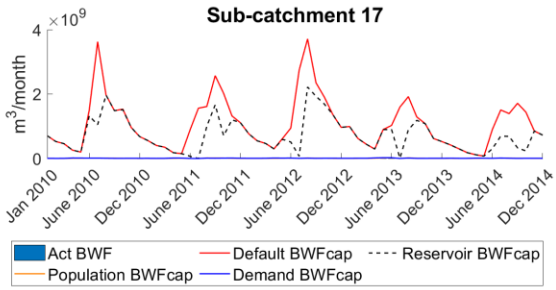

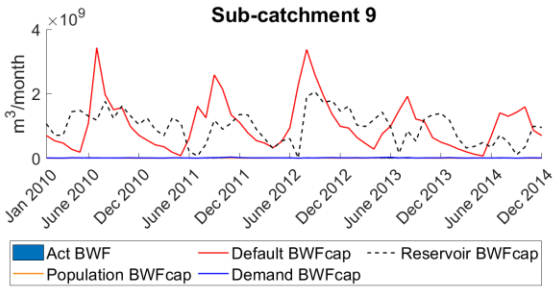

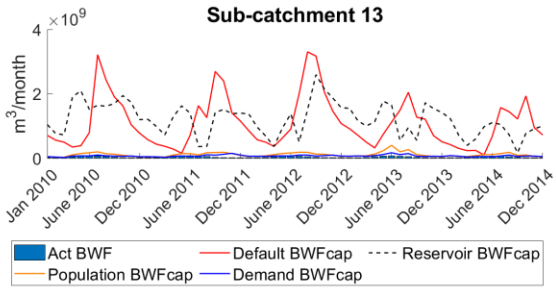

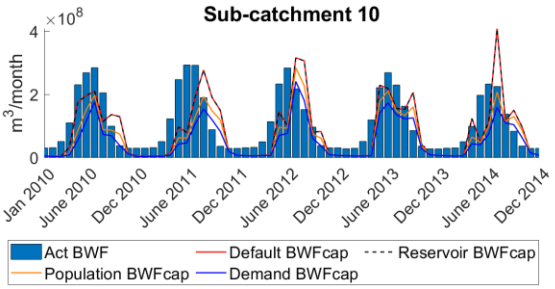

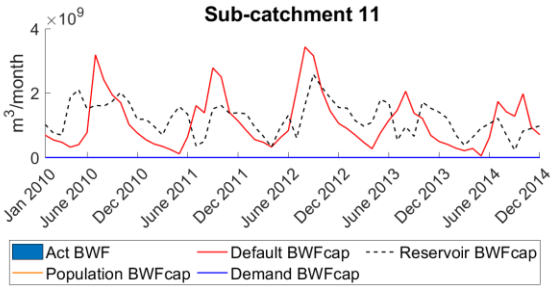

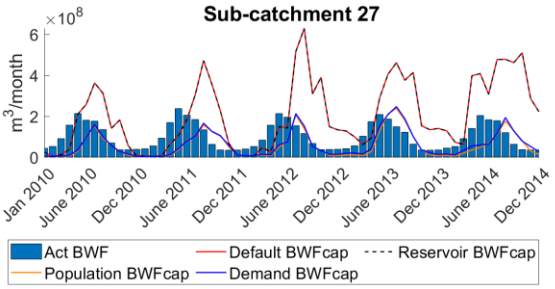

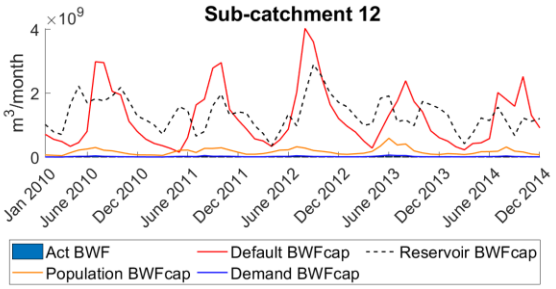

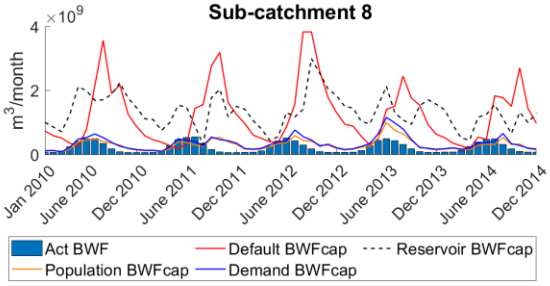
Sub-catchment 8
×10^9
m^3/month
Jan 2010
June 2010
Dec 2010
June 2011
Dec 2011
June 2012
Dec 2012
June 2013
Dec 2013
June 2014
Dec 2014
Act BWF
Default BWFcap
Reservoir BWFcap
Population BWFcap
Demand BWFcap

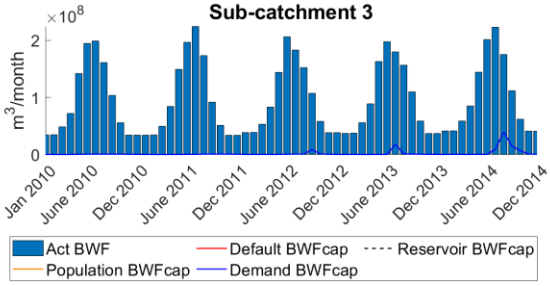
Sub-catchment 3
×10^8
m^3/month
Jan 2010
June 2010
Dec 2010
June 2011
Dec 2011
June 2012
Dec 2012
June 2013
Dec 2013
June 2014
Dec 2014
Act BWF
Default BWFcap
Reservoir BWFcap
Population BWFcap
Demand BWFcap

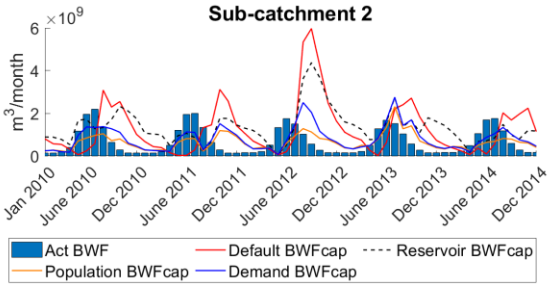
Sub-catchment 2
×10^9
m^3/month
Jan 2010
June 2010
Dec 2010
June 2011
Dec 2011
June 2012
Dec 2012
June 2013
Dec 2013
June 2014
Dec 2014
Act BWF
Default BWFcap
Reservoir BWFcap
Population BWFcap
Demand BWFcap

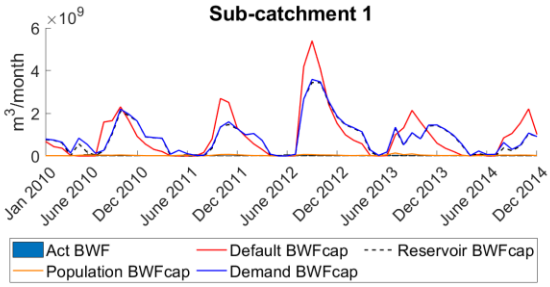
Sub-catchment 1
×10^9
m^3/month
Jan 2010
June 2010
Dec 2010
June 2011
Dec 2011
June 2012
Dec 2012
June 2013
Dec 2013
June 2014
Dec 2014
Act BWF
Default BWFcap
Reservoir BWFcap
Population BWFcap
Demand BWFcap

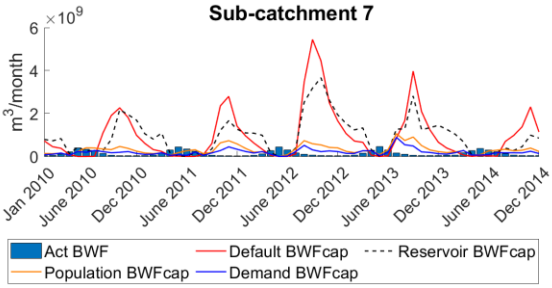
Sub-catchment 7
×10^9
m^3/month
Jan 2010
June 2010
Dec 2010
June 2011
Dec 2011
June 2012
Dec 2012
June 2013
Dec 2013
June 2014
Dec 2014
Act BWF
Default BWFcap
Reservoir BWFcap
Population BWFcap
Demand BWFcap

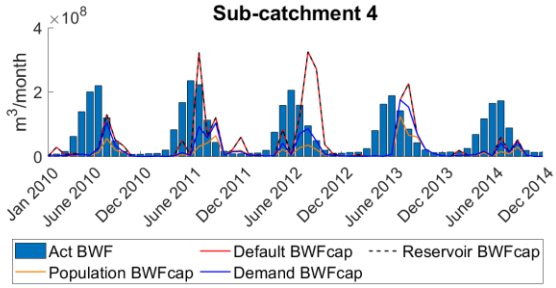
Sub-catchment 4
×10^8
m^3/month
Jan 2010
June 2010
Dec 2010
June 2011
Dec 2011
June 2012
Dec 2012
June 2013
Dec 2013
June 2014
Dec 2014
Act BWF
Default BWFcap
Reservoir BWFcap
Population BWFcap
Demand BWFcap

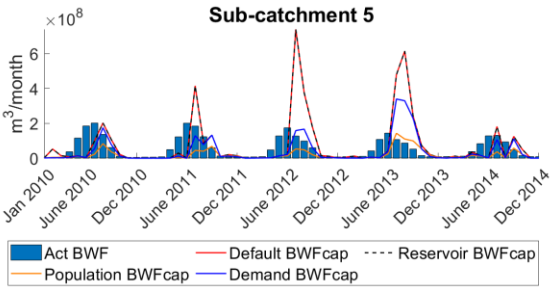
Sub-catchment 5
×10^8
m^3/month
Jan 2010
June 2010
Dec 2010
June 2011
Dec 2011
June 2012
Dec 2012
June 2013
Dec 2013
June 2014
Dec 2014
Act BWF
Default BWFcap
Reservoir BWFcap
Population BWFcap
Demand BWFcap

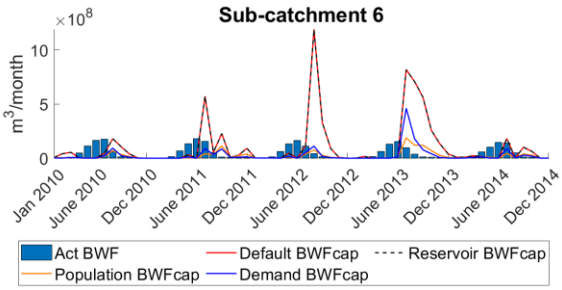
Sub-catchment 6
×10^8
m^3/month
Jan 2010
June 2010
Dec 2010
June 2011
Dec 2011
June 2012
Dec 2012
June 2013
Dec 2013
June 2014
Dec 2014
Act BWF
Default BWFcap
Reservoir BWFcap
Population BWFcap
Demand BWFcap

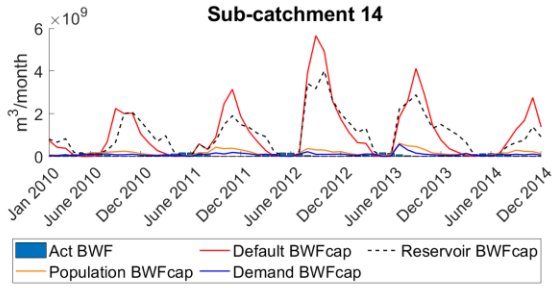
Sub-catchment 14
×10^9
m^3/month
Act BWF
Default BWFcap
Reservoir BWFcap
Population BWFcap
Demand BWFcap

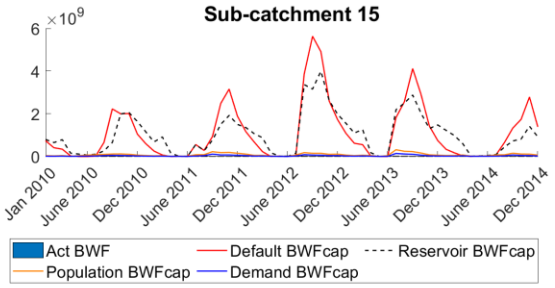
Sub-catchment 15
×10^9
m^3/month
Act BWF
Default BWFcap
Reservoir BWFcap
Population BWFcap
Demand BWFcap

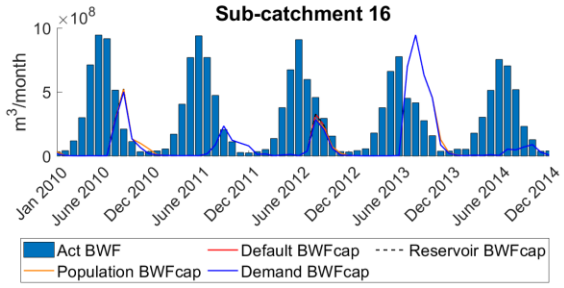
Sub-catchment 16
×10^8
m^3/month
Act BWF
Default BWFcap
Reservoir BWFcap
Population BWFcap
Demand BWFcap

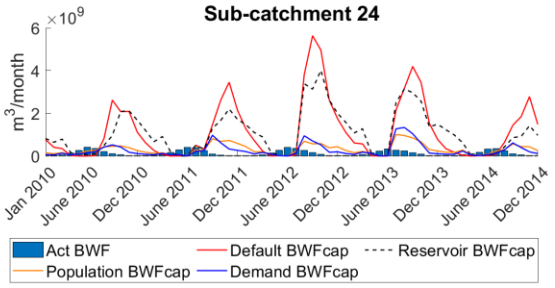
Sub-catchment 24
×10^9
m^3/month
Act BWF
Default BWFcap
Reservoir BWFcap
Population BWFcap
Demand BWFcap

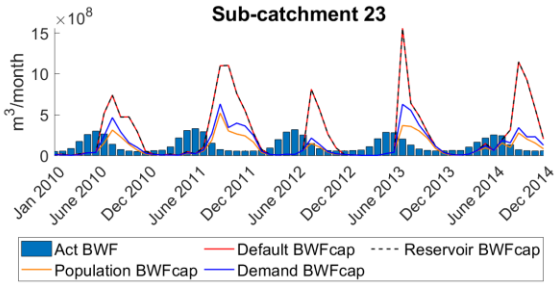
Sub-catchment 23
×10^8
m^3/month
Act BWF
Default BWFcap
Reservoir BWFcap
Population BWFcap
Demand BWFcap

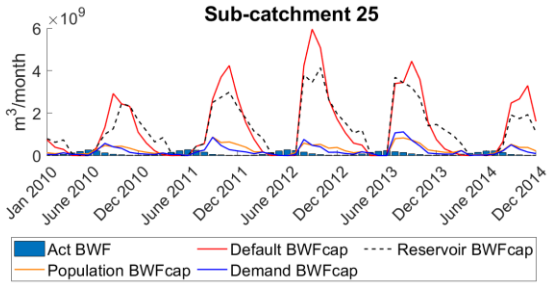
Sub-catchment 25
×10^9
m^3/month
Act BWF
Default BWFcap
Reservoir BWFcap
Population BWFcap
Demand BWFcap

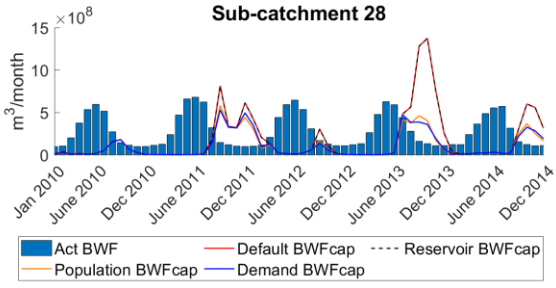
Sub-catchment 28
×10^8
m^3/month
Act BWF
Default BWFcap
Reservoir BWFcap
Population BWFcap
Demand BWFcap

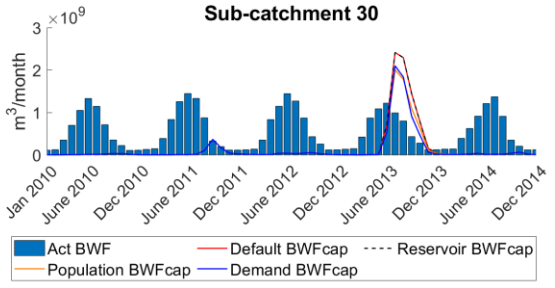
Sub-catchment 30
×10^9
m^3/month
Act BWF
Default BWFcap
Reservoir BWFcap
Population BWFcap
Demand BWFcap

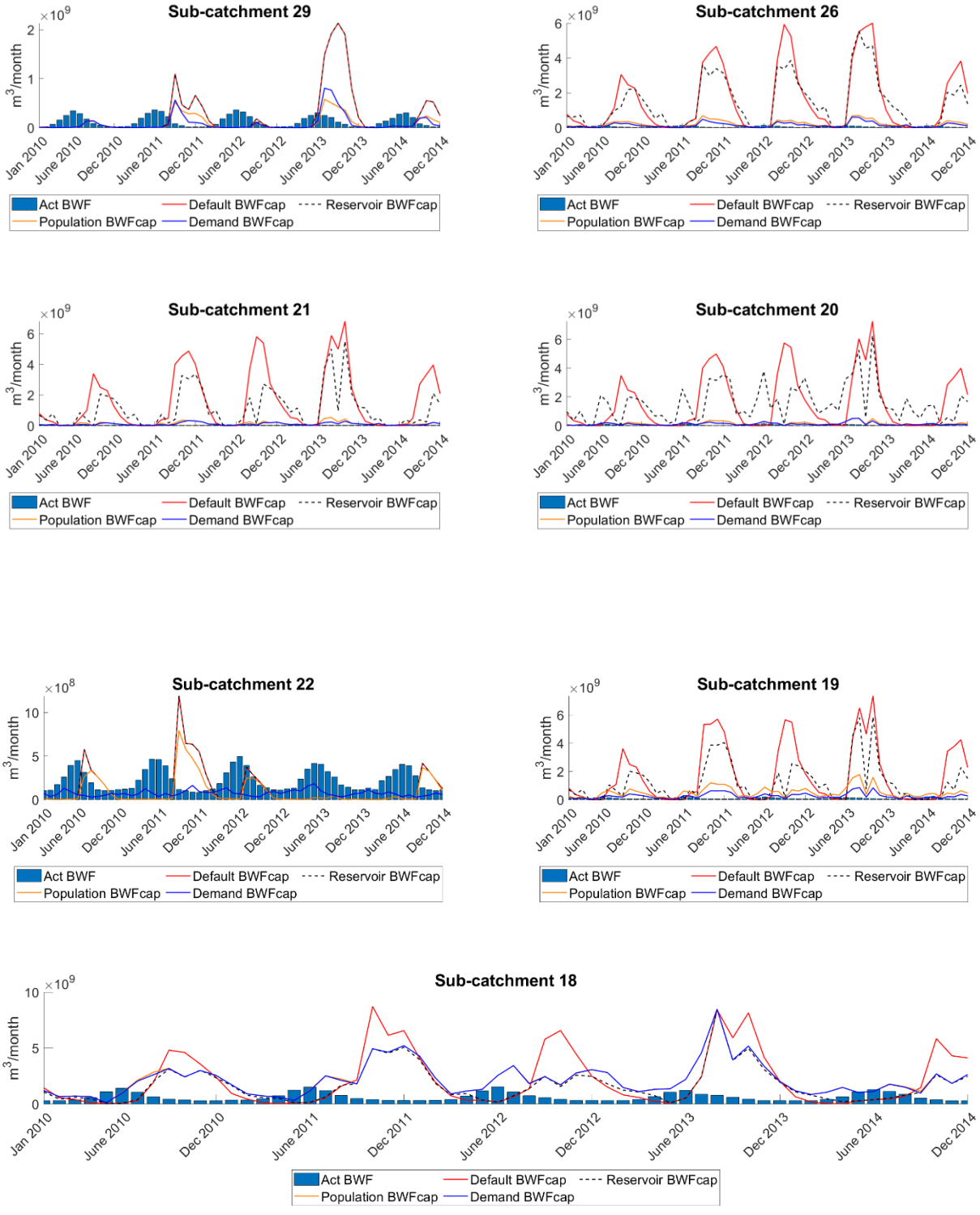

FIGURE 48: VMF METHOD BWF CAPS PER SUB-CATCHMENT INDIVIDUALLY FOR ALL FOUR SCENARIOS WITH THE ACTUAL BWF AS BARS.

K.2. Presumptive standard approach

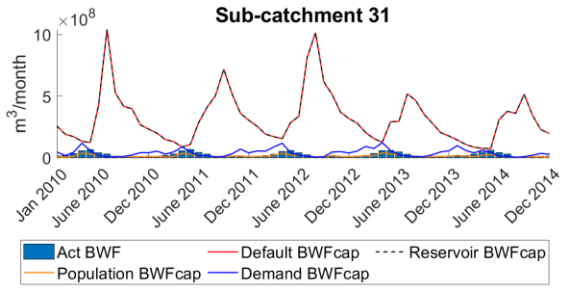

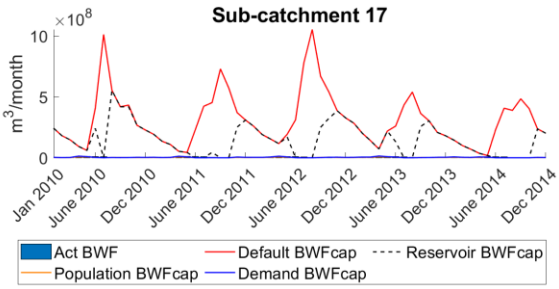

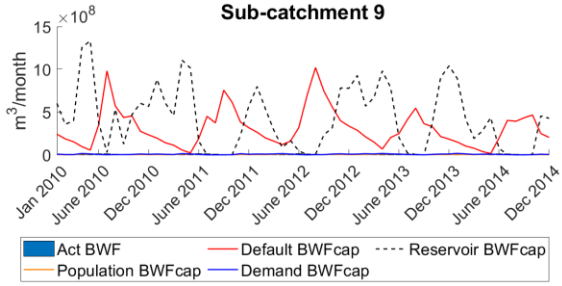

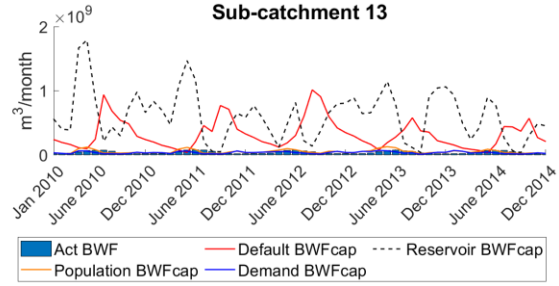

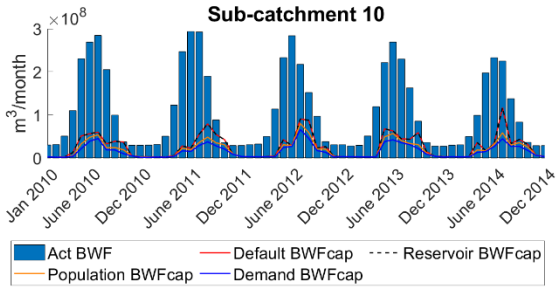

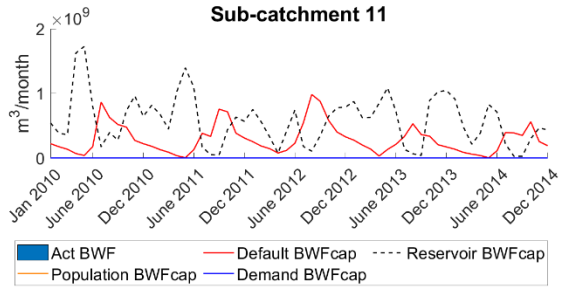

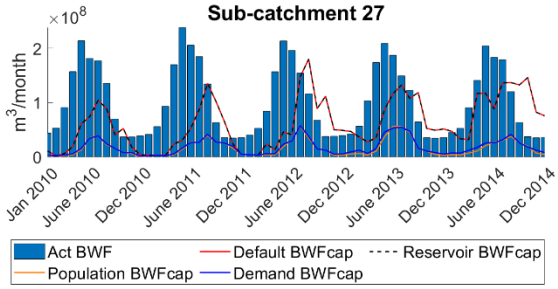

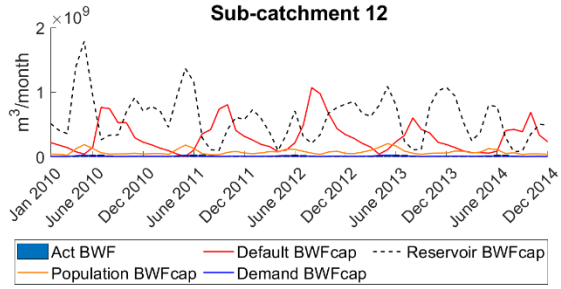

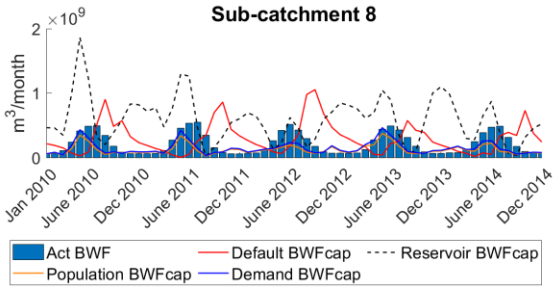
Sub-catchment 8
×10^9
m^3/month
Jan 2010
June 2010
Dec 2010
June 2011
Dec 2011
June 2012
Dec 2012
June 2013
Dec 2013
June 2014
Dec 2014
Act BWF
Default BWFcap
Reservoir BWFcap
Population BWFcap
Demand BWFcap

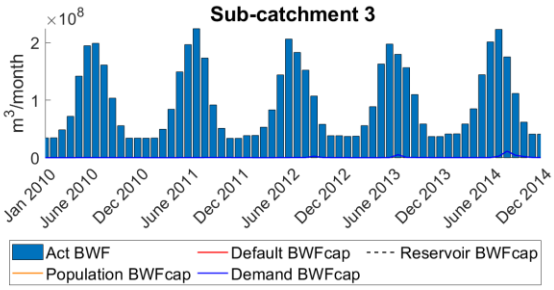
Sub-catchment 3
×10^8
m^3/month
Jan 2010
June 2010
Dec 2010
June 2011
Dec 2011
June 2012
Dec 2012
June 2013
Dec 2013
June 2014
Dec 2014
Act BWF
Default BWFcap
Reservoir BWFcap
Population BWFcap
Demand BWFcap

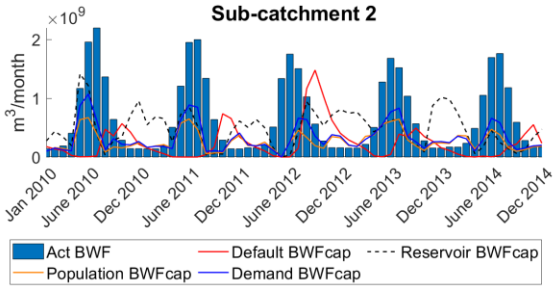
Sub-catchment 2
×10^9
m^3/month
Jan 2010
June 2010
Dec 2010
June 2011
Dec 2011
June 2012
Dec 2012
June 2013
Dec 2013
June 2014
Dec 2014
Act BWF
Default BWFcap
Reservoir BWFcap
Population BWFcap
Demand BWFcap

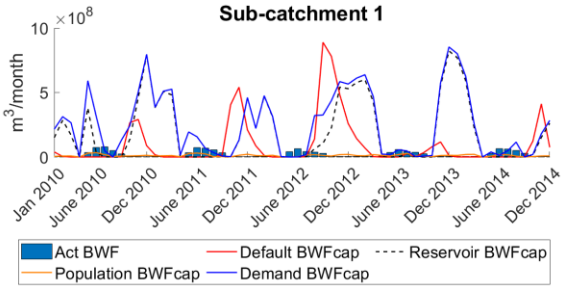
Sub-catchment 1
×10^8
m^3/month
Jan 2010
June 2010
Dec 2010
June 2011
Dec 2011
June 2012
Dec 2012
June 2013
Dec 2013
June 2014
Dec 2014
Act BWF
Default BWFcap
Reservoir BWFcap
Population BWFcap
Demand BWFcap

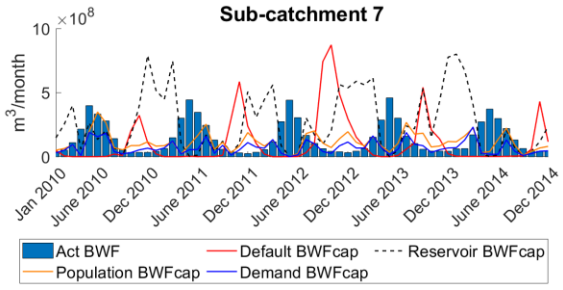
Sub-catchment 7
×10^8
m^3/month
Jan 2010
June 2010
Dec 2010
June 2011
Dec 2011
June 2012
Dec 2012
June 2013
Dec 2013
June 2014
Dec 2014
Act BWF
Default BWFcap
Reservoir BWFcap
Population BWFcap
Demand BWFcap

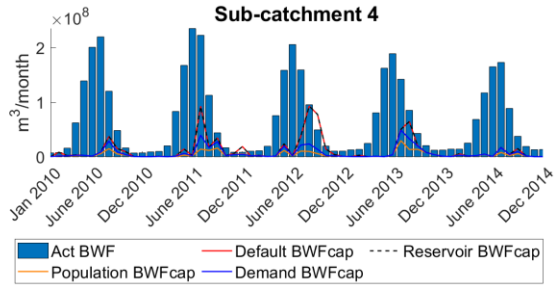
Sub-catchment 4
×10^8
m^3/month
Jan 2010
June 2010
Dec 2010
June 2011
Dec 2011
June 2012
Dec 2012
June 2013
Dec 2013
June 2014
Dec 2014
Act BWF
Default BWFcap
Reservoir BWFcap
Population BWFcap
Demand BWFcap

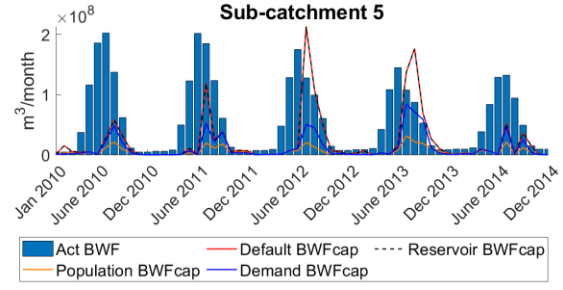
Sub-catchment 5
×10^8
m^3/month
Jan 2010
June 2010
Dec 2010
June 2011
Dec 2011
June 2012
Dec 2012
June 2013
Dec 2013
June 2014
Dec 2014
Act BWF
Default BWFcap
Reservoir BWFcap
Population BWFcap
Demand BWFcap

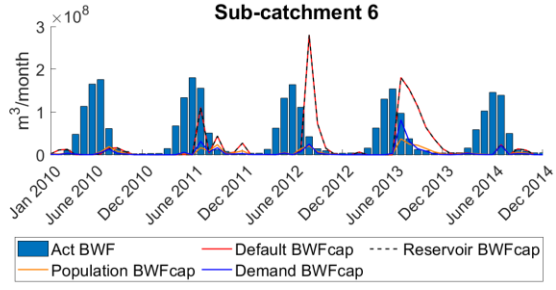
Sub-catchment 6
×10^8
m^3/month
Jan 2010
June 2010
Dec 2010
June 2011
Dec 2011
June 2012
Dec 2012
June 2013
Dec 2013
June 2014
Dec 2014
Act BWF
Default BWFcap
Reservoir BWFcap
Population BWFcap
Demand BWFcap

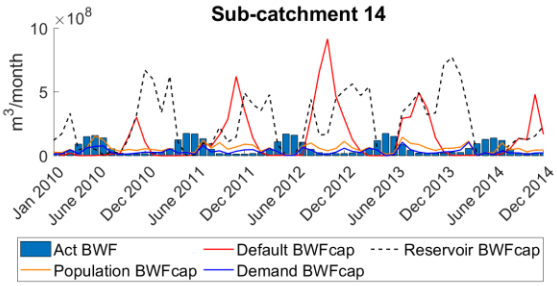
Sub-catchment 14
×10^8
m^3/month
Act BWF
Default BWFcap
Reservoir BWFcap
Population BWFcap
Demand BWFcap

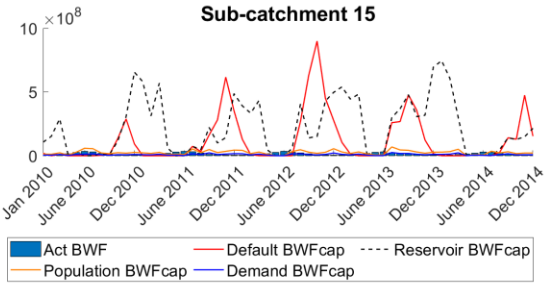
Sub-catchment 15
×10^8
m^3/month
Act BWF
Default BWFcap
Reservoir BWFcap
Population BWFcap
Demand BWFcap

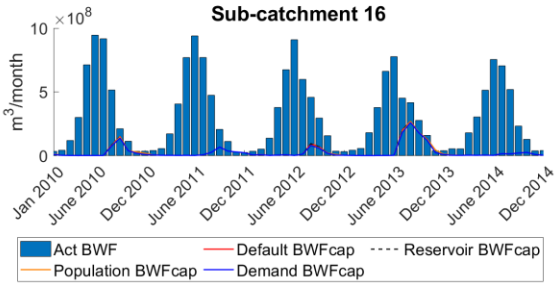
Sub-catchment 16
×10^8
m^3/month
Act BWF
Default BWFcap
Reservoir BWFcap
Population BWFcap
Demand BWFcap

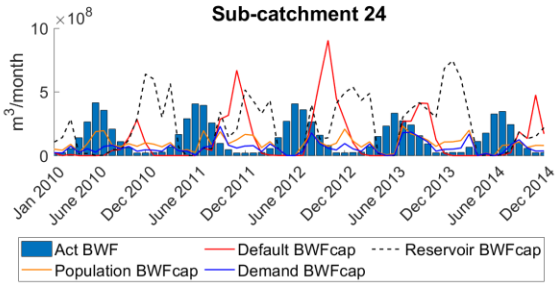
Sub-catchment 24
×10^8
m^3/month
Act BWF
Default BWFcap
Reservoir BWFcap
Population BWFcap
Demand BWFcap

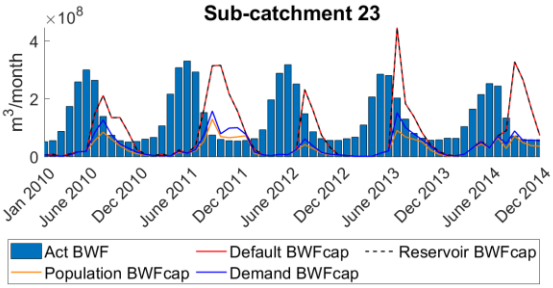
Sub-catchment 23
×10^8
m^3/month
Act BWF
Default BWFcap
Reservoir BWFcap
Population BWFcap
Demand BWFcap

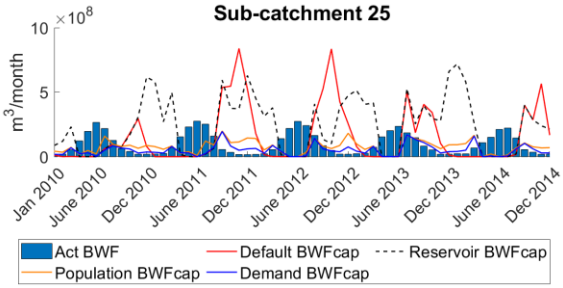
Sub-catchment 25
×10^8
m^3/month
Act BWF
Default BWFcap
Reservoir BWFcap
Population BWFcap
Demand BWFcap

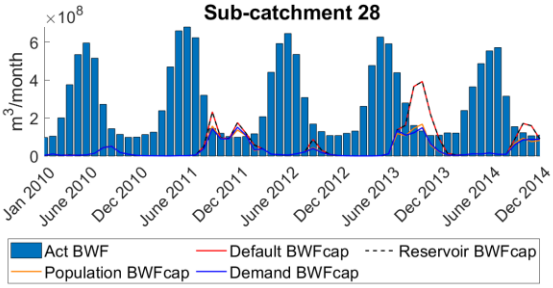
Sub-catchment 28
×10^8
m^3/month
Act BWF
Default BWFcap
Reservoir BWFcap
Population BWFcap
Demand BWFcap

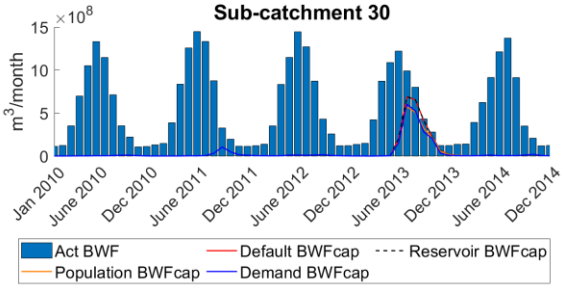
Sub-catchment 30
×10^8
m^3/month
Act BWF
Default BWFcap
Reservoir BWFcap
Population BWFcap
Demand BWFcap

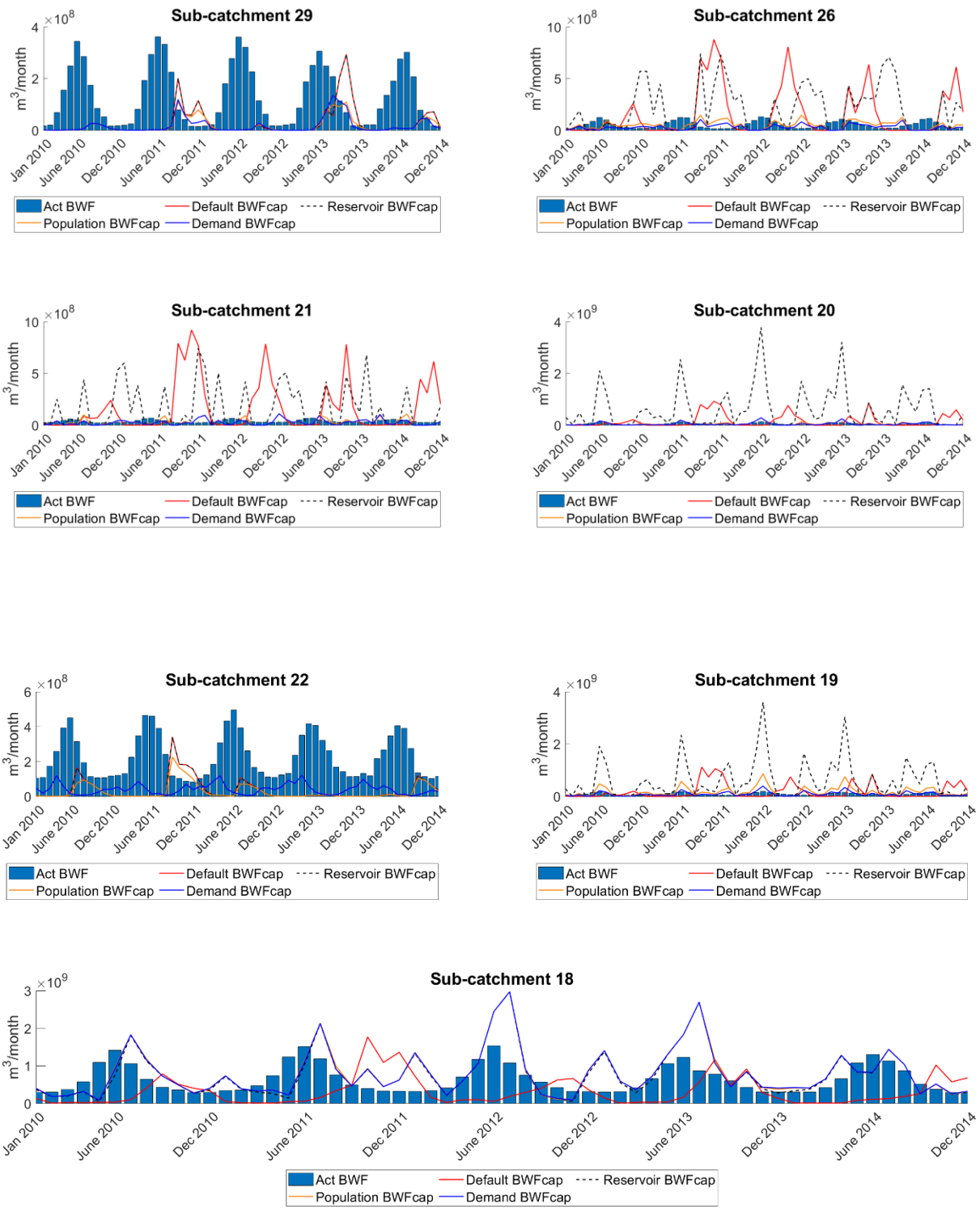

FIGURE 49: PRE METHOD BWF CAPS PER SUB-CATCHMENT INDIVIDUALLY FOR ALL FOUR SCENARIOS WITH THE ACTUAL BWF AS BARS.

Appendix L – Seasonal water scarcity maps presumptive standard approach

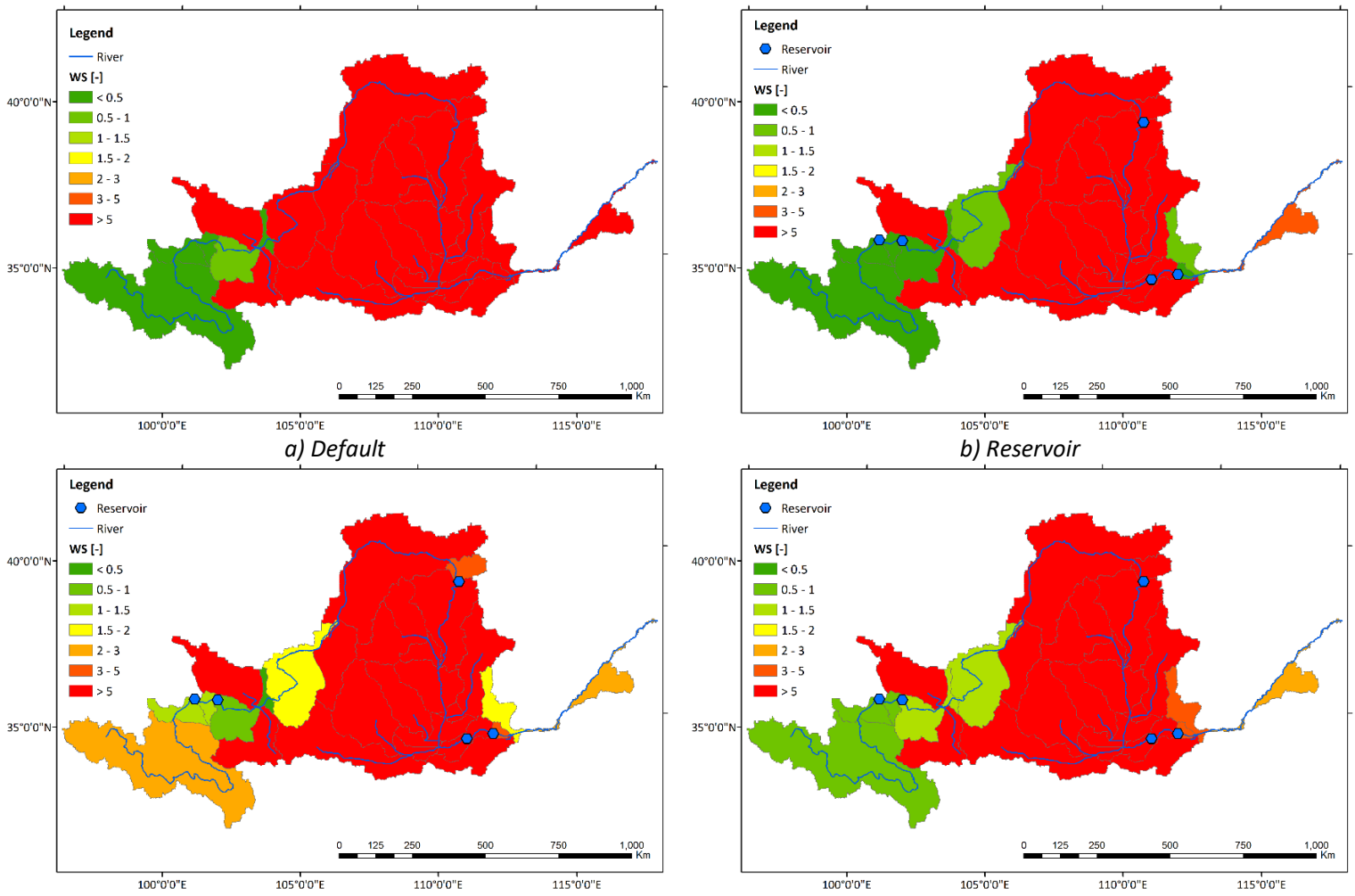

FIGURE 50: AVERAGE BLUE WATER SCARCITY SPRING (MARCH – MAY) PER SUB-CATCHMENT YRB (2010 – 2014) USING BWF CAPS ACCORDING TO A) DEFAULT SCENARIO, B) SCENARIO CONSIDERING RESERVOIRS, C) POPULATION-BASED SCENARIO, AND D) DEMAND-BASED SCENARIO USING PRE EFR METHOD.

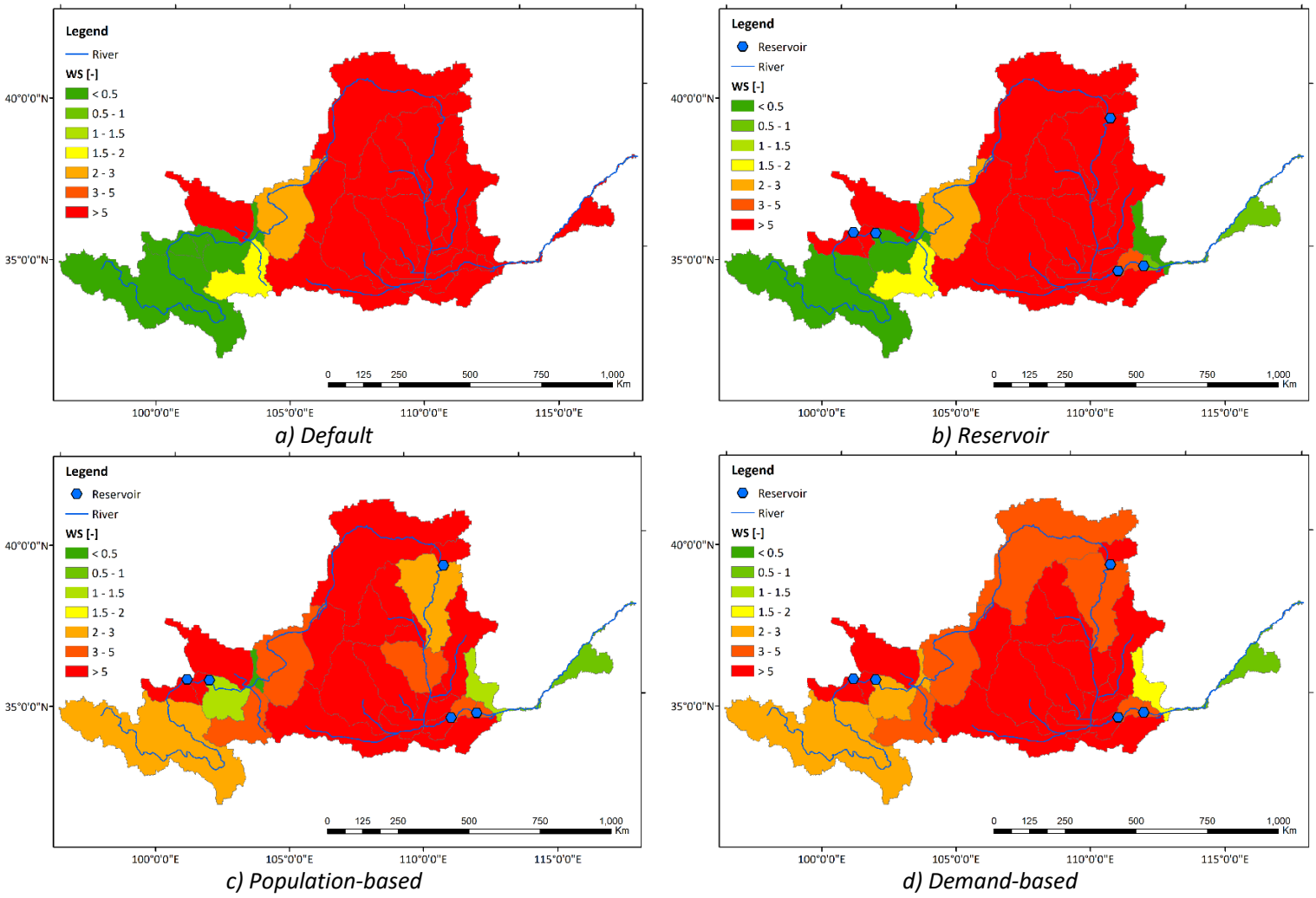

FIGURE 51: AVERAGE BLUE WATER SCARCITY SUMMER (JUNE – AUGUST) PER SUB-CATCHMENT YRB (2010 – 2014) USING BWF CAPS ACCORDING TO A) DEFAULT SCENARIO, B) SCENARIO CONSIDERING RESERVOIRS, C) POPULATION-BASED SCENARIO, AND D) DEMAND-BASED SCENARIO USING PRE EFR METHOD.

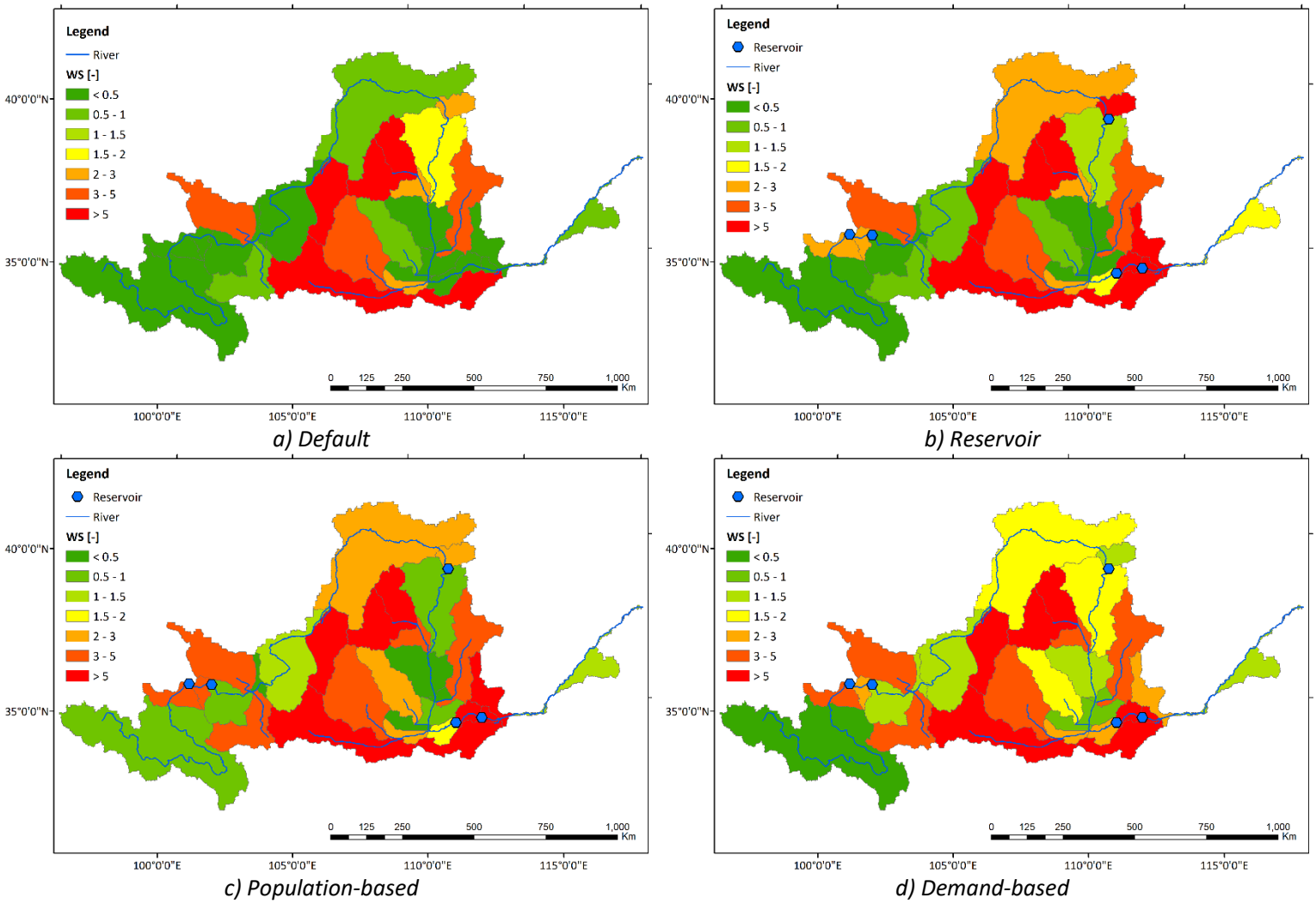

FIGURE 52: AVERAGE BLUE WATER SCARCITY AUTUMN (SEPTEMBER – NOVEMBER) PER SUB-CATCHMENT YRB (2010 – 2014) USING BWF CAPS ACCORDING TO A) DEFAULT SCENARIO, B) SCENARIO CONSIDERING RESERVOIRS, C) POPULATION-BASED SCENARIO, AND D) DEMAND-BASED SCENARIO USING PRE EFR METHOD.

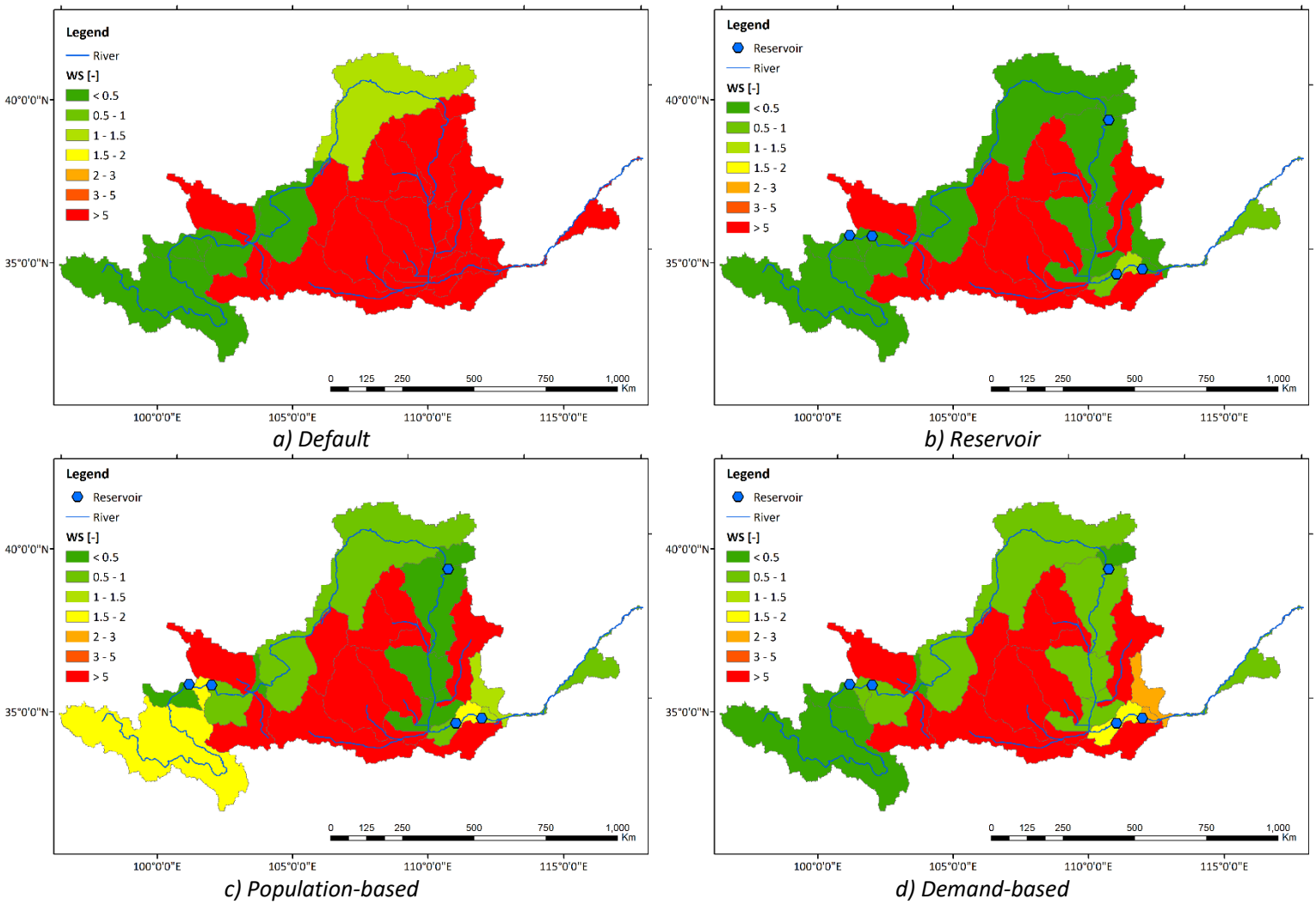

FIGURE 53: AVERAGE BLUE WATER SCARCITY WINTER (DECEMBER – FEBRUARY) PER SUB-CATCHMENT YRB (2010 – 2014) USING BWF CAPS ACCORDING TO A) DEFAULT SCENARIO, B) SCENARIO CONSIDERING RESERVOIRS, C) POPULATION-BASED SCENARIO, AND D) DEMAND-BASED SCENARIO USING PRE EFR METHOD.